Soil erosion of plastic-contaminated arable soils

Connecting the terrestrial microplastic sink to the inland water system

2024 | Raphael Rehm

Soil erosion of plastic-contaminated arable soils - connecting the terrestrial microplastic sink to the inland water system

Inaugural-Dissertation
zur Erlangung des Doktorgrades an der
Fakultät für Angewandte Informatik
der Universität Augsburg

vorgelegt von

Raphael Rehm

2024

First Examiner:	Prof. Dr. Peter Fiener, University Augsburg
Second Examiner:	Prof. Dr. Karl-Friedrich Wetzel, University Augsburg
Third Examiner:	Dr. Jörg Klasmeier, University Osnabrück
Date of oral examination:	March 14, 2024

Soil erosion of plastic-contaminated arable soils

Connecting the terrestrial microplastic sink to the inland water system

2024 | Raphael Rehm

Foreword

I am very pleased to present my work on "Soil erosion of plastic-contaminated arable soils - connecting the terrestrial microplastic sink to the inland water system". This work represents a broad research approach to better understand the complex interplay between microplastic pollution of agricultural soils and the transport of microplastic particles through a landscape via the soil erosion pathway.

Soil is one of our most important natural resources, serving not only as a source of food for humans and animals but also as a habitat for a variety of organisms and a filter for groundwater. However, this valuable resource is increasingly threatened by human activities such as agriculture, industry, sealing, erosion, and pollution. One worrying aspect of recent times is the growing contamination of soils with microplastic: tiny particles of plastic smaller than 5 millimeters entering the terrestrial environment through a variety of pathways and posing a significant threat.

The ubiquity of microplastic in the environment is already known, and it is undeniable that we need to address this problem. However, it is important to understand that soil erosion must be considered a significant mechanism for the transport of microplastic from soils into our inland waters, where it can continue to harm the aquatic environment.

I hope that this work will contribute to the discussion on the terrestrial transport mechanism of eroded microplastic and thus provide a basis for future studies in this research field.

“What we do today determines what the world will look like tomorrow.”

- Marie von Ebner-Eschenbach -

Acknowledgments

I would like to thank my family and friends from the bottom of my heart. Without your support, it would not have been possible for me to complete my doctoral thesis. I thank my family for their unconditional love and support during all stages of my education. Thank you for your understanding during the stressful periods and the constant motivation you gave me.

My thanks also go to my colleagues, who have always cheered me up and supported me in every request. Thank you for the breaks we took together, which helped us to clear our minds, and for the many conversations and discussions that broadened my horizons.

Special thanks go to my supervisor, who has been with me for the past few years. Thank you for the patience, professional support, and inspiring conversations that have shown me that research is not just a job, but also a calling.

I would also like to thank all those who have been directly or indirectly involved in my work. Without your help and contributions, my research would not have been possible.

I am incredibly grateful for all the support I have received and look forward to maintaining these relationships in the future.

Contents

Foreword I
Acknowledgments II
Contents III
Summary 1
Zusammenfassung 4
1 Introduction 7
2 Field experiment and laboratory analysis about potential transport of MP from on agricultural soils 20
2.1 Introduction 20
2.2 Methods 22
2.2.1 Setup of field experiment 22
2.2.2 Rainfall simulation – lateral MP fluxes 25
2.2.3 MP degradation and vertical fluxes 26
2.2.4 Prevention of MP contamination 27
2.2.5 MP extraction from soil samples 27
2.2.6 Microscopic MP detection 30
2.2.7 Quality control of MP extraction and microscopy detection 32
2.2.8 Statistical evaluation 32
2.3 Results 33
2.3.1 Surface runoff and sediment delivery 33
2.3.2 Microplastic delivery 34
2.3.3 Preferential erosion and transport of MP 36
2.3.4 Degradability and vertical movement 36
2.4 Discussion 38
2.4.1 Preferential erosion and transport of MP 38
2.4.2 Change in MP delivery over time 40
2.4.3 Experimental and environmental behavior 42
2.5 Conclusion 43
3 Model-based analysis of erosion-induced MP delivery from arable land to a stream network 45
3.1 Introduction 45
3.2 Methods 48

3.2.1 Modeled test catchment 48
3.2.2 MP erosion model 49
3.2.3 Model data 51
3.2.4 Model testing 59
3.2.5 Modelled scenarios 59
3.3 Results 60
3.3.1 Sediment delivery 60
3.3.2 MP erosion and delivery to stream network 61
3.3.3 Scenario S1 – business-as-usual 63
3.3.4 Scenario S2 – spatially targeted application of soil amendments 65
3.3.5 Scenario S3 – stop MP input: 66
3.4 Discussion 66
3.4.1 Modelled erosion rates & sediment delivery 66
3.4.2 Plausibility of MP soil input estimates 67
3.4.3 The modelled fate of MP 69
3.4.4 Soil erosion as a potential MP source for inland waters 70
3.4.5 The MP sink function of soil results in a long-term MP source 71
3.4.6 Targeted application of MP-loaded organic fertilizer 72
3.5 Conclusion 73
4 General discussion 75
4.1 Specific erosion and transport behavior of MP 75
4.2 Importance of soil erosion as input pathway to the stream network 78
4.3 Challenges and uncertainties related to erosion-induced MP delivery to the stream network 81
4.4 Soil erosion a specific MP stressor of inland waters 83
5 General conclusion 87
List of figures 90
List of tables 93
References 94

Summary

Microplastic (MP) contamination has been detected in all ecosystems and environments worldwide and is currently an important topic in various research fields. It is now known that MP particles pollute marine environments, freshwaters, and terrestrial ecosystems. This is partly because MP also spreads and is deposited via the atmosphere. Despite the public awareness of MP contamination of oceans as a major environmental problem, soils are suspected to contain more MP than the oceans. Arable land, in particular, represents a large human-made MP sink due to agricultural practices, including the application of MP-contaminated organic fertilizer and the direct plastic use, e.g., mulch films. Even in compost, the basis for healthy soil, MP concentrations with up to several hundred plastic particles per kilogram were already detected. The fate of the MP particles after deposition on arable land their spatial distribution in an agricultural landscape, e.g., by wind or water erosion, is largely unknown. However, the effectiveness of soil as an MP sink could be significantly reduced in areas exposed to regular water erosion. Against this background, this study focuses on the erosion of microplastic-polluted arable soils and aims to connect and evaluate the terrestrial microplastic sink with the inland water system. Concerning the possible transport of MP on agricultural topsoil via surface runoff, this work examines the extent to which soil erosion represents a potentially important MP entry path for aquatic ecosystems and tries to quantify this with corresponding uncertainties.

This thesis analyzes, on the one hand, experimentally the erosion and transport behavior of MP during heavy rainfall events. Therefore, a specific focus is set to preferential MP transport and MP-soil interactions, potentially leading to a more conservative transport behavior. On the other hand, a model-based estimation provides information on how much MP enters the river network due to erosion from a mesoscale catchment (400 km^2). In this context, the amounts of MP applied to cropland are specifically analyzed and runoff rates are calculated taking into account the spatial distribution in the landscape.

The experimental part of the thesis is based on a series of rainfall simulations on paired plots (4.5 m x 1.6 m) of silty loam and loamy sand located in Southern Germany. The simulations (rainfall intensity 60 mm h^{-1}) were repeated 3 times within 1.5 years. An amount of 10 g m^{-2} of fine (MP_f, size 53-100 µm) and 50 g m^{-2} of coarse (MP_c, size 250-300 µm) high-density polyethylene as common polymer was added to the topsoil (<10 cm) of the plots. The experiments showed a selective behavior of MP within the process of soil erosion, leading to a higher enrichment ratio in the eroded sediment and indicating MP losses from the plow horizon. Increasing interaction with mineral soil particles or aggregates leads to a decreasing MP delivery over time, showing that MP and soil interactions play a crucial role in the MP erosion process. There was a higher MP enrichment on the loamy sand but a higher sediment delivery on the silty loam resulting in nearly equal MP deliveries from both soil types. This implies that even less erosive coarse-textured soils can exhibit a substantial potential for MP transport. If soil presents a sink for MP depends on the size of the MP particles. The rain simulations have shown that more coarse MP was laterally lost via soil erosion, while the fine MP showed higher topsoil loss rates via vertical transport below the plow layer. The results generally indicate that arable land mainly retains the applied MP. However, in erosion-prone landscapes, arable land can be a substantial MP source for other land uses and aquatic.

In the modeling part of the thesis, a soil erosion model was adapted to account for MP erosion, transport and deposition following water and tillage erosion. This modeling tool estimated the MP redistribution within and the MP delivery from a mesoscale (~ 400 km^2) catchment in Southern Germany. To do so, an extensive evaluation of the potential MP contamination of especially the arable land in the catchment since 1950 was performed. The modeling analysis showed that most eroded MP is deposited within the catchment. Especially, the grassland areas along the stream network act as the most important MP sinks. Also important to note is that especially tillage erosion leads to a substantial burial of MP below the plow layer. Almost 5% of applied MP since 1950 is moved below the plough layer, while less than 1% of the MP potentially accumulated in the arable soils is transported to the stream network. However, in terms of mass, this amount is comparable to the MP delivery from wastewater treatment plants (WWTPs) within the same river system. Through the modeling, it could be concluded that in rural regions like the study area, the MP delivery into the river system caused by soil erosion can exceed the MP input from

WWTPs. However, as only small proportions of MP in soils are transported, it also means that soils are long-term MP sources. Based on the scenario ‘stop MP input in 2020’, in 100 years, MP delivery to the river network will have only decreased by 14% compared to 2020. In the 'business-as-usual' scenario, on the other hand, the MP input into the stream network would increase fourfold within the next century.

This study provides valuable insights into the erosion and transport of MP from agricultural soils to inland waters. The process study shows that lower-density MP particles are preferentially eroded and transported. The erosion rates of MP decrease over time due to the binding of the particles to or in soil aggregates, and particle size is critical to the transport of MP in soil. Soil erosion is essential in transferring MP from arable land to water bodies. Modeling shows that MP delivery from soil erosion can exceed MP inputs to streams from wastewater treatment plants, and reducing MP inputs to the environment will require targeted actions and changes in agriculture management. The modeling highlights the importance of tire wear as a major source of MP in the environment. Overall, arable soils present an MP sink but due to soil erosion, act as a long-term MP source for inland water systems.

Zusammenfassung

Die Verunreinigung durch Mikroplastik (MP) wurde in allen Ökosystemen und Umweltkompartimenten weltweit festgestellt und ist derzeit ein wichtiges Thema in verschiedenen Forschungsbereichen. Es ist inzwischen bekannt, dass MP-Partikel nicht nur die Meere, sondern auch Inlandsgewässer und terrestrische Ökosysteme verschmutzen. Dies ist zum Teil darauf zurückzuführen, dass sich MP auch über die Atmosphäre ausbreitet und ablagert. Trotz des öffentlichen Bewusstseins für die MP-Verschmutzung der Meere als großes Umweltproblem, ist wenig bekannt, dass davon ausgegangen wird, dass Böden mehr MP enthalten als die Meere. Insbesondere Ackerland stellt eine große, vom Menschen verursachte MP-Senke dar. Aufgrund landwirtschaftlicher Praktiken wie der Ausbringung von MP-haltigem organischem Dünger und der direkten Verwendung von Kunststoffen (z. B. Mulchfolien), erfahren Ackerböden eine besondere Belastung. Selbst in Kompost, der Grundlage für gesunde Böden, wurden bereits MP-Konzentrationen mit bis zu mehreren hundert Kunststoffpartikeln pro Kilogramm nachgewiesen. Der Verbleib der MP-Partikel nach der Ablagerung auf Ackerflächen und ihre räumliche Verteilung in der Agrarlandschaft, z. B. durch Wind- oder Wassererosion, ist weitgehend unbekannt. Die Wirksamkeit des Bodens als MP-Senke könnte jedoch in Gebieten mit regelmäßigen Wassererosionsereignissen langfristig reduziert sein. Vor diesem Hintergrund konzentriert sich diese Studie auf die Erosion von MP-belastetem Ackerböden und zielt darauf ab, die terrestrische Mikroplastiksenke mit dem Binnengewässersystem zu verbinden und zu bewerten. Im Hinblick auf den möglichen Transport von MP auf landwirtschaftlichen Oberboden über den Oberflächenabfluss wird in dieser Arbeit untersucht, inwieweit die Bodenerosion einen potentiell wichtigen MP-Eintragspfad für aquatische Ökosysteme darstellt und versucht, diesen mit entsprechenden Unsicherheiten zu quantifizieren.

Diese Arbeit analysiert einerseits experimentell das Erosions- und Transportverhalten von MP bei Starkregenereignissen, wobei ein besonderer Fokus auf den präferentiellen MP-Transport und die MP-Boden-Wechselwirkungen gelegt wird, die zu einem konservativeren Trans-

portverhalten führen könnten. Auf der anderen Seite bietet eine modellbasierte Schätzung Informationen darüber, wie viele MP aufgrund von Erosion aus einem mesoskaligen Einzugsgebiet (400 km^2) in das Flussnetz gelangen. In diesem Zusammenhang werden die MP-Mengen, die auf Ackerflächen ausgebracht werden, gezielt analysiert und Austragsraten unter Berücksichtigung der räumlichen Verteilung in der Landschaft kalkuliert.

Der experimentelle Teil der Arbeit basiert auf einer Reihe von Regensimulationen auf Beregnungs-Parzellen (4,5 m x 1,6 m) auf schluffigem Lehm und lehmigem Sand in Süddeutschland. Die Simulationen (Niederschlagsintensität 60 mm h^{-1}) wurden innerhalb von 1,5 Jahren dreimal wiederholt. Eine Menge von 10 g m^{-2} feinem (MP_f, Größe 53-100 µm) und 50 g m^{-2} grobem (MP_c, Größe 250-300 µm) High-Density-Polyethylen als gängiges Polymer wurde in den Oberboden (<10 cm) der Parzellen eingebracht. Die Experimente zeigen ein selektives Verhalten von MP während des Prozesses der Bodenerosion. Dieser führt zu einer höheren Anreicherung im erodierten Sediment, was auf einen beschleunigten MP-Verlust aus dem Pflughorizont hinweist. Eine zunehmende Interaktion mit mineralischen Bodenpartikeln oder Aggregaten führt zu einer abnehmenden MP-Lieferung über die Zeit. Dies zeigt, dass MP-Bodeninteraktionen eine entscheidende Rolle im MP-Erosionsprozess spielen. Auf dem lehmigen Sand wurde eine höhere MP-Anreicherung, auf dem schluffigen Lehm jedoch eine höhere Sedimentfracht gemessen, so dass der MP-Austrag bei beiden Bodentypen nahezu gleich war. Dies bedeutet, dass auch wenig erosive Böden mit grober Textur ein erhebliches Potenzial für den Transport von MP aufweisen können. Ob die Böden eine Senke im MP-Kreislauf darstellen, hängt unter anderem von der Größe der MP-Partikel ab. Die Regensimulationen haben gezeigt, dass ein größerer Teil des groben MP lateral durch Bodenerosion verloren ging, während das feine MP höhere Verlustraten aus dem Oberboden durch den vertikalen Transport bis unter die Pflugschicht aufwies. Im Allgemeinen deuten die Ergebnisse darauf hin, dass die Ackerböden die ausgebrachten MP-Partikel hauptsächlich zurückgehalten haben. In erosionsanfälligen Agrarlandschaften kann die Bodenerosion auf Ackerland jedoch eine bedeutende MP-Quelle für andere Landnutzungen und aquatische Ökosysteme darstellen. Wenn man bedenkt, wie viel Kunststoff auf Ackerböden und in der gesamten terrestrischen Umwelt enthalten ist, stellt dies eine nicht zu unterschätzende langfristige MP-Quelle dar.

Für die Modellierung wurde ein Bodenerosionsmodell angepasst, um die Erosion, den Transport und die Ablagerung von MP auch Wasser- und Bodenerosion zu berücksichtigen. Dieses

Modellierungswerkzeug wurde verwendet, um die MP-Umverteilung innerhalb und den MP-Austrag aus einem mesoskaligen (~ 400 km²) Einzugsgebiet in Süddeutschland abzuschätzen. Zu diesem Zweck wurde eine umfassende Bewertung der potenziellen MP-Belastung insbesondere der Ackerflächen im Einzugsgebiet seit 1950 durchgeführt. Die Modellanalyse zeigte, dass der größte Teil der erodierten MP innerhalb des Einzugsgebietes abgelagert wird, wobei die Grünlandflächen entlang des Bachnetzes als wichtigste MP-Senken fungieren. Wichtig ist auch die Feststellung, dass die Bearbeitungserosion zu einer erheblichen Verlagerung von MP unter den Pflughorizont führt. Insgesamt sind durch Prozesse der Wasser – und Bearbeitungserosion fast 5 % des seit 1950 ausgebrachten MPs unter den Pflughorizont verlagert worden, während weniger als 1 % des potenziell in den Ackerböden akkumulierten MP in das Fließgewässernetz ausgetragen wurde. Die Masse dieses MP-Austrages ist vergleichbar mit dem MP-Austrag aus den Kläranlagen im selben Einzugssystem. Durch die Modellierung konnte gezeigt werden, dass in ländlichen Regionen, wie dem Untersuchungsgebiet, der durch Bodenerosion verursachte MP-Eintrag in das Flusssystem den MP-Austrag aus den Kläranlagen übersteigen kann. Da jedoch das meiste MP im Boden verbleibt, bedeutet dies auch, dass Böden langfristige MP-Quellen sind. Basierend auf dem Szenario "Stopp des MP-Eintrags im Jahr 2020" wird der MP-Eintrag in das Flusssystem in 100 Jahren im Vergleich zu 2020 nur um 14% zurückgegangen sein. Im Szenario "Business-as-usual" würde sich der MP-Eintrag in das Fließgewässernetz innerhalb des nächsten Jahrhunderts hingegen vervierfachen.

Die Studie liefert wertvolle Erkenntnisse über die Erosion und den Transport von MP aus landwirtschaftlichen Böden in Binnengewässer. Zusammenfassend zeigt die Prozessstudie, dass MP-Partikel mit geringerer Dichte bevorzugt erodiert und transportiert werden. Die Erosionsraten von MP nehmen mit der Zeit aufgrund der Bindung der Partikel an oder in Bodenaggregate ab und die Partikelgröße ist entscheidend für den Transport von MP. Die Bodenerosion spielt eine wichtige Rolle bei der Übertragung von MP von Ackerland in Gewässer. Die Modellierung zeigt, dass die durch Bodenerosion verursachten MP-Einträge in Flüsse die Einträge aus Kläranlagen übersteigen können, und die Verringerung der MP-Erosion erfordert gezielte Maßnahmen und Veränderungen in der Landwirtschaft und Landschaft. Die Modellierung unterstreicht außerdem die Bedeutung von Reifenabrieb als Hauptquelle von MP in der Umwelt. Grundsätzlich stellen Ackerböden eine MP-Senke dar, die aber ihrerseits aufgrund von Bodenerosion eine langfristige MP-Quelle für Binnengewässer ist.

1 Introduction

In the Anthropocene, plastic has replaced many traditional materials such as wood, glass and metal. Plastics are widely used in many fields due to their diverse properties and versatility (malleable, lightweight, durable, insulating, hygienic, etc.). In 2021, more than 390 million tons of plastic were produced worldwide (Hachem *et al.*, 2023). Most of the plastic produced each year is need for packaging (146 million tons), construction (65 million tons), textiles (59 million tons), transportation (27 million tons), electrical (18 million tons) and industrial machinery (3 million tons) (Geyer *et al.*, 2017). Currently, plastics production is estimated to double within the next 20 years (Williams and Rangel-Buitrago, 2022; Lebreton and Andrady, 2019). Due to the predicted increase in global plastic production (Horton, 2022; Bergmann *et al.*, 2022), more environmental inputs are to be expected (Shekhar *et al.*, 2022; Machado *et al.*, 2018). Due to their versatility and low cost (Moulé, 2010; Samuel, 2004), plastic products are part of everyday

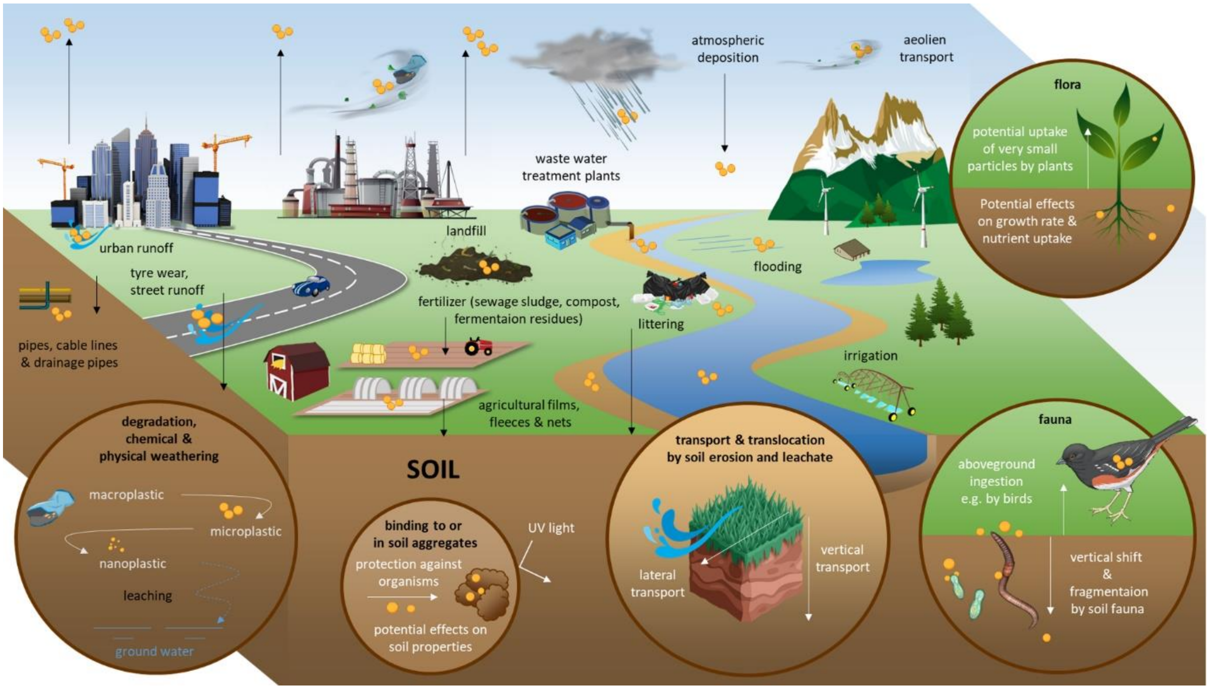

Figure 1: Schematic representation of emission and immission processes of microplastics in the soil system, including potential sources, input pathways, and ecological effects (adopted from Rehm and Fiener 2020).

life, but in many cases only with a very short use time (Moritz and Echterhoff, 2016). This leads to high consumption and loss rates (Luan *et al.*, 2022; Amadei *et al.*, 2022).

Estimates of global plastic emissions into the environment currently range from 9 to 23 million tons per year for the aquatic environment and from 13 to 25 million tons per year for the terrestrial environment (Lechthaler, 2020; MacLeod *et al.*, 2021; Bergmann *et al.*, 2022). The ranges and estimates substantially vary between studies and are overall associated with large uncertainties. For example, Horton et al. (2017) estimated that terrestrial ecosystems in the European Union contain approximately 4 to 23 times more plastic than oceans. The large emissions of plastic and the longevity of most plastic types also pose an obvious threat to our environment (Ng *et al.*, 2018). The issue of plastic in the environment is a global concern and has become one of the greatest environmental pollutions of the 20st and 21st century (Su *et al.*, 2022; Guo *et al.*, 2021; Klingelhöfer *et al.*, 2020). In the Anthropocene, with humanity as the dominant geophysical influence, plastic pollution has already reached such proportions that special terms like “plastisphere” (ecosystems that have evolved to live in human-made plastic environments) and “technofossils” (material footprints that humans will leave behind through their material goods) have emerged (Ramkumar *et al.*, 2022; Chen *et al.*, 2022).

The topic is mainly associated with the entry and the associated negative effects in different ecosystems (Su *et al.*, 2022; Sarker *et al.*, 2020; Ajith *et al.*, 2020). Plastic can become a problem when it enters natural ecosystems (Tekman *et al.*, 2022; Zhang *et al.*, 2022b), accumulates (van Emmerik *et al.*, 2022; Huang *et al.*, 2023a; Barnes *et al.*, 2009) and is ingested by organisms (Hodkovicova *et al.*, 2022; Bhattacharyya *et al.*, 2022; Rillig *et al.*, 2019). There are great uncertainties about the actual amounts of plastic pollution within the respective ecosystems and its effects (Schell *et al.*, 2020; van Leeuwen *et al.*, 2022). This is particularly the case with particles of very small size - so-called microplastic (MP) (Koelmans *et al.*, 2022; Lamichhane *et al.*, 2022). By definition, the size of MP is between 1 µm and 5 mm (Kim *et al.*, 2021; Miklos *et al.*, 2016; Frias and Nash, 2019). Larger pieces of plastic are referred to as mesoplastic (5-25 mm) or macroplastic (> 25 mm), smaller ones as nanoplastic (< 1 µm) (Miklos *et al.*, 2016; Frias and Nash, 2019). In addition, a distinction is made between primary and secondary MP (Miklos *et al.*, 2016; Rillig, 2012). The primary MP is deliberately added to certain products such as cosmetics, coatings or paints to change their properties (Mitrano and Wohlleben, 2020).

In contrast, secondary MP are formed through macroplastic's physical, chemical, or biological and biochemical fragmentation (Miklos *et al.*, 2016; Bertling *et al.*, 2021).

The most common plastics found in the form of microplastic particles are polyethylene (PE) as the most common plastic in many everyday items such as plastic bags, packaging, cosmetic products and textile fibers (Jahn, 2020; Lozano *et al.*, 2021; Sajjad *et al.*, 2022). Polypropylene (PP) and polystyrene (PS) used as packaging or disposable tableware. Polyethylene terephthalate (PET) mainly used in beverage bottles, food packaging and textile fibers such as polyester; polyvinyl chloride (PVC) used as pipes, cable insulation or flooring. In addition, many other plastics are developed for specific applications, such as polyvinyl acetate (PVA) in adhesives and coatings. Polyurethane (PU) for foams and insulation materials. Polycarbonate (PC) is characterized by its high transparency, impact strength and heat resistance. Polyamide (PA) also known as nylon, in textiles, carpets and ropes, or polymethyl methacrylate (PMMA) in the form of acrylic glass (Plexiglas). Nowadays, biodegradable plastics are often used as an alternative to conventional plastic in various sectors such as packaging, agriculture, medicine and disposables (da Luz *et al.*, 2014; Moshood *et al.*, 2022a). However, the degradation of biodegradable plastics often requires specific conditions and does not always occur efficiently in natural environments, such as soil (Sintim and Flury, 2017; Tábi, 2022). In addition, improper disposal or mixing with conventional plastics can compromise the effectiveness of the biodegradable material and cause environmental problems as with normal plastic (Moshood *et al.*, 2022b).

Microplastic pollution has become an increasingly important area of research in recent years, as scientists have recognized the potential impact of MP on ecosystem function (Lambert and Wagner, 2018; Tagg and do Sul, 2019; Xu *et al.*, 2020). While plastic (and MP) pollution was first recognized as a problem in marine environments (Ryan, 2015), it is now known to occur in many other environmental compartments, including freshwater systems (Dris *et al.*, 2015; Nasseri and Azizi, 2022), air (Gasperi *et al.*, 2018; Yurtsever *et al.*, 2018), and soil (Rillig, 2012; Sa'adu and Farsang, 2023). Estimation of terrestrial microplastic pollution is still associated with very high uncertainties. Koutnik *et al.* (2021) analysed MP concentrations reported in 196 studies from 49 countries concluding that the concentration of MP can vary up to 8 orders of magnitude depending on the location. In this study it is for example shown that the MP concentration decreased by up to two orders of magnitude from inland urban areas to estuaries in coastal areas. This result indicates that the terrestrial MP-pollution seems to be higher than in the water of coastal areas (Koutnik *et al.*, 2021). MP are widely distributed in terrestrial ecosystems, with the highest concentrations found in urban areas, followed by rural and natural areas (Nizzetto *et al.*, 2016b; Kim *et al.*, 2021; Chauhan and Basri, 2022).

Studies have shown that microplastic can accumulate in the soil through various pathways, including tire wear (TW), stated as the primary source (Knight *et al.*, 2020; Sommer *et al.*, 2018), littering (Scheurer and Bigalke, 2018) and atmospheric deposition (Brahney *et al.*, 2020) (Figure 1). Arable soils, in particular, experience increased MP inputs due to agricultural management (Brandes, 2020). Foils or films are used for various purposes such as greenhouse coverings (Espí *et al.*, 2016), mulching (Steinmetz et al., 2016), or protective barriers to control pests and weed growth, regulate soil temperature and moisture, and therefore enhance crop productivity. Films are subject to numerous fragmentation processes during use (whereas only biodegradable plastic is transformed into CO_2 via microbial degradation), so parts of the film material remain in the soil and are converted to MP over time (Ng *et al.*, 2018). Silage foils preserve and store forage crops, such as grass or corn, as silage and plastic foils for packaging are also used in agriculture, causing macro and microplastic emissions (Bertling *et al.*, 2021). Compost and sewage sludge have been used as organic fertilizers for a long time to support the circular economy (Braun *et al.*, 2021; Liu *et al.*, 2014; Zhang *et al.*, 2020a). They can contain different amounts of plastic, with compost containing a wide range of particle sizes or even macroplastic, while sewage sludge mainly contains smaller MP (e.g., textile fibers). In contrast to compost, fertilization with sewage sludge is decreasing (instead it is burned to produce energy), as it contains undesirable and sometimes toxic components. In addition, binding material in particular crops (Rehm *et al.*, 2018), irrigation with contaminated (waste) water (Pérez-Reverón *et al.*, 2022), as well as MP associated with coated fertilizer and seeds (Accinelli *et al.*, 2021; Lian *et al.*, 2021), have proven to be also potential input pathways for agricultural soils.

In general, relevant input pathways are sufficiently known, but data on the spatial distribution of input still need to be provided. MP-concentration measurements cannot compensate for this gap in the soil because no allocation to the sources can be made. The extent to which individual MP sources contribute to the input into the soil cannot yet be reliably quantified (He *et al.*, 2023; Sa'adu and Farsang, 2023). The main reason for this is: (i) MP pollution of soil strongly varies depending on the location, type of soil, and other factors (Khan *et al.*, 2023; Rafique *et al.*, 2020), (ii) the analysis of MP in soil is challenging, and there are no standardized sampling and analysis methods available (Praveena *et al.*, 2022; Radford, 2023).

Detecting MP particles in the soil presents a significant challenge because separating the few particles from a matrix of numerous other mineral and organic particles is a complex task. Nevertheless, detection methods are critical to determining the extent of MP pollution in soils. Three groups of methods are predominantly used for MP particle analysis. Thermoanalytical techniques such as pyrolysis gas chromatography/mass spectrometry (Pyr-GC/MS) (Li *et al.*, 2021b), microscopy for optical determination (Baruah *et al.*, 2022; Santander, 2021), and microspectroscopic methods such as Raman microspectroscopy (Raman) and Fourier transform infrared microspectroscopy (FTIR) (Raj and Maiti, 2023; Kappler *et al.*, 2015). While the pyrolysis method only provides MP mass units, the microspectroscopy method captures the MP particle number. All groups of methods are difficult to compare, so combining the methods with a sample would ensure the most significant possible information gain (Elert *et al.*, 2017; Adhikari *et al.*, 2022).

Py-GC/MS combines the thermal decomposition of organic or carbon materials, including MP, at high temperatures in an atmosphere without reactive gases with the analysis of the resulting volatile compounds using gas chromatography and mass spectrometry (Mansa and Zou, 2021; Li *et al.*, 2021b). The combustion of synthetic polymers at a temperature of 600 °C produces specific degradation products that can be detected using Py-GC-MS. By analyzing the outgassing, polymer types can be identified, similar to a fingerprint. The advantage of py-GC/MS is the detection of polymer types of microplastic particles (Fries *et al.*, 2013). By analyzing selected pyrolysis products, it is also possible to indirectly quantify synthetic polymers in complex environmental samples. This method provides information on the chemical composition of MP and allows the identification of different types of plastics and the quantitative determination of MP in soil samples. When using mass spectrometers to analyze soil samples, the exact particle count is not essential to identify MP. However, if the MP concentration or particle number is low, the detection limit may not be reached, which would call for a complex enrichment of the plastic concentration within the sample (Dierkes *et al.*, 2019; Dümichen *et al.*, 2015). A further disadvantage of py-GC/MS is the destruction of the investigated particles during the analysis. It is important to emphasize that py-GC/MS only provides information on the mass of microplastic (MP) particles. However, this approach falls short in assessing the environmental impact, as it does not take into account the size and quantity of plastic particles, which are of great importance.

Methods based on spectroscopy or microscopy techniques require the extraction of polymers from the sample matrix beforehand. The choice of processing methods for the extraction of microplastics from soil samples and sediments is based on the respective environmental matrix and the detection method. The correct sequence of steps is vital to ensure optimal sample preparation. It is essential to keep the number of preparation steps as low as possible to minimize the particles' losses, contamination, and possible fragmentation. Among the various methods available, density separation and electrostatic separation are among them (Santander, 2021). These methods aim to separate the inorganic matrix from the microplastic particles. Density separation uses saturated salt solutions, while electrostatic separation is based on the different electrical charges of the particles. The chemical treatment represents another method. Here, oxidative processes, acid or base digestions decompose organic components and isolate the microplastic particles (Braun *et al.*, 2020). It must be considered here that some polymers can react sensitively to chemical conditions. Enzymatic processing methods gently remove organic contaminants from the microplastic particles. Enzymes such as cellulase, protease, lipase, amylase, chitinase, and pectinase are used in this process (Braun *et al.*, 2020). This method is time-consuming and often requires complementary oxidative steps. Also of importance is chemical extraction. The microplastic particles are dissolved from the sample using increased temperature and pressure. This allows the concentration of the particles from larger sample volumes. The method can be automated, but toxic solvents are used. Separating the plastic particles from the soil matrix becomes more complex and methodologically more difficult as the particle size decreases. As a result, the technically possible detection is limited, and so far, most studies about MP in soil focus on particles > 50 µm (Chauhan and Basri, 2022; Liu *et al.*, 2022b).

After separation of MP from soil, microscopy is a method to examine MP (Santander, 2021). Visual observation can identify MP particles and determine their properties, such as shape and size. Plastic particles of 1-5 mm can be detected with the naked eye. To identify MP in the range of hundreds of micrometers, the help of microscopy is needed. Commonly used microscopy techniques for the detection of MP are light microscopy (Sierra *et al.*, 2020), stereomicroscope

(Pervez *et al.*, 2020), fluorescent microscopy (Liu *et al.*, 2022a), and scanning electron microscopy (SEM) (Huang *et al.*, 2023b). The microscopy method involves magnified images that provide detailed surface texture and structural information for identifying plastic-like particles. While most particles in this size range can be determined, sub-hundred-micron particles without color or typical shape are challenging to characterize as plastics (Baruah *et al.*, 2022). Sediment samples with poorly separated light sediment particles and biogenic materials can interfere with microscopic identification. In various field monitoring studies, fibers were found to be the dominant MP particles and the distinction between synthetic and natural fibers is difficult. Previous studies have shown high false identification rates using microscopy, particularly for transparent particles (Shim *et al.*, 2017).

Raman spectroscopy is a spectroscopic technique based on the interaction of light with chemical bonds in a material (Krekelbergh *et al.*, 2022). It uses a laser beam directed onto the sample and produces a unique spectrum based on its composition. As this technique uses a small-diameter laser beam, it can also detect MP of smaller sizes. Raman microscopy can achieve a lateral resolution of up to 500 nm (Kappler *et al.*, 2015). It allows the identification and characterization of MP particles based on their specific Raman spectra, which are unique to different types of plastics. This method records the number of MP particles and the different types of polymers. However, it is necessary to eliminate disturbing biological components by an efficient sample preparation to avoid fluorescence during the Raman measurement. Otherwise, fluorescence due to the presence of a biofilm superposes the Raman signal, which can entirely hamper particle identification (Kappler *et al.*, 2015). Refractive errors are also a significant drawback due to non-interpretable spectra produced by irregularly shaped MP (Harrison et al. 2012). Furthermore, an automated process ensuring optimal focusing on each potential MP particle is needed. These are current challenges to cope with.

Fourier transform infrared spectroscopy (FTIR) technique uses the absorption of infrared light by molecules to obtain information about the chemical composition of a material (Krekelbergh *et al.*, 2022; Kappler *et al.*, 2015). FTIR is a widely used method for identifying MP and can also be used to determine the type of polymer. FTIR produces unique spectra that differentiate MP from other organic and inorganic particles and gives specific information on chemical bonds and polymer composition, giving clues of origin or source (Cincinelli et al. 2017; Besseling et al. 2015). The complete environmental sample is concentrated on a filter.

Subsequently, the whole or a specific filter area (about 10 mm in diameter) is measured automatically without visual presorting and analyzed via FTIR imaging (Löder *et al.*, 2015). This optimized analytical approach allows the detection of MP with particle size down to about 20 μm.

The different approaches generally result in two types of data sets: mass or particle-number-related. By assuming the average densities, size, and shape of particles, polymer masses can empirically be calculated from microscopy or spectroscopy data and compared with mass-based results (Primpke *et al.*, 2020). Since the methods determine either the weight or the number, such a conversion is always associated with errors or uncertainties since all particles' exact shape and weight are unknown.

After considering various treatment methods for extracting MP from soil samples, it is critical to understand the potential impact of these tiny plastic particles on the soil and surrounding environment. These effects are complex and can have multiple consequences for soil quality and soil organisms. The interactions between microplastics and soil can involve short-term and long-term consequences requiring thorough investigation. Below, the physical, chemical, and toxic effects of MP are discussed.

Physical effects refer to soil structure and to aggregates. Soil aggregates are essential for soil structure and have important roles in water and nutrient management, microbial activity, and soil layer stabilizing. The presence of MP affects soil structure by influencing aggregate formation and porosity (Figure 1), which can affect soil drainage, water infiltration, and aeration (Li *et al.*, 2022a; Chia *et al.*, 2022). The effects of MP on soil structure depend on their morphology, material properties, and chemical factors. Microplastic films can accelerate evaporation, reduce soil water content, decrease soil tensile strength, increase soil porosity, and alter pore size distribution (Zhang *et al.*, 2022a). In laboratory experiments using field and pot soils supplemented with 0.1% and 0.3% microplastic films, it was observed that after one year, there was an increase in the volume of larger pores (macropores) and a decrease in the volume of smaller pores (micropores) (Zhang *et al.*, 2022a). This change in pore distribution could potentially enhance drainage capacity in the soil. MP impacts various physical properties of soil, including soil aggregates, bulk density, and water content. Little is known about the long-term effects of this interaction, and further research is needed to understand the long-term consequences on soil functions and ecosystems.

In addition to soil physical effects, the presence of MP in soils can also have effects on soil chemistry and toxicity. MP can adsorb to organic compounds in the soil or sorb them to their surface, which can alter the availability of nutrients and reduce their accessibility for plants, potentially leading to nutrient deficiencies (Kumar *et al.*, 2022). MP can also affect soil pH and increase soil acidity by releasing chemical additives or interacting with soil components (Hale *et al.*, 2020; Liu *et al.*, 2017). This can have implications for nutrient availability and soil health. Additionally, MP can be a carrier for organic pollutants and heavy metals, potentially increasing soil contamination and posing toxic risks to organisms and plants (de Souza Machado *et al.*, 2017). Plastic debris is often associated with dead marine animals and seabirds whose stomachs are filled with macroplastics. Conversely, MP leaves the organism again, making possible consequences difficult to predict (Gong and Xie, 2020). The harmful effects of MP can be subdivided into physical and chemical effects (Ding *et al.*, 2022). While pure polymers are not very reactive, and direct toxicity is low (Brown *et al.*, 2022). Many additives (plasticizers, UV-stabilizers, etc.) can add toxic effects (Qiao *et al.*, 2022; Okoye *et al.*, 2022). The activities of soil enzymes and bacterial communities can change (Wang *et al.*, 2022b), as can the germination success (De Silva *et al.*, 2021), growth and biomass of plants (Li *et al.*, 2022b), the biomass of earthworms and the gut microbiome of springtails (Ju *et al.*, 2019). Microplastic particles can have various effects on organisms: Known effects include functional disorders (e.g., instability of the quiver of caddisfly larvae) (Ehlers *et al.*, 2019), malnutrition, inflammation, and developmental disorders (Sharma *et al.*, 2022; Li *et al.*, 2022b). The interaction and the effect on the organism depend on numerous factors, such as the size, shape, and concentration of the particles, the material, the species of organism, its nutritional type, and the developmental stage (Verla *et al.*, 2019; Ju *et al.*, 2019). It is difficult to transfer the results on the toxicity of the particles, which are mostly determined in laboratory experiments, to the field. Laboratory experiments are often conducted at very high concentrations. While standard spherical particles are mostly used in the tests, fibers, and fragments dominate the environment. Furthermore, MP is further modified in the environment, for example, by oxidation and colonization with biofilms.

The problem with MP is its diffuse entry and ubiquity. MP enters the soil system primarily via the surface and is mixed into the soil column via bioturbation (Heinze *et al.*, 2022; Li *et al.*, 2021a) and, in the case of small particles, via infiltration (Li *et al.*, 2021a). The transport towards the groundwater via preferential flow pathways such as root canals, worm burrows, and drying cracks has also been described (Maass *et al.*, 2017; Li *et al.*, 2021a; Heinze *et al.*, 2022). The extent of these translocation processes can only be roughly estimated since previous detection studies are scarce or based on experiments with artificially high MP loadings. In arable land, it is actively mixed into the plow layer via tillage operations (Weber *et al.*, 2022; Zhao *et al.*, 2022; Zubris and Richards, 2005). Depending on the tillage technique, the MP is worked into the soil at different depths and homogenized more or less after multiple processing (Fiener *et al.*, 2018; Weber *et al.*, 2022). Moreover, tillage potentially leads to mechanical fragmentation of macroplastic but also reduces photochemical decomposition at the soil surface and reduces MP transport via water and wind (Colin *et al.*, 1981; Corcoran, 2022; Feuilloley *et al.*, 2005). Plastic degrades very slowly in the environment (Corcoran, 2022; Weber *et al.*, 2022). As it can be assumed that plastic will accumulate in the soil over long-term periods if inputs remain unchanged (Gasperi *et al.*, 2018; Horton *et al.*, 2017; Saling *et al.*, 2020). Most estimates based on MP input into soils consider agricultural soils a significant MP sink (Rochman, 2018; Waldschläger *et al.*, 2020; Zubris and Richards, 2005).

However, soils might not only be a long-term sink of plastic slowly fragmenting in smaller sizes, but might be also a MP source for other environmental compartments. Whether the accumulation of MP in the soil leads to a permanent sink (until the plastic disintegrates after centuries), or is lost again through leaching into the groundwater or through surface runoff and erosion, is often discussed, but it is hardly quantified (Mai *et al.*, 2018; Nizzetto *et al.*, 2016a; Rillig *et al.*, 2017a). Initial studies suggest a significant MP delivery from agricultural soils (Crossman *et al.*, 2020). An important pathway removing MP from especially arable soils are different soil erosion pathways transporting soil and MP via wind and water (Han *et al.*, 2022; Bullard *et al.*, 2021).

Wind erosion may transport light MP across soil systems, potentially reaching streams and rivers (Horton *et al.*, 2017). Arid regions prone to wind erosion may be particularly vulnerable, and climate change-induced aridity could exacerbate the issue. Zylstra (2013) revealed the role of wind action in spreading light macroplastic particles to other terrestrial locations. He indicated that trash densities were largely independent of road proximity, suggesting that wind could carry plastic bags and balloons > 2 km into remote areas. Knowledge of the transport of MP with soil wind erosion is sparse because of inadequate research. Rezaei *et al.* (2019) first revealed the key role of wind erosion in the spread of MP in terrestrial environments using a portable wind tunnel in the field. They reported that wind-eroded sediments from both agricultural and natural lands were enriched with microplastics. Bullard *et al.* (2021) explored the extent to which MP was preferentially transported by wind erosion and concluded that MP shape was an important factor in such transportation.

The redistribution within terrestrial systems but might also lead, especially in case of water erosion, to an input into aquatic systems (Liu *et al.*, 2021; Lwanga *et al.*, 2022). Soil erosion and surface runoff are potential sources of MP entering aquatic ecosystems. MP is carried through stormwater runoff in urban and suburban regions. A study by (Liu *et al.*, 2019) identified runoff as a significant source of MPs in retention ponds. Lutz *et al.* (2022) studied the movement of microplastics (MPs) within sediment samples taken from stormwater drainage systems in Australia. They discovered fewer microplastics in sediment collected from an agricultural area than sediment collected from an urban area. In the Rhône River, a peak in plastic transport was measured a few days after precipitation events, indicating that surface runoff may have an essential effect on MP input to water bodies compared to other processes (Castro-Jiménez et al., 2019). Just a few studies have investigated how MP behaves during the transport via water erosion on agricultural soils so far. One study by Schell *et al.* (2022) examined the lateral transport of MPs in runoff from agricultural fields treated with biosolids as fertilizer and observed the sludge application significantly increased the MP concentration in eroded soil sediments. Han *et al.* (2022) focused on examining the horizontal transport of MP through surface runoff in soil influenced by vegetation. It was observed that smaller-sized and low-density plastics exhibited a higher susceptibility to be carried along by surface runoff. Notably, vegetation cover played a crucial role in mitigating the horizontal transport of plastics through surface runoff. Furthermore, the research indicated that the quantity of rainfall, rather than the frequency of rain events, had a more pronounced influence on the transportation of plastics. However, it's important to note that these observations about MP transport were based on limited study plots.

MP transport in terrestrial environments is also analyzed using various models. One process-based model, INCA-Contaminants, simulates plastic storage, entrainment, and deposition in soils and streams based on hydrological and pedological factors (Nizzetto *et al.*, 2016c; Nizzetto *et al.*, 2016a). Empirical data limitations have constrained its application, but it has highlighted the significance of size and soil characteristics on MP transport. Zhang *et al.* (2020b) used geographical data sets to create maps of MP emissions for different compartments like soil, freshwater, and air. Conceptual models like the Source–Pathway–Receptor (SPR) model summarize knowledge on plastic pollution, describing sources, transport pathways, concentrations, and receptors in various environments (Waldschläger *et al.*, 2020; Waldschläger and Schüttrumpf, 2020). This model aids in assessing the consequences of MP pollution and suggests control measures. Koutnik *et al.* (2021) analyzed microplastic concentrations in urban soil, water, and remote glaciers, emphasizing the role of wind-driven transport. Models offer insights into MP transport in terrestrial environments, highlighting the importance of various factors such as size, soil characteristics, emissions pathways, and transport mechanisms.

The relationship between microplastics and erosion, particularly water erosion, is a complex and poorly understood area of research (Surendran *et al.*, 2023; Horton *et al.*, 2017). Windsor *et al.* (2019) adopted a hydrological catchment as a distinct and well-defined analytical unit to assess plastic pollution. However, their findings highlighted the insufficient quantification of sources, flow rates, and accumulation points within these catchments. The relationship between MP and these soil properties is not fully understood, particularly in field situations. Empirical evidence supporting MP transport through runoff and erosion is scarce.

The motivation of this thesis is, therefore, to address the following research gabs. A lack of knowledge exists regarding the specific behavior of MP in water erosion and how this behavior changes over time. Studies on how MP behaves under erosion are still rare in the present research process. This thesis aims to present research on how the concentration of MP in topsoil changes both laterally and vertically. Furthermore, knowledge about the area-specific exposure to MP in agricultural landscapes will be gained, especially with regard to agricultural management. Therefore, the PhD thesis encompasses five central research inquiries. (i) Firstly, it examines the differences in surface runoff induced erosion and transport of MP compared to other soil compartments. (ii) Secondly, it explores whether the erosion and transportation behavior of MP exhibit dynamic changes over time. (iii) Thirdly, the study assesses the significance of lateral and vertical losses of MP in changing MP concentrations within the plow layer. (iv) Additionally, it delves into the role of water erosion within an agricultural catchment regarding MP redistribution and MP delivery into the stream network. (v) Lastly, the research investigates the primary sources of MP responsible for inducing erosion-driven MP fluxes into water stream networks.

Regarding the above research questions, the thesis will test the following hypotheses:

1. Due to the low density, MP particles are preferentially eroded with water, resulting in MP enrichment in the delivered sediment compared to topsoil MP contamination.
2. The MP enrichment increases with decreasing MP size, while overall MP enrichment is more pronounced if the MP is in the same or a smaller size range as the mineral soil particles.
3. MP delivery rates change over time as interactions between MP and soil (aggregation and binding to mineral particles) increase and concentrations of MP in topsoil decrease due to subsequent erosion events and vertical transport below the plow layer.
4. Tillage erosion substantially reduces MP transport via water erosion as it decreases MP concentration at erosional sites and a burial of MP below the plow layer at depositional sites.
5. Soil erosion of MP leads to a long-term redistribution within the catchment and is a long-term source of MP delivery to water streams.
6. Targeted or reduced application of MP contaminating organic fertilizer only slightly affects MP delivery to the stream network as tire wear fluxes dominate this process.

To test the hypotheses the theses is subdivided in an experimental part focusing on processes of MP erosion and transport during heavy rainfall events, and a modelling part analyzing the long-term importance of MP erosion, redistribution and delivery in a semi-virtual catchment setting.

2 Field experiment and laboratory analysis about potential transport of MP from on agricultural soils[1]

2.1 Introduction

Overall, there is little knowledge regarding the specific erosion and transport behavior of MP during heavy rainfall events. One could either speculate that MP due to its lower density than mineral soil compartment, is preferentially eroded and transported, or that it behaves more or less like mineral particles as the compactly small number of MP particles immediately interact with heavier mineral particles. As there is little research (Han *et al.*, 2022; Schell *et al.*, 2022) regarding this behavior same analogies to another light weight soil compartment, namely soil organic carbon (SOC) in general and especially particular soil organic carbon (POC) might give fast insights. In general, a large number of soil erosion and soil organic carbon (soil) studies indicate that SOC is preferentially eroded and transported (Franzluebbers and Stuedemann, 2002; Wilken *et al.*, 2017). However, this preferential removal is mostly associated to the fact that SOC is bound to finer mineral particles (fine silt and clay) (Li *et al.*, 2016; Rhoton *et al.*, 2006; Six *et al.*, 2000). In contrast to bulk SOC, the behavior of MP might be more similar to the behavior of particular organic carbon (POC) consisting on more or less degraded, light weight plant residues. Therefore, the also well documented preferential transport of POC with water erosion (Cerro *et al.*, 2014; Martinez-Mena *et al.*, 2000; Martínez-Mena *et al.*, 2012) should be a good indication for a preferential erosion and transport of also light-weight MP.

[1] *This chapter was partly published in Rehm, R., Zeyer, T., Schmidt, A., Fiener, P. (2021): Soil erosion as transport pathway of microplastic from agriculture soils to aquatic ecosystems. Science of the Total Environment, 795, 148774. https://doi.org/10.1016/j.scitotenv.2021.148774.*

The second important aspect which might affect MP erosion and transport is its interaction with organic matter and mineral particles. Recent studies have demonstrated the presence of MPs within soil aggregates, suggesting their potential impact on transport processes (Li *et al.*, 2022a; Chia *et al.*, 2022). However, the extent to which this interaction influences MP transport behavior is still under investigation. Comparisons with the behavior of particulate organic carbon (POC) again could shed light on potential patterns. Similar to POC, there's a conceivable hypothesis that MP concentrations might decrease over time due to binding with soil aggregates (Bertol et al., 2007; Martínez-Mena et al., 2012; Wang et al., 2013a). In agricultural settings, MPs are predominantly found in fiber form, with a higher prevalence in micro-aggregates than macro-aggregates. A study by Zhang and Liu (2018) in agricultural soils revealed that 72% of MPs were present within soil aggregates, primarily as fibers, followed by films and fragments. In contrast, particles seem to have a lesser impact on aggregate stability (Lehmann *et al.*, 2021), underscoring the significance of aggregation in MP retention within the soil matrix.

The interaction of microplastics with different-sized mineral soil particles emerges as a pivotal determinant of MP erosion. This interplay gains further complexity when considering the role of soil organic carbon (SOC). Extensive research has illuminated the intricate relationship between MPs and SOC, resulting in a range of effects (Rillig et al., 2021; Liang et al., 2021; de

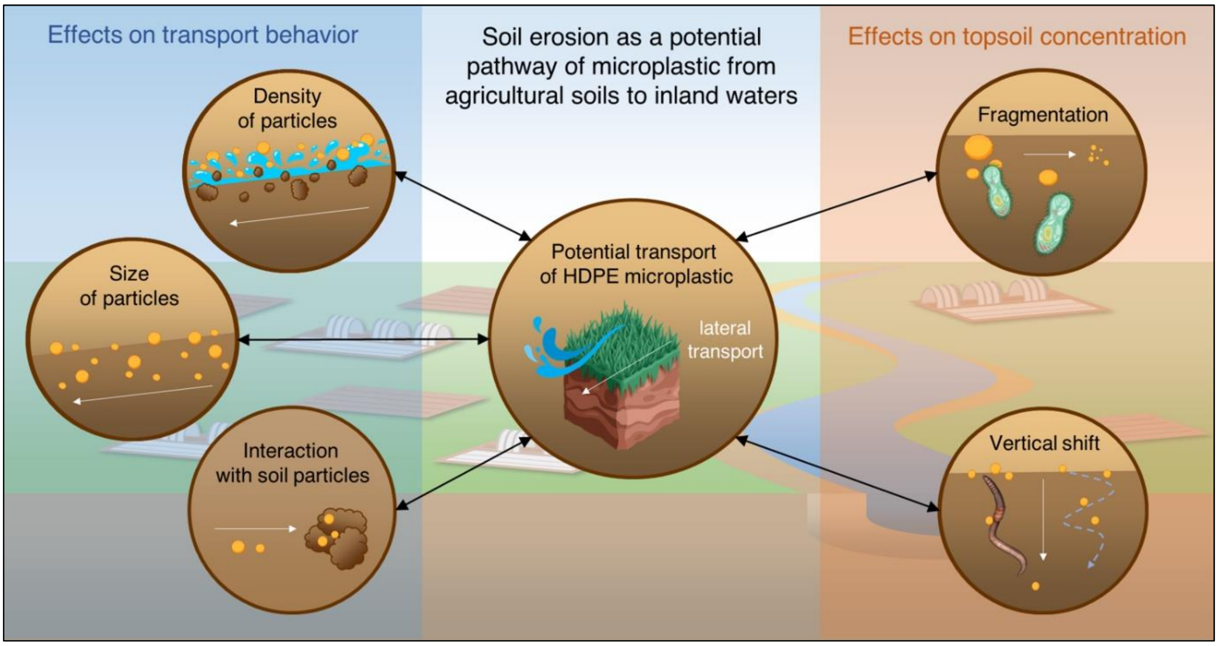

Figure 2: Graphical overview about field experiment and laboratory analysis. In the field experiment, considered and investigated factors related to MP transport behavior and MP topsoil concentration and thus determining effects on the potential transport of HDPE MP particles.

Souza Machado et al., 2018). MP's high carbon content, typically around 80%, contributes to its interaction with soil organic carbon (Zhang and Liu, 2018; Klíč et al., 2022). Laboratory investigations have underscored the propensity of MPs to aggregate both internally (intra-aggregation) and with organic matter (inter-aggregation) within soils (Bastos and De las Nieves, 1994; Bouchard et al., 2013; Walker and Bob, 2001).

In conclusion, the intricate interplay between microplastics, organic matter, and mineral particles significantly shapes the erosion and transport dynamics of microplastics within the soil environment. Understanding these interactions is essential for devising effective strategies to mitigate microplastic contamination and its potential consequences.

The general objective of this experimental chapter was to shed light on the specific behavior of MP during erosion and transport due to heavy rainfall events. The analysis is based on a series of rainfall simulations on MP spiked plots over 1.5 years to also address the changes in MP behavior.

The following hypotheses will be tested: (i) Due to the comparatively low density of plastic particles, preferred erosion leads to an accumulation of MP in the delivered sediments compared to the parent soil contaminated with MP. (ii) The MP enrichment will increase with decreasing MP size, while overall MP enrichment is more pronounced if the MP is in the same or a smaller size range as the mineral soil particles. (iii) Over time, MP delivery will decrease as MP-soil interactions (aggregation and binding to mineral particles) increase, and topsoil MP concentrations will decline due to subsequent erosion events and vertical transport below the plough layer.

2.2 Methods

2.2.1 Setup of field experiment

This study was carried out at two experimental farms representing intensively used arable land in Southern Germany, located in Freising (latitude 48°24´16´´; longitude 11°41´42´´) and Strass (latitude 48°42´28´´; longitude 11°03´05´´). Both sites show distinctively different soil textures, namely a silty loam (16% sand, 59% silt, 25% clay) with somewhat higher mean topsoil organic carbon contents of 1.3% in Freising and a loamy sand (72% sand, 18% silt, 10% clay) with lower mean topsoil organic carbon contents of 0.9% in Strass. At both sites, slopes of 3° were chosen, where two paired rainfall simulation plots were installed in August 2018 to study the lateral transport of HDPE particles in a size of 53-100 µm and 250-300 µm. The choice of MP size was based on the fraction sizes of soil micro- and macro-aggregates (see section 2.5). The plots had a 1.6 m x 4.5 m dimension and were boarded by metal plates reaching 0.15 m deep into the soil. At the downslope end of the plots, a stainless-steel funnel was installed to measure runoff during the experiments (Figure 3). Next to the plots, six stainless-steel cylinders (0.25 m diameter, 0.5 m height) were inserted into the soil for 0.45 m to study the vertical movement of the identical HDPE microplastic particles (Figure 3). To investigate whether the MP used in this study degraded during the 1.5-years experimental phase, MP samples of 250-300 µm HDPE were buried in stainless-steel mesh bags (30 mm x 60 mm, 180 µm mesh size) at a depth of 0.05 m.

The plots and the cylinders were spiked with the two different MP size fractions. Commercially available dry milled HDPE (Schaetti AG; Wallisellen, Switzerland) without additives, at a density of 0.975 g cm^{-3} and a melting point of 127-135 °C was dry-sieved in the laboratory to obtain a fine MP with a diameter of 53-100 µm (MP_f) and a coarse MP with a diameter of 250-300 µm (MP_c) fraction. Mainly HDPE particles were used for pragmatic reasons as their production costs are much lower than low-density polyethylene (LDPE) due to more accessible milling procedures. The size distribution within each MP fraction was determined using a digital microscope (Keyence VHX 6000, Japan) and proofed for normal distribution using QQ plots.

At the beginning of the experimental phase, 10 g m^{-2} of MP_f and 50 g m^{-2} of MP_c was added to all plots. Due to the known properties of the MP, this corresponds to $1.02 \cdot 10^9$ (MP_f) and $40.7 \cdot 10^6$ (MP_c) particles added per plot (Figure 3). To ensure spatial homogeneity within the plots, the same amount of MP was added per m² on the surface using a fine-meshed kitchen strainer. After surface application, the MP was mixed into the upper 10 cm of topsoil by plowing using an electric garden hoe (Hecht 745; Hecht; Germany), followed by a 30 kg lawn roller (Hecht 501; Hecht; Germany). The topsoil of the stainless-steel cylinders was loaded with the same MP concentrations. In contrast to the plots, the upper 5 cm of the topsoil was removed, and MP was mixed into the 3–5 cm layer and covered by 2 cm of MP free topsoil to avoid potential MP loss via splash or wind erosion (Figure 3). At each study site, three of the six cylinders were loaded with MP_f, and the others were loaded with MP_c. The stainless-steel mesh bag nets were filled with 0.2 g of MP_c only.

The topsoil of the plots was loaded with a relatively high MP concentration (MP_f: about 77 mg or $1.1 \cdot 10^6$ particles kg^{-1} soil; MP_c: about 385 mg or 4.35 10^4 particles kg^{-1} soil) for three reasons: (i) Adding MP was only done at the beginning of the experimental period to determine changes in erosion and transport behavior over time. As such, the MP concentrations needed to

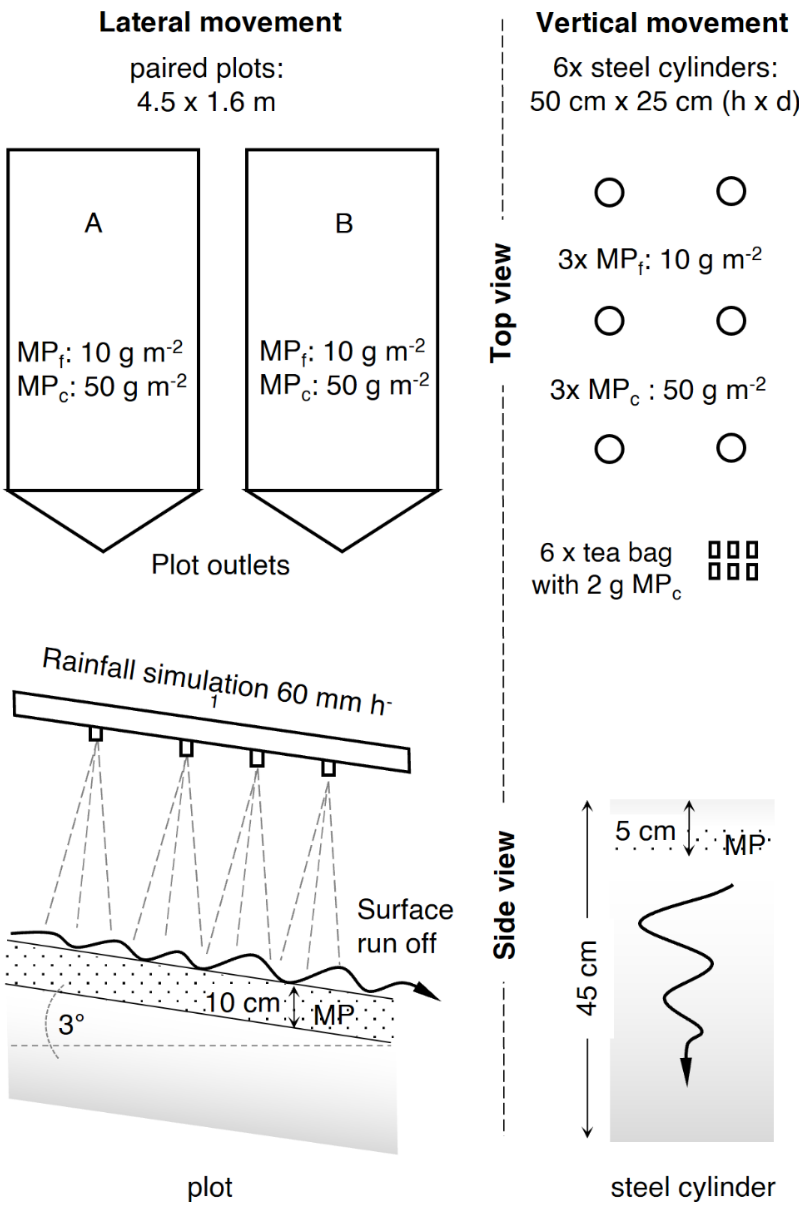

Figure 3: Top and side view of the set up in the field for a 1.5 years experiment for lateral (left side) and vertical (right side) high density polyethylene (HDPE) microplastic (MP) movement observation. For lateral movement, MP (MP_f is fine MP, 53-100 µm; MP_c is coarse MP, 250-300 µm) was added to the topsoil of paired plots (A and B) and treated with a series of rainfall simulations. For vertical movement, stainless-steel cylinders were inserted into the soil to study the vertical movement of MP.

be high enough to ensure that even after a series of rainfall simulations and a potential loss below the plough layer, a substantial amount of MP was left in the topsoil. (ii) The added concentrations were also high enough to avoid potential bias via minimal background concentrations. (iii) The concentrations needed to be above the detection limit of the used MP measurements (see Section 2.7). Even if the used MP concentrations are relatively high, similar concentrations are documented in heavily contaminated soils; e.g., Vollertsen and Hansen (2017) found concentrations of up to 2.4 10^5 MP (10-500 µm) particles kg^{-1} soil in farmland soils in Denmark.

2.2.2 Rainfall simulation – lateral MP fluxes

The rainfall simulation (RS) was carried out with a 'Weihenstephaner Schwenkdüsenregner' after Kainz *et al.* (1992). The rainfall simulator works with four swiveling nozzles (Veejet 80/100), producing a median drop diameter of 1.9 mm, a mean (± standard deviation) kinetic energy of 19.1±2.3 J m^{-2} mm^{-1} rain, and a mean drop falling velocity of 6.8±0.82 m s^{-1} (Auerswald *et al.*, 1992; Kainz *et al.*, 1992). The rainfall simulator was calibrated in four test runs to reach a near-constant rainfall intensity of 60.9±5.28 mm h^{-1}. In contrast, spatial homogeneous rainfall coverage of the plot area was shown using 96 cups placed in a 0.3 m x 0.3 m grid (mean coefficient of variation within the plot for four simulations: 8.66%).

At both test sites, three series of rainfall simulations were carried out in August 2018 (RS1), July 2019 (RS2), and November 2019 (RS3). One RS consisted of a sequence of two 30-minute runs (rainfall intensity 60.9 mm h^{-1}) with a gap of 30 min in between to simulate heavy rain on dry (dry run) and wet (wet run) soil. This rainfall sequence roughly equals a rainfall event with a recurrence interval of 50 to 100 years at both test sites (Junghänel *et al.*, 2010). During each RS run, the surface runoff was collected via the covered plot outlets (Figure 3). From the moment the first runoff reached the plot outlet, a water sample of 2 liters was taken every 2 minutes in a glass bottle with plastic-free screw caps.

Before each RS, the ploughing and rolling procedure, as described in Section 2.1, was repeated to establish the same starting conditions on each plot. After soil preparation, the topsoil was sampled for bulk density and MP concentration. The core method determined the bulk density using standard sharpened steel 100 cm^3 sized Kopecky rings (diameter 57 mm, height 40.5 mm). Before each RS, the MP concentration of each plot was measured three times (à

50 g) from a composite topsoil (< 1 cm) sample taken at ten randomly distributed plot locations to calculate the enrichment ratio (ER) comparing the MP concentration of the topsoil and the sediments of each RS (Eq. 1).

$$ER = \frac{mean\ MP\ concentration\ in\ sediments}{mean\ MP\ concentratin\ in\ topsoil} \qquad \text{(Eq. 1)}$$

ER values > 1 indicate an enrichment, and values < 1 a depletion of MP in the delivered sediment. In addition, soil moisture of the topsoil (< 6 cm) was measured before and 15 min after each run (dry and wet) at ten locations within each plot using a Soil Moisture Sensor (ML3 ThetaProbe, Delta-T devices, UK).

Between RSs the plots were covered with a weed tile fleece (GTM 13013, 80 g m^{-2}, colour: brown, material: Polypropylene) to suppress plant growth. The water permeable fleece was stretched over the plots without surface contact. Hence, the soil was exposed to natural rain amounts but drop energy was minimized to avoid splash erosion, soil crusting and hence minimize potential surface runoff. Moreover, MP loss via wind erosion or photo degradation was avoided.

2.2.3 MP degradation and vertical fluxes

In December 2019, following the last rainfall simulation RS3, the stainless-steel cylinders were excavated (after being buried for 475 days). The soil monoliths were extracted from the cylinders and sliced into 1 cm increments. To avoid overestimation of vertical MP movement potentially resulting from preferential transport along the soil-steel interface, only an inner square section (12 cm x 12 cm) of the cylinders were analysed. It is assumed that the relative vertical loss from the soil layer of MP application (depths: 3-5 cm) in the stainless-steel cylinders represents the potential loss from the plough horizon of the plots (depths: 0-10 cm). This is acceptable as the soil was ploughed several times in the course of the experiments so that the 0-10 cm top layer can be considered to be well-mixed.

The mesh bags were also excavated (after being buried for 475 days) and quantified based on mass and the outer appearance of the MP_c particles (section 2. 5).

2.2.4 Prevention of MP contamination

Potential contact with plastic materials was reduced to a minimum during the experimental process to avoid MP contamination of the samples. Nevertheless, there were potential sources of MP contamination by pre-contamination of the soil during the RS and the lab work, as there were no cleanroom conditions. A 50 g composite sample out of 10 topsoil samples was taken to ensure no pre-contamination of the plots before adding MP. Based on the procedures to extract and determine HDPE microplastic (see Sections 2.5 and 2.6), no pre-contamination with similar MP as the reference material could be found. The sediment and runoff samples were transported, dried (60 °C), and stored in 2-liter glass jars. The only plastics used during lab work were wash bottles (PE) and the density separation unit made of polyvinyl chloride (PVC). For both wash bottles and density separators, colored plastic was used because the added MP particles were white, and their color was one of the criteria used for their detection in the soil and sediments. In addition, the particle sizes of the MP particles used in this study are too large to become airborne in the laboratory. As a result, the chance of airborne contamination with similar particles during laboratory work was minimized as no MP_f and MP_c particles were found in the topsoil before contaminating, general proof that any contamination with similar particles during sample handling is minimal to neglectable. Together with the high MP concentrations used, our method should be sufficient in avoiding remarkable sample contamination.

2.2.5 MP extraction from soil samples

To investigate whether the MP transport is influenced by soil aggregation, the sediment samples were separated into micro- (53-100 µm) and macro-aggregates (250-300 µm) (Figure 4). The applied fractionation scheme follows Six *et al.* (1999), whereas aggregates in dried soil were separated by wet sieving through two sieves (250 and 53 µm). The sediment samples were submerged in distilled water on the 250 µm sieve for 15 minutes. Samples were sieved under distilled water by gently moving the sieve 3 cm vertically 50 times over 2 min through distilled water in a shallow pan. The material remaining on the sieve was added to a first-density separation (DS I). Sediment passing the 250 µm sieve and remaining in the shallow pan was transferred to the 53 µm sieve and repeated. The remaining sediments on the 53 µm sieve were also added to DS I (Figure 4). During DS I, the MP particles, which were not bound to soil particles or aggregates, were separated (MP_{free}). MP and organic material, floats to the surface, while the mineral soil particles and bounded MP (MP_{bound}) particles sink to the bottom.

The density separation was performed using a Sediment-Microplastic-Isolation (SMI) unit (for details see Coppock *et al.*, 2017). The SMI consists of a 30 cm long PVC pipe with a diameter of 5 cm (volume = 0.5 l), which was hot-air bound on a PVC plate. A ball valve was installed in the center of the pipe to separate floating and sinking particles. The SMI was filled with distilled water (density at 20°C: 0.998 g cm^{-3}) as floating media and the respective soil/sediment fraction. After 12 hours, the ball valve was closed, and the water with the floating organic and MP_{free} particles was poured over a 350 µm and, subsequently, a 53 µm stainless steel sieve. Its upper part was extensively washed with distilled water to prevent MP_{free} particles from attaching to the SMI. Sieving through the 350 µm sieve was performed to remove larger organic matter particles, while all MP_{free} particles (MP_c and MP_f) should pass the sieve. Due to the second sieving through 53 µm, all MP_{free} particles remain in the sieve. From the 53 µm sieve, the MP_{free} and left organic material was poured on black colored paper filters with a diameter of 8 cm (Figure 5 a, c). The filter size was adapted to the digital microscope's maximum scanning area (10 x 10 cm) (Keyence VHX 6000, Japan). Black filters improved the color contrast between the filter and white reference MP particles. The MP and organic particles were fixed with hairspray on the still-wet filter. The filters were dried at 30 °C and stored in a flat aluminum can until they were analyzed with the digital microscope.

To destroy the macro- and micro-aggregates and separate MP_{bound} from soil aggregates, a plastic-free magnetic stirrer was added to the under chamber of the SMI. The complete SMI was placed alternately on a magnetic stirrer plate and in an ultrasonic bath (130/300 W, 40 kHz). The dispersing procedure was as follows: 5 min magnetic stirrer, 5 min ultrasonic bath, 5 min magnetic stirrer, 5 min ultrasonic bath, short stirring pulses to stir up the settled sediment again to release trapped MP particles. After the dispersing procedure, the upper chamber of the SMI was refilled with distilled water for the second-density separation DS II (Figure 4). This releases the MP_{bound} particles previously bound to soil particles or incorporated in micro- and macro-aggregates (Figure 4). After DS I, the suspended MP_{bound} and organic material after DS II was filtered and transferred on black filters, fixed with hairspray, and dried at 30 °C. The soil minerals that remained in the lower part of the SMI were dried at 105 ° C. and weighed. After each density separation, the SMI was disassembled, and the individual components were first cleaned in a laboratory dishwater and then rinsed with distilled water.

In contrast to the sediment samples, no aggregate fractionation was applied to the soil samples taken from the plots and the vertical MP movement in the steel cylinders. The dried soil samples (50 g) were wet-sieved through a 2 mm sieve to remove the stone content. The sieved

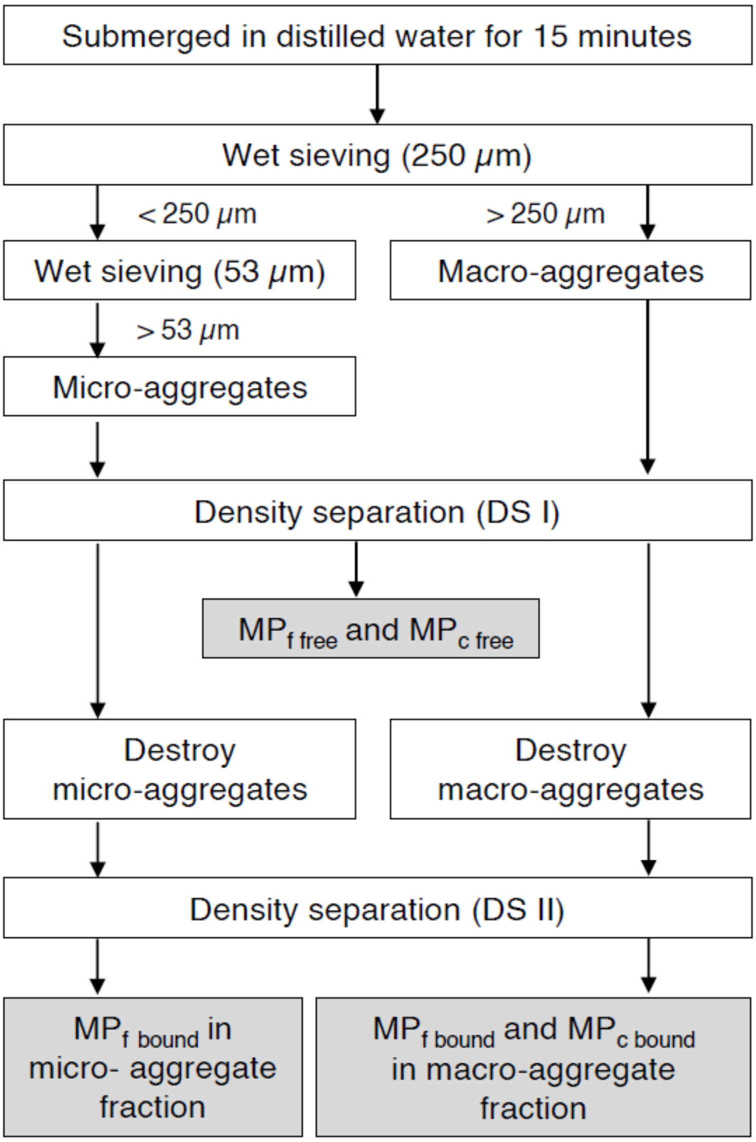

Figure 4: Scheme of the laboratory extraction of high density polyethylene (HDPE) microplastic (MP) from the soil samples, considering the micro- and macro-aggregates (MP_{free} is MP not bound to soil particles and aggregates; MP_{bound} is MP bound to soil particles or aggregates). MP_f is fine MP, 53-100 µm; MP_c is coarse MP, 250-300 µm. Grey boxes represent filters that have been analysed with the digital microscope.

soil samples were mixed in 500 ml beakers filled with about 400 ml distilled water. MP potentially attached to soil aggregates and mineral substances were treated in a magnetic stirrer and ultrasonic bath, the same as the sediment samples described above. After this procedure, a single density separation (DS I) was performed, followed by sieving with a 350 µm and a 53 µm sieve and, lastly, placing on black colored paper filters.

The mesh bags were cleaned from soil and roots and washed with distilled water. Afterward, they were treated three times for 15 min with an ultrasonic bath (130/300 W, 400 kHz) to remove small soil particles from the MP_c. Afterward, the MP_c samples were weighted for potential weight loss and reviewed optically under the digital microscope. Therefore, a precision balance (Excellence Plus XP6, Mettler Toledo, USA; 0.000 mg) was used, and a digital microscope (Keyence VHX-6000, Japan) with a magnification of 200x.

2.2.6 Microscopic MP detection

The black paper filters with MP_{free} and MP_{bound} were analyzed using a digital microscope (Keyence VHX 6000, Japan) with a magnification of 20x, an incident light ring illumination of the 10 cm x 10 cm scan area, and the ability to control the lens height (Z stage control) to adjust the focus automatically. Therefore, even when filters are uneven, sharp images can be produced (Figure 5). A panorama scan function can capture a whole filter in one picture (Figure 5 a, b). The picture was further analyzed with automatic image processing within the microscope to detect and count particles. Because the color of the particles used was known, the extraction of the MP particles could be specified manually according to particular image brightness, hue, and saturation. The white-colored HDPE microplastic was detected in its full size using brightness, saturation, and hue values of 150–250, 5–50, and 0, respectively. The organic matter could be excluded in these settings due to contrast differences (Figure 5 b, d). Contamination of the filters through natural MP pollution of the soil was excluded by a preliminary soil sampling and high start concentration to make the possible error negligibly small (**chapter 2.2.4**).

The microscope outputs a complete size distribution (µm²) of all single detected MP particles. Further data analysis was performed in R (R: Development Core Team, 2021). The area size distribution (µm²) of the used reference MP was known by a pronounced size distribution of the pure MP_f and MP_c via the digital microscope and amounted to 1000 to 10 000 µm² for MP_f and 50 000 to 100 000 µm² for MP_c particles. Therefore, all detected particles < 1000 µm² were excluded. Particles > 10 000 µm² but < 50 000 µm² were interpreted as clustered MP_f. Particles > 100 000 µm² were interpreted as clustered MP_c. The cluster surface area was divided by the median surface area of MP_f or MP_c to estimate the number of single particles within a cluster.

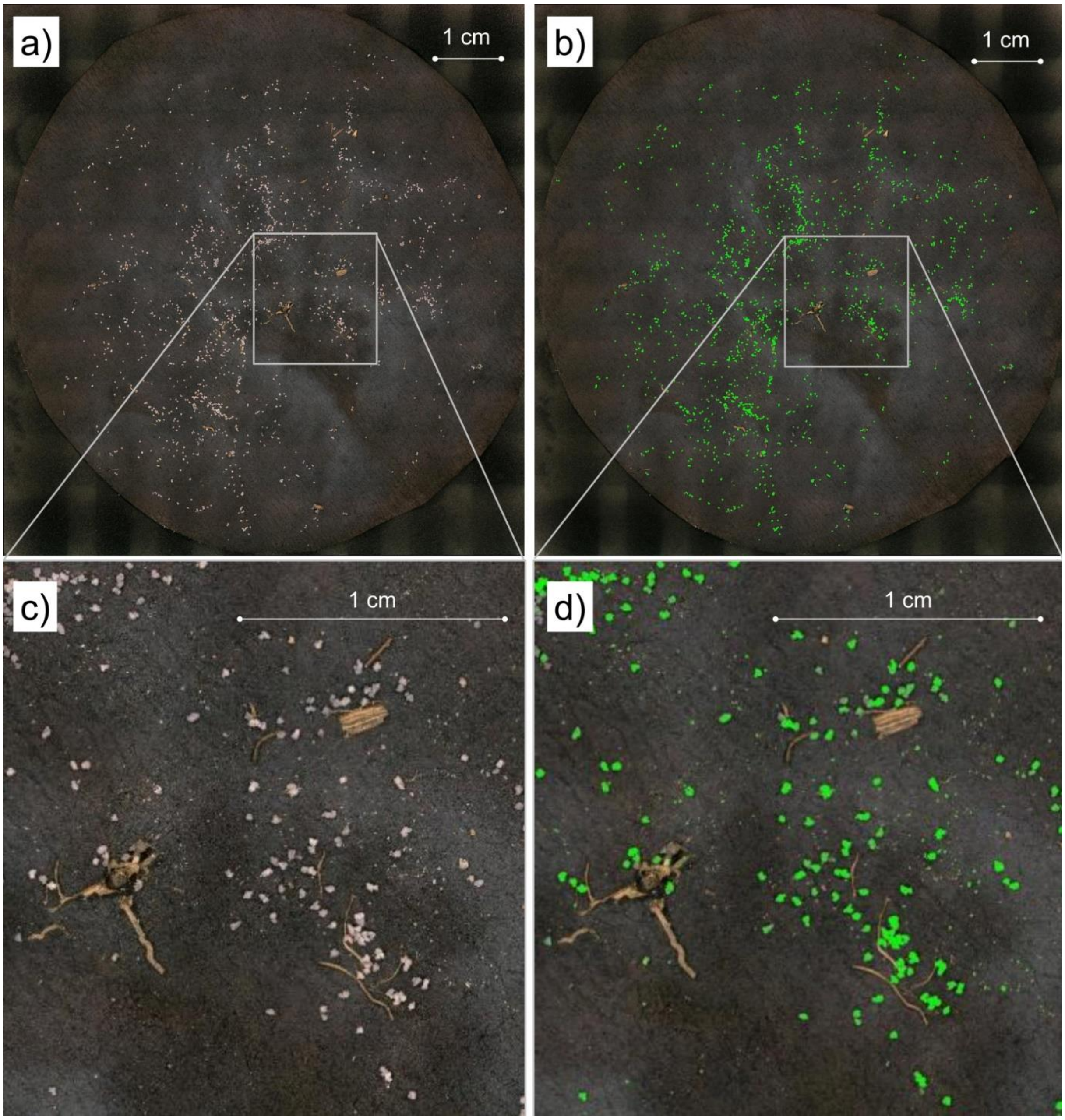

Figure 5: After density separation, high density polyethylene (HDPE) microplastic (MP) and organic matter particles from the sediment samples were filtered out on black filters (a, c). For the detection of the white MP reference particles a digital microscope was used based on color. The white MP particles were captured (green = detected particles), while the brown colored organic material remained undetected (b, d).

2.2.7 Quality control of MP extraction and microscopy detection

To assess the quality of the MP extraction and detection procedure, a pilot study was performed to detect the recovery rates of the reference MP particles. For this reason, soil samples of both field sites were sieved < 2 mm to remove stones and thus imitate eroded sediment samples. Afterwards 20 g soil blanks were taken and mixed with four different MP concentrations I-IV (Table 1). For each concentration, MP size and soil type 3 replicates were prepared. The concentrations between 0.01-0.2 mg MP_f g^{-1} soil and 0.25-5 mg MP_c g^{-1} soil were used to cover the range of the start concentration in the field with 0.08 mg MP_f and 0.38 mg MP_c g^{-1} soil. The mean recovery rate for MP_c reached 85±1.68% (± standard deviation, n =24) and 83±5.43% (n = 24) for MP_f.

Table 1: Used microplastic (MP) concentrations (I-IV) (mg g^{-1} soil) for quality controlof the microplastic extraction method. Each concentration was mixed with 20 g soil and presents 3 replicates in two soil types (total n = 48). MP_f = fine MP, 53-100 µm; MP_c = coarse MP, 250-300 µm.

	Concentration of MP (mg g^{-1} soil)			
	I	II	III	IV
MP_f	0.01	0.02	0.08	0.20
MP_c	0.25	0.50	2.50	5.00

2.2.8 Statistical evaluation

The data preparation of the digital microscope, the evaluation of the MP size distribution, and the test for normal distribution were carried out in R (R: Development Core Team, 2021). The statistical evaluation of the RS runs was carried out with CoStat (CoHort Software, California). All data were normally distributed (after the Pearson K^2 normality test); therefore, mean values were presented per run (dry and wet run separated). To investigate if there were significant differences due to soil type or MP size, a Welch's *t*-test (unequal variances *t*-test) was carried out to test the hypotheses of equal means ($p < 0.05$). The Pearson correlation coefficient was used to assess the correlation between soil moisture and sediment delivery during dry runs, and significance was evaluated at the $p < 0.05$ level. The data variability is given as ± standard deviation if means are provided.

2.3 Results

2.3.1 Surface runoff and sediment delivery

The simulations of heavy rainfall produced runoff coefficients of 0.43 ± 0.19 (n = 12) and 0.60 ± 0.09 (n =12) for dry and wet runs, respectively. Overall, runoff rates were much more variable for the dry runs (Figure 6 a, b) due to the high variability in soil moisture at the beginning of the RSs (Table 2). The wet runs resulted in very similar runoff rates on all plots (Figure 6 a, b), which also corresponds to the very similar starting soil moisture conditions at the beginning of the wet runs (Table 2). Overall, mean runoff volumes during the wet runs did not significantly differ between the loamy sand and silty loam plots. It is also important to note for the interpretation of the data that the two-paired plots (A, B) of each site and simulation produce very similar runoff volumes (Figure 6 a, b).

Table 2: Mean soil moisture conditions measured at ten plot locations before starting the rainfall simulations (RS), 15 min after the dry runs and 15 min after the wet run; within plot moisture, variability is indicated as ± standard deviation.

Soil	RS	Before RS (vol.-%)	After dry run (vol.-%)	After wet run (vol.-%)
Loamy sand	1	9.86 ± 2.35	35.4 ± 3.18	35.4 ± 3.56
	2	18.4 ± 3.69	35.8 ± 1.65	36.1 ± 1.14
	3	34.9 ± 2.94	36.6 ± 2.19	41.0 ± 2.74
Silty loam	1	21.1 ± 4.22	35.6 ± 3.17	36.1 ± 2.92
	2	23.0 ± 6.77	39.7 ± 3.40	40.4 ± 2.84
	3	33.9 ± 3.83	35.4 ± 3.52	37.8 ± 2.50

In general, sediment delivery rates of dry and wet runs follow surface runoff dynamics (Figure 6 c, d). There are noteworthy differences, especially in the case of RS3 on loamy sand and RS2 and RS3 on silty loam, where the highest sediment delivery rates were reached during the dry runs with peaks in sediment concentration up to 253 g min^{-1} at the beginning of surface runoff. In contrast to surface runoff, mean sediment delivery during wet runs differ significantly ($p = 0.03$) between the soils. Silty loam plots were producing, on average, 31% more sediments. The mean sediment delivery rates during wet runs increased from RS1 to RS3 (Figure 6 c, d). In the cases of the silty loam and the loamy sand, the sediment delivery between the first and the last wet run increased by 1.54 and 2.96, respectively. This increase was even more pronounced, including the dry runs rising by a factor of 2.27 (silty loam) and 4.45 (loamy sand), respectively. Sediment delivery during dry runs significantly correlated with soil moisture at the beginning of these simulations ($R^2 = 0.36$; p = 0.04; n = 82).

2.3.2 Microplastic delivery

During the dry runs, the MP concentrations were much more variable as compared to the sediment concentrations (Figure 6). MP concentrations peaked in the first runoff reaching the plot outlets, while runoff was minimal at this stage of the experiment. Total mean delivery rates during dry and wet runs ranged between $3 \pm 1 \cdot 10^4$ (n = 12) and $2.9 \pm 1.1 \cdot 10^4$ MP_c particles min^{-1} (n = 12) and $12 \pm 3.31 \cdot 10^4$ (n = 12) and $13 \pm 3.47 \cdot 10^4$ MP_f particles min^{-1} (n = 12) for the silty loam and loamy sand plots, respectively (Figure 6 e-h).

Table 3: Mean lateral microplastic (MP_f = fine MP, 53-100 µm; MP_c = coarse MP, 250-300 µm) loss after rainfall simulation 1, 2 and 3 (RS1, RS2 and RS3) and mean vertical MP_c and MP_f loss (steel cylinders) relative to MP_c and MP_f amounts added to topsoil at the beginning of the experiment in percent. The lateral loss presents the mean of two plots per soil type (n = 2), vertical loss presents mean ± standard deviation of three pipes per soil type (n = 3).

	Rainfall simulation plots				Steel cylinders
	Lateral loss (%)				Vertical loss (%)
	RS1	RS2	RS3	Total	
MP_c					
silty loam	4.70	4.65	4.01	12.8	1.51 ± 1.67
loamy sand	4.80	3.86	3.75	11.9	2.95 ± 1.17
MP_f					
silty loam	0.79	0.80	0.50	2.08	5.01 ± 1.67
loamy sand	0.84	0.68	0.67	2.18	5.87 ± 3.20

During the wet runs there was no significant difference in MP delivery rates for MP_c and MP_f caused by soil type, while the total sediment delivery of the silty loam plots was significantly (p = 0.03) lager by a factor of 1.91 as compared to the loamy sand plots. In contrast to the increasing sediment delivery between wet runs of RS1 and RS3, MP_c and MP_f delivery decreased over time at both test sites. Overall MP_c was delivered more effectively compared to MP_f (Table 3).

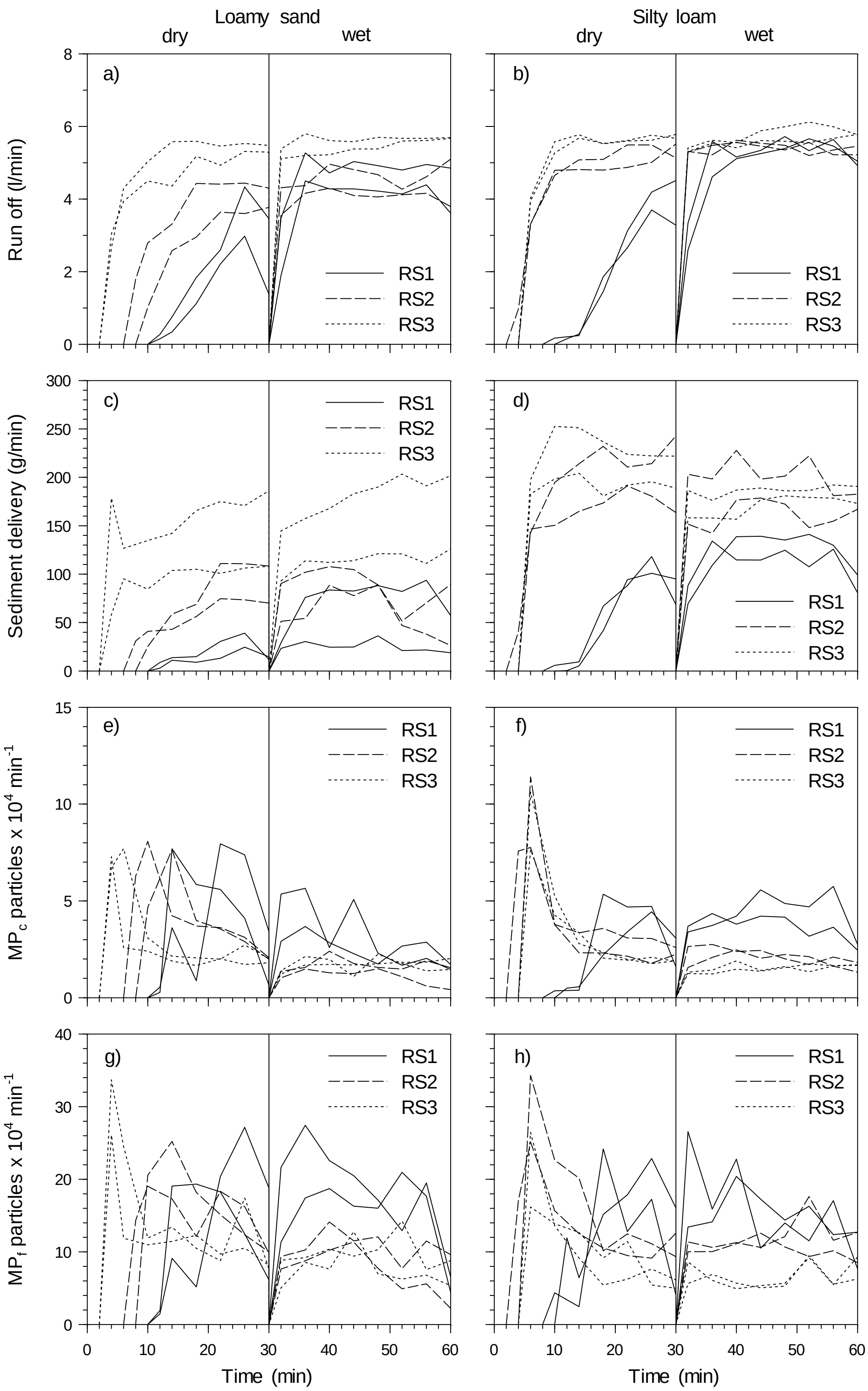

Figure 6: Surface run off (a, b), sediment delivery (c, d), coarse microplastic (MP_c, 250-300 µm) delivery (e, f) and fine microplastic (MP_f, 53-100 µm) delivery (g, h) of the rainfall simulations 1, 2 and 3 (RS1, RS2 and RS3) in both soil types (silty loam and loamy sand). Each simulation is shown with two lines, which represent the two installed plots A and B on each soil type. The X-axis shows the time of a rainfall simulation run (0-30 min dry run, 30-60 min wet run).

2.3.3 Preferential erosion and transport of MP

The rainfall simulations showed a preferential erosion and transport of the MP_c and MP_f with a mean ER of 3.95 ± 3.71 and 3.17 ± 2.58 for all RSs (n = 24), respectively (Figure 7 a, b). Despite the larger mean in case of MP_c, the size of MP did not show any significant difference due to the high variability between all the runs (Figure 7). Even more pronounced differences were found between the two soil types with substantially larger mean MP ER in case of loamy sand (MP_c ER = 5.90 ± 4.38; MP_f ER= 4.72 ± 2.76; n = 12) compared to the mean MP ER of silty loam (MP_c ER = 1.99 ± 0.77; MP_f ER= 1.63 ± 0.99; n = 12). These differences were also not significant due to the high variability of the single sample values (Figure 7). Overall, the enrichment factors for MP_c and MP_f were substantively higher and more variable during dry runs (MP_c ER = 5.45 ± 4.48; MP_f ER = 3.90 ± 2.93; n = 12) compared to the wet runs (MP_c ER = 2.43 ± 1.69; MP_f ER = 2.44 ± 1.94; n = 12) ($p < 0.01$).

The sediment fractionation and two-step density separation (Figure 4) show an increasing interaction between MP and mineral particles over time (Figure 8). However, this interaction was more dominant in the case of $MP_{f\ bound}$ (53.9 ± 12.5% of particles were bound to soil minerals; n = 24) compared to $MP_{c\ bound}$ (26.4 ± 12.9% of particles were bound to soil minerals; n = 24) ($p < 0.01$). Considered across all RSs, no significant difference could be found between the two soil types regarding the interaction between MP_c or MP_f and soil. However, including the chronological sequence from RS1 to RS3, there was a significantly higher interaction between MP_f and soil minerals/aggregates in the silty loam during RS1 ($p = 0.03$) but not during RS2 and RS3. For MP_c, also the MP-soil interaction was more pronounced for the finer soil matrix (silty loam) but only was significant in RS3 ($p = 0.03$). Over time, significant differences disappear in the case of MP_f and arise in the case of MP_c. No significant difference in the interaction between MP_c/MP_f and soil minerals and aggregates were found between the dry and wet runs. During the last simulation (RS3), 38.9 ± 10.2% ($MP_{c\ bound}$; n = 8) and 62.1 ± 13.1% ($MP_{f\ bound}$; n = 8) of the eroded MP was bound to soil particles or aggregates.

2.3.4 Degradability and vertical movement

As expected, no significant degradation of the used HDPE particles was found after being buried in the soil for 475 days. The weight of the MP_c buried slightly increased (mean difference

+ 2.03 ± 1.03%; n = 6) because attached clay particles could not be entirely removed with the ultrasonic treatment. There was also no visible change in particle surface using a microscopy magnification 200x.

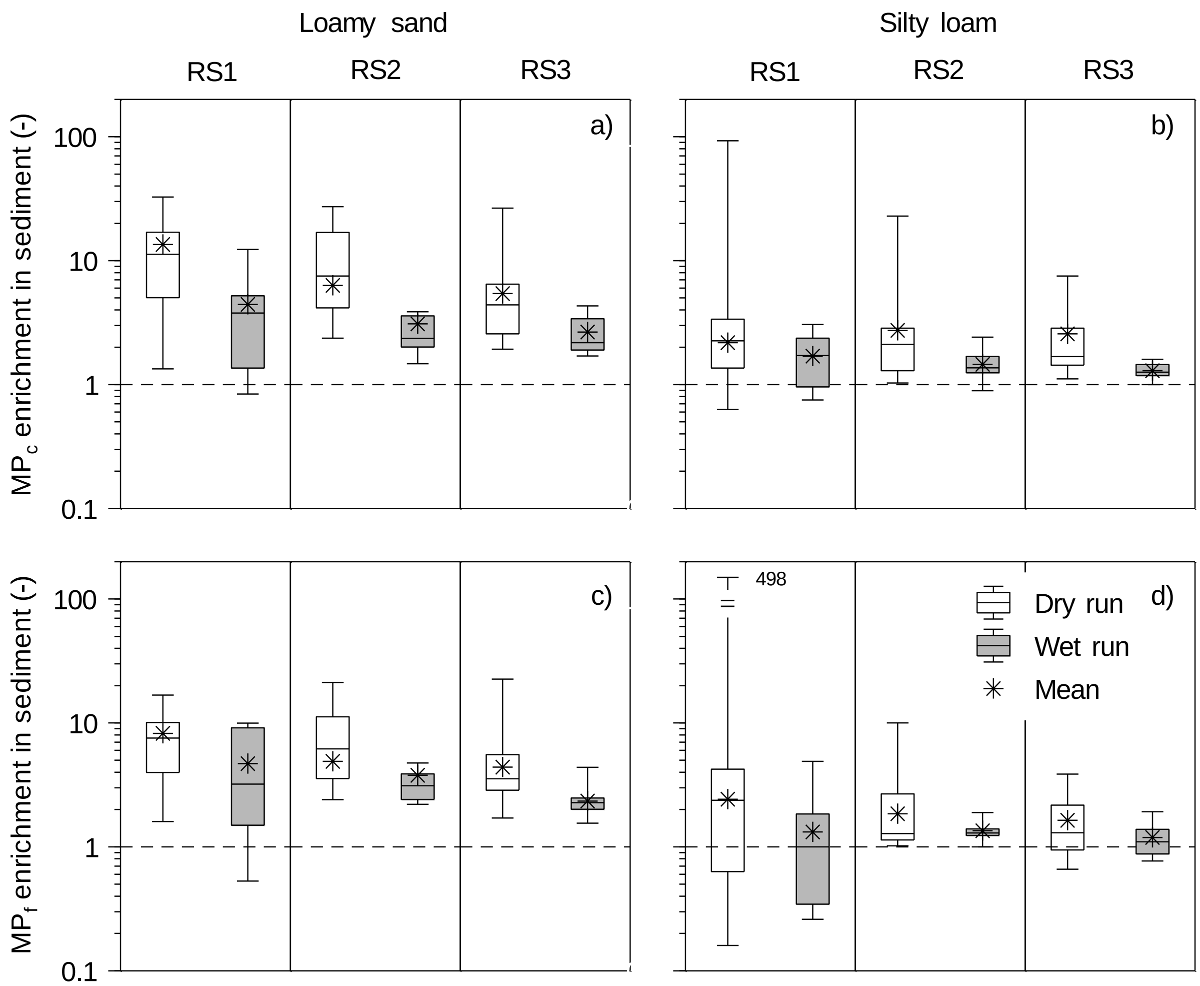

Figure 7: Microplastic (MP) enrichment ratios of coarse MP (MP_c, 250-300 µm) particles (a, b) and fine MP (MP_f, 53-100 µm) particles (c, d) in the delivered sediment of two soil types (loamy sand and silty loam) during the rainfall simulations 1, 2 and 3 (RS1, RS2 and RS3). A preferential erosion of MP is shown by a mean enrichment factor >1 in all simulations. Boxes present all single sample values during the runs and show the median and the 1st and 3rd quartile, whiskers give the minimum and maximum; the stars present mean values per run; the dashed line indicates the relative initial concentration in topsoil < 1 cm (factor 1).

The observation of the vertical MP movement in the stainless steel cylinders showed an average MP_c loss of 1.51 ± 1.67% (n = 3) and 2.95 ± 1.17% (n = 3) to soil depths below the MP application layer (3-5 cm) for silty loam and loamy sand, respectively. This vertical transfer was more pronounced for MP_f, whereas 5.01 ± 1.67% (n = 3) for silt loam and 5.87 ± 3.20% (n = 3) for loamy sand of applied MP was found below a soil depth of 5 cm.

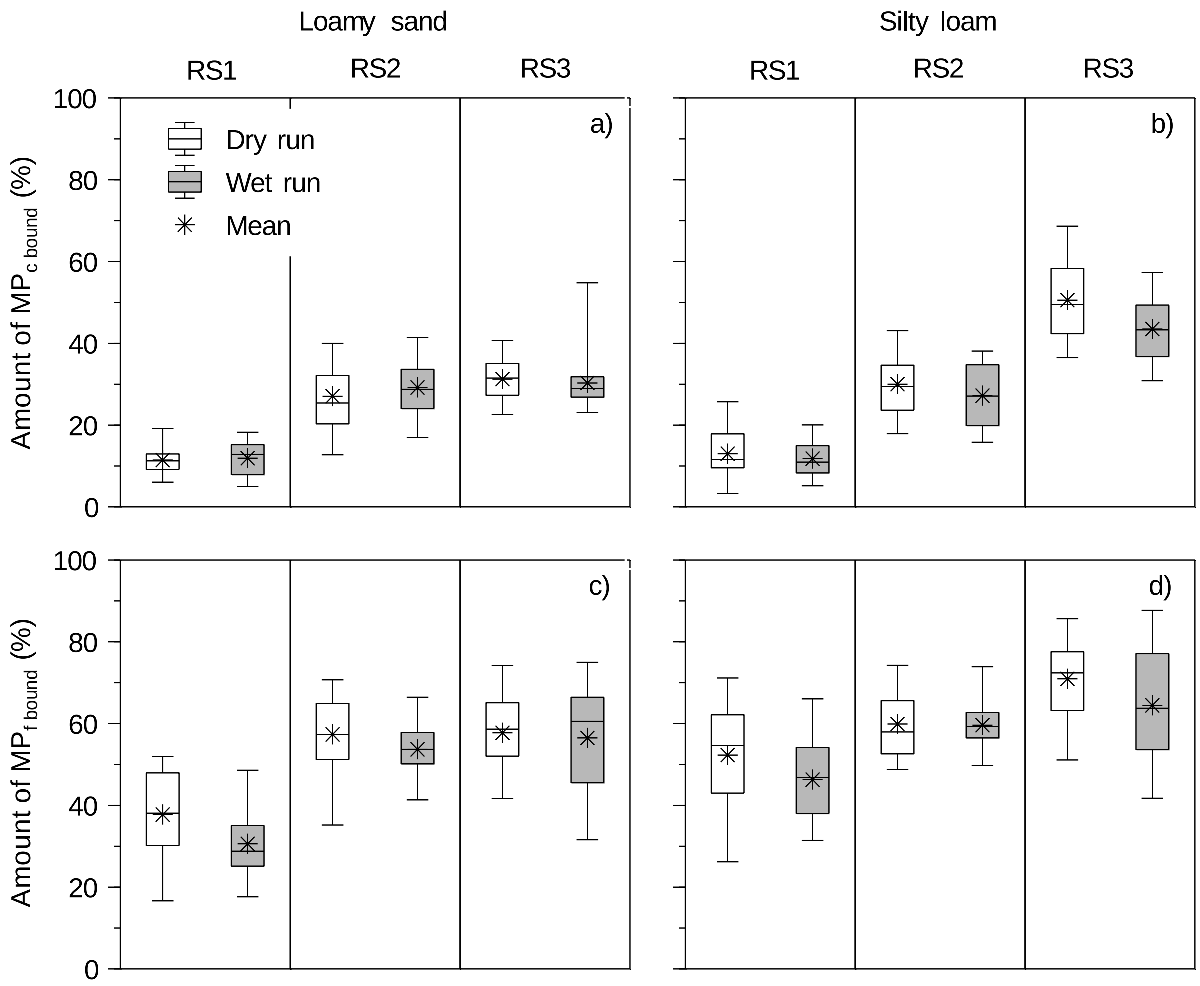

Figure 8: The increasing amount of coarse microplastic ($MP_{c\ bound}$, 250-300 µm) particles (a, b) and fine microplastic ($MP_{f\ bound}$, 53-100 µm) particles (c, d) in the delivered sediment which was bound to soil particles or aggregates during the rainfall simulations 1, 2 and 3 (RS1, RS2 and RS3) on two soil types (loamy sand and silty loam). Boxplots present all single sample values during the rainfall simulation runs and show the median and the 1st and 3rd quartile, whiskers give the minimum and maximum; the stars present mean values per run.

2.4 Discussion

2.4.1 Preferential erosion and transport of MP

In the case of the MP particles tested in the experiment (diameter 53-100 µm and 250 – 300 µm, density 0.957 g cm^{-3}), preferential erosion and transport were found in comparison to the mineral soil, reflected in a mean enrichment ratio > 1 during all RSs (Figure 7). This verifies the hypothesis that less dense materials are preferentially eroded and transported. So far, the results can hardly be compared with other scientific studies that investigated the accumulation of MP in detail during soil erosion. However, Han *et al.* (2022) also found during their MP erosion experiments on vegetation that MP particles < 1 mm and lower density are preferentially eroded and accumulated in the sediment. Also, studies by Schell et al. (2022) on the interaction of MP and soil erosion at the plot level revealed then lower density of MP facilitated transport by surface runoff. Next, the results align with experimental findings on particulate organic matter (POM) erosion (also with densities below 1.0 g cm^{-3}). For example, Martínez-Mena *et al.* (2012), Muller-Nedebock and Chaplot (2015), and Wang *et al.* (2013b) found POM enrichment ratios between 1.37 to 2.9. Recent work on the mobilization of MP by wind erosion also confirmed the preferential MP transport of 212 µm particles with enrichment factors of up to 5 due to the low density (Bullard *et al.*, 2021).

A higher enrichment of MP_c in the delivered sediment can be explained by the less pronounced connection to soil particles. Based on the analysis of MP_{free} and MP_{bound} (Figure 8), it is evident that there are more vital binding forces between the smaller MP_f compared to the coarser MP_c and the mineral soil, a fact which generally can be found for smaller soil particles (He *et al.*, 2008; Hu *et al.*, 2015; Wagner *et al.*, 2007). This association of MP with soil minerals leads to a less pronounced density-induced MP enrichment in delivered sediments, with a more significant effect on MP_f. This is also mirrored in the less pronounced MP enrichment ratios in the case of the silty loam (Figure 7 b, d), even in the case of the first runs where encapsulation in aggregates can be neglected.

A minor enrichment of MP_f in delivered sediments might also indicate aggregation and encapsulation in aggregates, e.g., following repeated dry and wetting cycles, which might play an essential role in the more limited erosion and transport of fine MP particles. By splitting the topsoil (before the RS sequence started) into the different size fractions used for sediment analysis (section 0), a potential depletion of micro- (water-stable) and macro-aggregates (non-water stable) can be assumed in delivered sediments (ER < 1). Whereas, comparing the sediment size fraction < 53 µm with the soil fraction < 53 µm gives some indication that, as expected, non-aggregated particles are preferentially eroded (ER of sediments < 53 µm vs. soil fraction

< 53 µm; 1.73 ± 0.44 and 2.10 ± 1.01 in case of silty loam and loamy sand, respectively). Overall, the data indicate that the MP_f used in this study is more strongly bound to mineral particles and may also encapsulate in water-stable aggregates. The latter effect cannot be found in the case of the MP_c, which might be encapsulated in larger aggregates (> 250 µm), as the larger soil aggregates are less water-stable (Angers *et al.*, 2008; Lal, 2015; Six *et al.*, 1999) and hence are potentially destroyed during erosion and transport.

Overall, aggregation between MP and mineral soil particles of different sizes and properties should substantially affect MP erosion. The general tendency to build aggregates was already shown in earlier laboratory studies indicating both a high intra (with one another) and inter (with organic matter) binding potential of MP in soils (Bastos and De las Nieves, 1994; Bouchard *et al.*, 2013; Walker and Bob, 2001). Zhang and Liu (2018) observed up to 72% of MP particles (> 500 µm) associated with soil aggregates in Nitisol and Gleysol in a semi-humid region of China. Even if such large aggregates might not be stable during erosion processes, their findings confirm the general importance of aggregation in MP stabilization in the soil.

It is also important to note that the ER of MP during erosion and transport was generally more pronounced for the dry runs than the following wet runs. This might have two reasons: (i) Loose, MP_{free} on the soil surface resulting from the tillage of the plots before each RS sequence might be flashed out during the dry runs. This assumption is partly underlined through the highest MP concentrations measured at the beginning of the dry runs (Figure 6 f, h). (ii) There might be some additional binding forces between wet MP and wet mineral particles in the case of the pre-wetted soils in the case of the wet runs. This would be consistent with the findings of several studies indicating stronger binding forces between soil particles under wet conditions (Lehrsch and Jolley, 1992; Luk, 1983; Swanson and Dedrick, 1967).

2.4.2 Change in MP delivery over time

Over the 1.5 years of the experiment, the enrichment ratio in the consecutive rainfall simulations decreased for both particle sizes (Figure 7). This decrease in ER is mirrored in an increase in the amount of $MP_{f\ bound}$ and $MP_{c\ bound}$ in the delivered sediments over time (Figure 8).

The near-constant mass flux of MP over time for all experiments resulted from decreasing MP concentrations in delivered sediments, whereas overall erosion and sediment delivery increased (Figure 6). This increase in sediment delivery over time most likely results by chance from increasing soil moisture between RS1 to RS 3 (Table 2). Interestingly, even under similar initial topsoil moisture conditions (Table 2) and similar surface runoff in the case of the wet runs (Figure 6 a, b), an increase in sediment delivery was still found with a factor of 1.54 (silty loam) and 2.96 (loamy sand) between RS1 and RS3. This might result from increased sediment connectivity (Boardman *et al.*, 2019) during these wet runs due to the more substantial erosion during the dry runs in case of higher initial soil moisture conditions (Figure 6 c, d; Table 2).

While the MP concentrations in delivered sediments decreased over time, the total delivery of MP per (wet) run was more or less stable for all runs and both soils. The near equal MP_c and MP_f delivery in the case of both soils occurred by chance from the combination of lower MP enrichment in the case of silty loam (Figure 7 b, d) and the higher probability of silty soils leading to more erosion and sediment delivery (Figure 6 c, d). However, it is essential to note that the results indicate that even sandy soils, typically not classified as very erodible, might be a substantial MP source.

The MP concentrations in delivered sediments declined over time due to decreasing enrichment caused by MP-soil binding and aggregation and a general reduction of topsoil MP concentrations. The latter has two main reasons: (i) Topsoil MP concentrations declined due to lateral loss with surface runoff and erosion. Compared to the start conditions, there was a total loss (dry and wet runs) of $5.20 \cdot 10^6$ MP_c particles (12.8%) per plot on silty loam (n = 2) and $4.86 \cdot 10^6$ MP_c particles (11.9%) on loamy sand (n = 2) overall RSs (Table 3). This results in an average MP_c loss of 4.25% (on silty loam) and 3.98% (on loamy sand) per heavy rain event. For MP_f, there was a total loss of $21.2 \cdot 10^6$ particles (2.08%) per plot on silty loam (n = 2) and $22.2 \cdot 10^6$ particles (2.18%) on loamy sand (n = 2) (Table 3). This leads to a mean MP_f loss of 0.69% (on silty loam) and 0.73% (on loamy sand) for a single heavy rain event. (ii) Topsoil MP concentrations declined over time due to vertical loss below the plough layer. Vertical MP transport via infiltration and bioturbation is widely discussed and partly observed in earlier studies, e.g., Rillig *et al.* (2017b), whereas especially earthworms play an important role in directly transporting MP via digestion and excretion (Huerta Lwanga *et al.*, 2016; Lwanga *et al.*, 2018) or in preparing preferential flow pathways for MP leaching (Yu *et al.*, 2019). In this study, the added MP_c and MP_f were found up to a depth of 0.42 m in the soil column. The overall loss within 1.5 years from the application horizon (3–5 cm) was 1.51 ± 1.67% and 2.95 ± 1.17%, as well as 5.01 ± 1.67% to 5.87 ± 3.20% (n = 3) for the MP_c and MP_f in the silty loam and loamy sand, respectively. This indicates that larger MP_c particles are dominantly lost via soil erosion in soils prone to erosion. In contrast, for small MP_f particles, erosion is less critical, and these particles are slowly but steadily stored below the plough horizon.

2.4.3 Experimental and environmental behavior

Through the experiment design of this study, the investigated transport behavior of the MP particles relates mainly to processes of interrill erosion. The analyzed enrichment of the MP in the delivered sediment must be seen in connection with the plot size. On a landscape scale, a different extent of enrichment or depletion of MP in delivered sediments might occur due to two opposing processes: (i) Non-selective rill and ephemeral gully erosion may play an essential role at the hillslope to catchment scale leading to a reduction of interill erosion-induced MP enrichment, while (ii) preferential deposition of heavier mineral particles within the landscape should increase the enrichment MP in sediments delivered to surface water bodies. To present knowledge, there are no MP studies available to prove this. However, there is some analogy to the erosion, transport, and deposition processes of soil organic carbon, which also shows enrichment on the plot-to-catchment scale (Bertol *et al.*, 2007; Rhoton *et al.*, 2006).

In this study, HDPE particles of one material in two size fractions were analyzed, so it is the question if the results of this study can be generalized. Other MP particles with similar size, shape, and density should behave similarly during erosion processes. As the most commonly used plastic materials alongside HDPE, different PE types, polypropylene (PP) and polystyrene (PS) (Koutnik et al., 2021), all have lower densities than mineral soils. There should be a similar size-dependent preferential erosion as long as these particles have a similar shape as the tested HDPE. There might be some differences in the case of the heavier polyethylene terephthalate (PET) (density up to 1.67 g cm^{-3}), especially in depositional areas where particles substantially heavier than water might settle.

Although there are many similar properties, the polymers behave differently under certain chemical conditions. For example, the sorption behavior of MP depends on the pH value. While PS is negatively charged with a pH solution below 7.1, the sorption behavior of PE and PP keeps it more stable and damaging up to a pH of 11 (Guo et al., 2018). On the field sides of this study, the pH was 7.1 (silty loam) and 6.9 (loamy sand), which could cause different kinetic sorption to the soil particles due to the type of polymer. PS could be more easily eroded due to a reduced sorption behavior compared to PE (Chen et al., 2021; Guo et al., 2018).

Another important aspect is the shape of the MP. A more conservative erosion and transport behavior would be expected, especially for fibers typically found in sewage sludge (Bayo et al., 2016; Carr et al., 2016; Zubris and Richards, 2005). However, this is somewhat speculative and calls for more research to shed light on erosion as a pathway of MP from soils to surface water bodies.

2.5 Conclusion

In chapter PI the behavior of a known MP contamination in soils during soil erosion was analyzed in a long-term plot experiment. Therefore, a series of controlled rainfall simulations were carried out. In general, HDPE particles of a diameter between 53-100 µm and 250-300 µm were preferentially eroded and transported, leading to a mean enrichment ratio of 3.17 ± 2.58 (n = 12) and 3.95 ± 3.71 (n = 12) in the eroded sediment, respectively.

For both MP fractions, the ER declined from RS1 to RS3. This indicates that MP-soil interactions (binding and aggregation in water-stable aggregates in the case of fine materials) play a crucial role in MP erosion. This is also underlined through the differences in MP concentrations in delivered sediments depending on soil texture, with lower concentrations in more fine-textured soils. The combination of lower MP concentrations in delivered sediments from the finer textured silty loam, with the higher erosion rates of these soils, leads finally to similar MP fluxes from the silty loam and the loamy sand plots. Therefore, it is essential to note that coarse-textured soils, typically not assumed to be very erosive, still exhibit a substantial potential for MP erosion.

Taking lateral MP loss via erosion and vertical redistribution of MP below the plough layer into account indicates that the MP source-sink function strongly depends on MP particle size. In this experiment, MP_c was predominantly lost via erosion-induced lateral transport, while the MP_f was predominantly redistributed below the plough layer and hence protected from further soil erosion.

There still needs to be more knowledge about the behavior of the MP particles during runoff and erosion events to estimate realistic MP inputs from arable land to inland waters. The results of this study allow some first estimates of the transport behavior of HDPE particles during soil erosion and show relevant interactions due to the conduct of MP in agricultural soils. Especially the binding to soil minerals, its incorporation in aggregates, and the vertical transport below the plough layer were important observations to understand the fate of MP in soil. However, the MP/soil interactions must be studied for a more extensive range of MP shapes and chemical properties. Overall, the results of chapter PI indicate that soil erosion can be a substantial source of MP entering neighboring ecosystems.

3 Model-based analysis of erosion-induced MP delivery from arable land to a stream network[2]

3.1 Introduction

Despite the generally known pathways into the soil, knowledge of the spatial distribution and the fate of MP particles, once they enter the soil system is limited (Guo *et al.*, 2020; Hurley and Nizzetto, 2018; Tian *et al.*, 2022). However, the question arises about whether the terrestrial MP sink releases relevant amounts of MP for water bodies via water erosion. If so, the soils, as an MP sink, could represent an important MP source for water bodies. The potential lateral transport via (water) erosion processes might be analyzed using existing modeling techniques. Such approaches face two major challenges: modeling approaches are required, which allow the cumulative loss of MP to adjacent ecosystems to be determined while considering spatial differences in MP contamination and site-specific erosion. Moreover, the long-term change in MP concentrations in the plough layer should be considered, following mixing with subsoil at erosional sites or burial of MP below the plough layer at depositional sites.

In general, there are different water erosion modeling approaches available, ranging from physically-oriented models (e.g. EROSION3D, Schmidt *et al.*, 1999; MCST, Fiener *et al.*, 2008), which might be suitable for dealing with the specific particle size and density of MP during transport in the case of individual erosion events, to conceptual approaches (e.g., WaTEM/SEDEM, (Van Oost *et al.*, 2000; Van Rompaey *et al.*, 2001), which are able to consider long-term cumulative MP soil contamination and the associated long-term soil and MP erosion, transport and deposition. Generally, models of the first type are very parameter and

[2] *This chapter was partly published in Rehm, Raphael, Fiener, P. (2024): Model-based analysis of erosion-induced microplastic delivery from arable land to the stream network of a mesoscale catchment. Soil. https://doi.org/10.5194/soil-10-211-2024.*

input data-intensive and primarily applied in small catchments. One of them is the Water Erosion Prediction Project (WEPP), a physically based distributed-parameter model intended to represent the essential mechanisms controlling water erosion and to estimate spatial distribution of soil loss, well validated at catchment scale (Raclot and Albergel, 2006). Another process-based model to analyze soil erosion dynamics within a catchment is EROSION 3D, simulating the main sub-processes of infiltration of precipitation, discharge generation and detachment of soil particles and transport and deposition of fine soil material (Saggau *et al.*, 2022).

In contrast, the second model type needs less detailed data and is often used for mesoscale catchments (Nunes *et al.*, 2018). WATEM/SEDEM is a sediment delivery model that predicts how much sediment is transported to the river channel on an annual basis (Van Rompaey et al., 2001). It is a spatially distributed model, which means that the landscape is divided into small spatial units or grid cells. It follows the three components soil loss assessment; sediment transport capacity assessment, and sediment routing with the option to simulate both tillage and water erosion (Haregeweyn *et al.*, 2013). Following the requirements outlined above, conceptual, long-term approaches that account for spatial variability in MP soil contamination and erosion processes are more appropriate than process-oriented models to simulate the magnitude of erosion-induced MP delivery to the stream network of mesoscale catchments. As MP loss below the plough layer might be also important in reducing topsoil MP contamination, such a model approach should simulate not only water erosion but also tillage erosion processes leading to a reduction of the MP concentration at erosional sites and MP burial below the plough layer at depositional sites. One of the few models simulating long-term water and tillage erosion in a spatial distribution context that updates the soil properties within the soil profile is the SPEROS-C model, used in the context of the analysis of erosion induced SOC turnover or more general erosion-induced C dynamics (Fiener *et al.*, 2015; Van Oost *et al.*, 2005b). The water and tillage erosion components of the model, originating from the WaTEM/SEDEM model (Van Oost *et al.*, 2000; Van Rompaey *et al.*, 2001), were tested in several micro- and mesoscale catchments (Krasa *et al.*, 2005; Verstraeten and Prosser, 2008).

The general objective of this chapter is to investigate the potential MP transport from arable land to the stream network within a mesoscale catchment. Therefore, the amount of MP applied to the fields between 1950 and 2020 was estimated, considering the significant uncertainties via minimum and maximum values (Figure 9). Moreover, the diffuse MP delivery into the

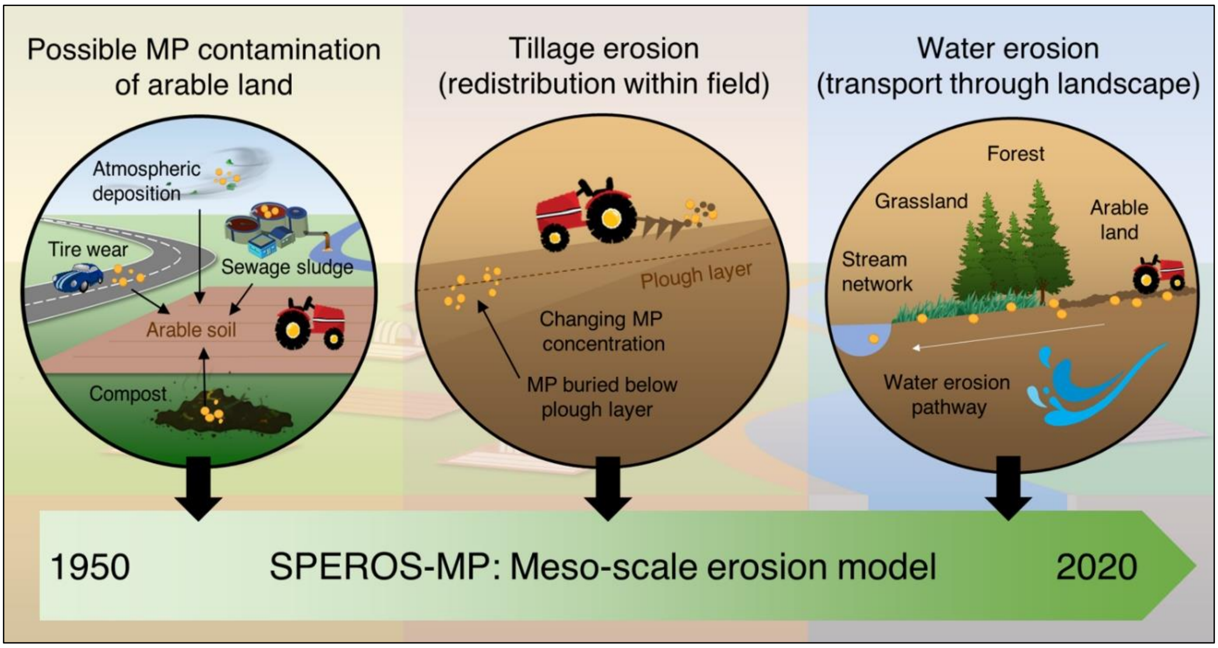

Figure 9: Graphical overview of the model-based analysis. The model-based approach considered and investigated factors related to MP transport through the landscape of a mesoscale river basin.

stream network was determined 100 years into the future for different scenarios of MP contamination of arable land. Therefore, the conceptual soil erosion and carbon transport model SPEROS-C was adapted to SPEROS-MP. A mesoscale river catchment of 400 km² was chosen as a study area, presenting a typical arable region of Southern Germany. The soil erosion-causing MP transport was spatially resolved in a 5 m x 5 m raster grid resolution. Next to water erosion, the model also calculates tillage erosion processes and takes changing MP concentration in the plough layer and buried MP below the plough layer at points of deposition into account (Figure 9).

This chapter will test the following hypotheses: (i) Tillage erosion substantially reduces MP transport via water erosion as it decreases MP concentration at erosional sites and a burial of MP below the plow layer at depositional sites. (ii) Soil erosion of MP leads to a long-term redistribution within the catchment and is a long-term source of MP delivery to water streams. (iii) Targeted or reduced application of MP-contaminating organic fertilizer only slightly affects MP delivery to the stream network as tire wear fluxes dominate this process.

3.2 Methods

3.2.1 Modeled test catchment

The catchment was chosen for two main reasons: (i) it represents an intensively used arable landscape in Southern Germany with hilly terrain and highly productive, loess-burden soils, and (ii) the Bavarian States Office for Environment has monitored discharge and sediment delivery at the outlet since 1968, which allows the erosion component of the model to be tested. The mesoscale Glonn catchment (48°22’N, 11°24’E) covers 400 km², and its altitude ranges from 578 m in its southwest to 447 m a.s.l. At its outlet in the northeast (Figure 10). The region's

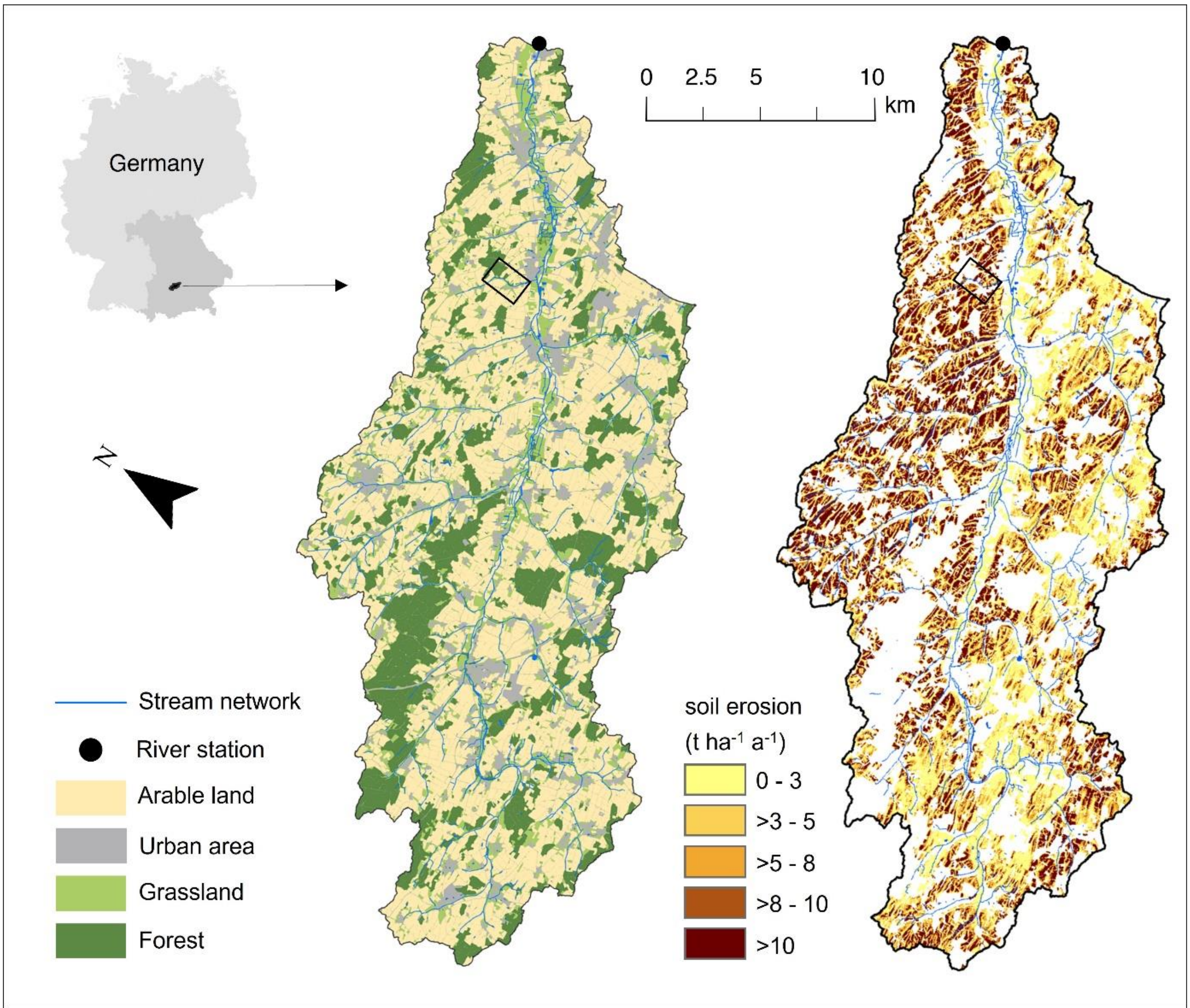

Figure 10: The Glonn catchment (400 km²) representing a typical intensively used arable landscape in Southern Germany with highly erosion rates. The left and right illustration shows the land use and the soil erosion in t ha^{-1} a^{-1} within in the catchment, respectively. The black rectangle in the catchment marks the section of the detailed maps in Fig. 13.

mean annual temperature and precipitation are 7.5°C and 876 mm, respectively, with the most intense summer rainfall events associated with convective rainfall. The hilly landscape (4.7±3.7° main slope) is characterized by loamy Cambisols (WRB, 2015) on the elevated terrain and loamy Gleysols (WRB, 2015) in the valleys. Land cover in this area is dominated by arable land (54%), followed by forest (21%), grassland (14%), and settlements (11%) (Figure 10). The main crops are arranged in a corn-grain rotation. Due to the topography and the soils, an average, long-term soil erosion of 5.9 t ha^{-1} a^{-1} (based on the German version of the Universal Soil Loss Equation ABAG) could be calculated for arable land (LfL, 2023). And 10 t ha^{-1} a^{-1} and more erosion rates can be reached (Figure 10).

3.2.2 MP erosion model

The erosion and MP transport is modeled using a modified version of the spatially distributed water and tillage erosion and carbon (C) turnover model SPEROS-C (Van Oost et al., 2005a; Fiener et al., 2015). The model was initially developed to analyze the long-term effect of soil erosion on landscape-scale carbon balance (e.g. Nadeu *et al.*, 2015). In contrast, the erosion components are based on the erosion and sediment transport model WaTEM/SEDEM, which was extensively tested and validated in different regions of the world (Krasa et al., 2005; Van Oost et al., 2000; Van Rompaey et al., 2001; Verstraeten and Prosser, 2008). The most crucial model components for this study are (i) the water erosion and sediment transport component, (ii) the tillage erosion component, and (iii) the lateral redistribution and the vertical mixing of MP in the soil profile following erosion and deposition processes. As the C turnover component of SPEROS-C was not used in this study, but the MP component was introduced, the model will subsequently be referred to as SPEROS-MP.

Water erosion component: The water erosion component of SPEROS-MP consists of two main parts. First, the erosion potential of each raster cell (5 m x 5 m) is estimated based on the German version of the Universal Soil Loss Equation ABAG (Schwertmann et al., 1987). The major advantage of this well-tested approach is that the input data to calculate the different USLE (ABAG) factors are available from the Bavarian State Office of Agriculture (Bayerische Landesanstalt für Landwirtschaft; LfL) and are regularly updated by the State Office administration. Sediment transport per raster cell, and hence deposition if transport capacity is smaller than sediment influx, is calculated using Eq. 2:

$$T_c = k_{tc} \cdot R \cdot C \cdot K \cdot LS_{2D} \cdot P \qquad \text{(Eq. 2)}$$

Where T_c is the transport capacity (kg m^{-1} a^{-1}), kt_c is the transport coefficient; R (N h^{-1} a^{-1}), C (-), K (kg h m^{-2} N^{-1}) and P (-) are the rainfall erosivity, soil cover, soil erodibility, and management factors of the USLE calculated for Bavaria following the approach of Fiener et al. (2020). LS_{2D} is a grid cell-specific topographic combined slope gradient and lengths factor calculated following Desmet and Govers (1996), using the digital elevation model (DEM) with a resolution of 5 m x 5 m.

Tillage erosion component (k_{til}): The tillage erosion module of SPEROS follows a diffusion-type equation adopted from Govers *et al.* (1994) that derives tillage erosion based on change in topography and management-specific coefficients:

$$Q_{til} = -k_{til} \cdot \Delta h/\Delta x \qquad \text{(Eq. 3)}$$

where Q_{til} is the soil flux in kgm^{-2} yr^{-1}, Δh is the elevation difference in metres, Δx is the horizontal distance in metres, and k_{til} is the tillage transport coefficient in kg m^{-1} yr^{-1}. Consequently, tillage erosion or deposition is most prominent if slope gradient changes, with most soil loss modelled at convexities and most soil accumulation at concavities. Tillage erosion has no direct effect on sediment or MP delivery into the stream network, but over time it modifies the MP concentration in the plough layer of different raster cells, leading to a decrease in MP delivery, because at erosional sites subsoil with little potential MP is mixed into the plough layer, while MP at depositional sites is buried below the plough layer.

MP redistribution and vertical mixing: It is generally assumed that MP enters the soil via its surface and is immediately mixed into the plough layer (upper 0.2 m). The MP input to arable land is estimated at field level (see input estimate below). For MP erosion, the concentration in the plough layer of each 5 m x 5 m raster cell was multiplied by the bulk soil erosion of this raster cell to calculate the MP outflux to neighboring cells. The MP concentration of the transported sediment is analogously used to calculate potential MP deposition. After each year of modeling water and tillage erosion, the soil profile is updated, assuming a tillage operation to a constant depth of 0.2 m. Consequently, MP-free subsoil is mixed into the plough layer at erosional sites, decreasing the topsoil MP concentration. In contrast, at depositional sites, the deposited MP is combined with the underlying old plough layer, creating a new topsoil MP concentration and some MP in the layer no longer reached by the plough. Over the years, this produces a steadily increasing variability in MP concentration within fields and transports MP into soils of other land uses (e.g., grassland and forest sites) assumed not to get other MP inputs.

MP component: The SPEROS-MP model calculates the input of MP in terms of mass (kg/m²) and does not consider the specific properties of MP particles, such as type, shape, density, size, or chemical properties. The model treats MP as a stable component without oxidation and decomposition processes. The C component in the model was designed for degrading soil organic carbon. It was modified to the MP component so the carbon no longer degrades. Thus, the modeled MP behaves like infinitely stable carbon and is considered particulate MP in the size range of the soil matrix. Mass fluxes are modeled; enrichment does not come into play.

Table 4: USLE factors used in SPEROS-MP.

Factors of the USLE	Value	Unit	Comment	Reference
k_{tc}	150	m		*Dlugoß et al. (2012)*
R	0.048 - 0.089	N h^{-1} a^{-1}	Varies annually, **controls the variability of the model**	*DWD (2020)*
C			Does not vary spatially within different land uses	*Brandhuber et al. (2018)*
Arable land	0.15	-		
Forest and grassland	0.004	-		
Urban area	0.001	-		
K	5-55	kg h m^{-2} N^{-1}	Varies spatially depending on soil texture	*Fiener et al. (2020)*
P	0.85	-		*Fiener et al. (2020)*
k_{til}	350	kg m^{-1} a^{-1}		*Van Oost et al. (2006)*

3.2.3 Model data

3.2.3.1 *Soil erosion inputs and parameters*

For the study area, the LfL provided a digital elevation model (DEM, raster 5 m x 5 m), land-use data (field-based), and a soil map (1:25,000), as well as most USLE factors (Table 4). A transport capacity coefficient k_{tc} of 150 m was used as the optimum value for cropland for a 5 m x 5 m grid resolution (Dlugoß *et al.*, 2012). For the sake of simplicity and because long-term data on soil management was missing, only the rainfall erosivity (*R* factor of the USLE) was calculated every year, following the approach of Schwertmann *et al.* (1987), using the mean annual precipitation N (mm/a). N was available in a 1 km x 1 km grid resolution from the German Weather Service (DWD, 2020). A corn-grain crop rotation (with a mixture of small grain crops and a proportion of row crops of 25%) was assumed to be typically found in the region. It used the USLE calculator Brandhuber et al. (2018) developed, resulting in a *C* factor of 0.15, which is constantly used for all arable land in the catchment (Table 4). For forest and grassland, a low *C* factor of 0.004 and for settlements, a *C* factor of 0.001, was applied (Brandhuber *et al.*, 2018). A *K* factor map was provided by the LfL (derived from the soil properties given by the soil overview map of Bavaria at a scale of 1:25,000) based on the calculation in Schwertmann *et al.* (1987). The LS_{2D} factor was derived from the 5 m x 5 m DEM, following the approach of Desmet and Govers (1996). Assuming some soil conservation methods to be in place, e.g., partial contour ploughing, the *P* factor was set to 0.85 (Fiener *et al.*, 2020). The tillage transport coefficient k_{til} depends on the tillage implementation, tillage speed, tillage depths, bulk density, texture, and soil moisture at the time of tillage (Van Oost *et al.*, 2006). For the Glonn catchment, a constant k_{til} value of 350 kg m^{-1} yr^{-1} (Table 4) was determined for another loess-dominated region within Germany by Wilken et al. (2020).

3.2.3.2 MP contamination of soils

Because sampling and sample analysis would be highly time-consuming and costly, it is impossible to determine the actual MP concentrations in a 390 km² catchment where estimates from MP inputs suggest considerable spatial heterogeneity. Hence, the potential soil-MP contamination must be estimated from different sources' potential MP input. As soil erosion is dominant on arable land, an exclusive input estimate was performed for arable land. However, it is essential to emphasize that most estimates are based on regional means for the whole of Bavaria and that any calculations of the MP accumulated in the catchment soils since the 1950s are based on several assumptions and simplifications, resulting in large uncertainties. To account for these uncertainties in the model outputs and arrive at a robust indication of the potential contribution of soil erosion as a source of MP in the stream network, the potential yearly mean was estimated as minimum and maximum soil-MP input for each input pathway (see below) and did separate and combined modeling runs for the different contamination estimates. As mentioned earlier, mean MP inputs from sewage sludge, compost, and atmospheric deposition were estimated from means for all arable land in Bavaria. In contrast, the input of tire wear was derived using catchment-specific road data and road-specific traffic data as far as possible.

These represent the typical sources in the agricultural landscape of Southern Germany, along with MP, applicable for SPEROS-MP. Potential MP input pathways, for instance, from plastic used in agricultural management (e.g., mulch films) or littering, were not considered for two reasons. (i) In Bavaria, mulch films are primarily associated with particular regions where specific crops or vegetables are grown, especially asparagus. For our test site, this is not the case, and using the average area of mulch cover in Bavaria to estimate the potential mean input in the catchment would have resulted in very small input amounts, not comparable with other regions in the world, which mulch films can be a significant source of MP (Li *et al.*, 2022c; Liu *et al.*, 2014). (ii) Larger macroplastic fragments from mulch films and littering should only be transported with severe rill and ephemeral gully erosion, which are not the dominant erosion processes in the region.

3.2.3.2.1 Sewage sludge and compost

Sewage sludge and compost as soil amendments (organic fertilizers) contain different quantities of microplastic and small macroplastic in the case of compost. The first step was to estimate the amount of sewage sludge and compost applied on Bavarian agricultural soils since 1950. Bavarian waste reports (LfU, 1990-2020) allowed us to determine the mean annual input on arable land from 1990–2020. Historical application rates of compost were selected based on a linear relationship between application rates and population numbers between 1990 and 2020 (the variability was continued at random) (LfStaD, 2022) (Figure 10 b, c). In the case of sewage sludge, the number of residents connected to the sewage system was considered (Schleypen, 2017). The gaps between historical individual values were interpolated. The development of plant technology and the use of sewage sludge between 1945 and 1990 were considered, as described by Schleypen (2017). While compost was constantly used as an organic fertilizer, the use of sewage sludge was quite variable over time (Figure 10 c). From 1970 onwards, new wastewater treatment plant (WWTP) technology meant that the sewage sludge was no longer allowed to accumulate dry but rather as wet sludge (Schleypen, 2017). This led to a sharp drop in the use of sewage sludge as a fertilizer, and it was not until the 1990s that it became popular again (Figure 10 c). Since 2017, sewage sludge has been banned mainly in Bavaria (Schleypen, 2017).

The second step was to estimate the MP concentrations in sewage sludge and compost. To do this, current literature values were used to estimate the MP concentrations for 2020. Minimum, mean, and maximum MP concentration were always considered based on the range of values from the literature. For sewage sludge, data from Edo et al. (2020) were used; this is, to present knowledge, one of the few studies providing a mass balance of MP for a WWTP by specifying the total wastewater volume and the total amount of sewage sludge per day. The sum of the MP particles filtered out (contained in sewage sludge), and the delivered MP from the WWTP effluent results in the number of MP detected in the WWTP input. Edo et al. (2020) consider size classes 25–104 µm, 104–375 µm and 375–5000 µm, and their data show that 95% of the MP in the WWTP is retained in the sewage sludge, which is consistent with other publications giving ranges of 93–98% (Habib et al., 2020; Tang and Hadibarata, 2021; Unice et al., 2019). For compost, data from Braun et al. (2021) were used, which contain all essential data on MP in compost from Germany. They examined MP in size ranges < 1000 µm, 1000–5000 µm and > 5000 µm. Macroplastics are also included for the mass calculation of the MP in compost.

Both publications, Edo et al. (2020) and Braun et al. (2021) provide information on the size distribution of the detected MP particles. This enabled the most accurate conversion possible between mass and particle number. The particle size, size distribution, and shape were considered when converting. While a spherical shape was assumed for sewage sludge, for compost, the most realistic possible volume for each detected particle was calculated (individual dimensions have been provided by the authors of Braun et al. (2021). Based on the type of plastic detected, an average density of 1 was assumed for all particles. An average MP load of 1.14 g MP kg^{-1} dry matter of sewage sludge (min.: 0.42 g, max.: 4.04 g) and 0.15 g MP kg^{-1} dry matter of compost (min.: 0.05 g, max.: 1.36 g) was assumed.

Based on the known amounts of sewage sludge and compost applied, it was possible to calculate the corresponding amount of MP on Bavarian agricultural soils (kg m^{-2}). When calculating the MP concentration back to 1950, the amount of plastics produced in Germany was considered for each year, as the MP concentration depends on the level of production (Figure 10 a, b). The annual amount of MP was then evenly distributed across all agricultural fields in Bavaria since spatial allocation within the study area was impossible.

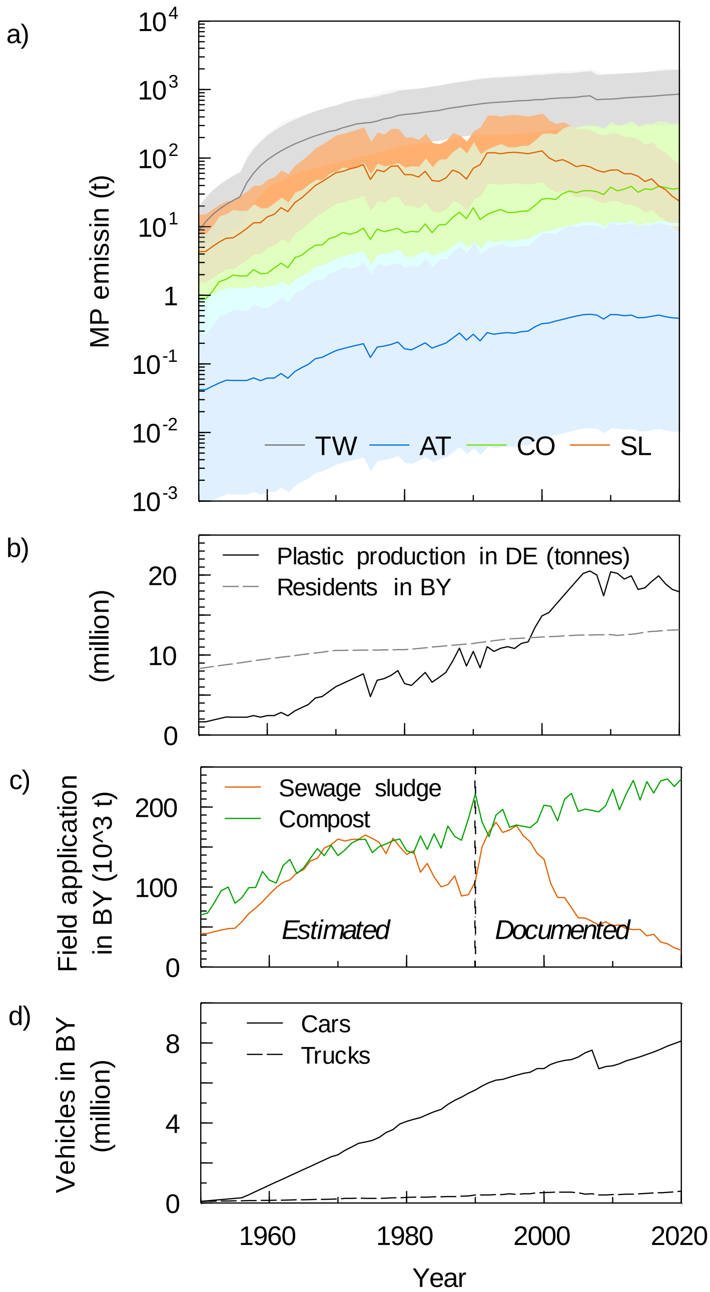

Figure 11: a) The MP emissions for arable land in Bavaria from the different sources, tire wear (TW), sewage sludge (SL), compost (CO) and atmospheric deposition (AT), from 1950 to 2020. b) The development of plastics production in Germany and the population of Bavaria since 1950. c) Amount of application of sewage sludge and compost as fertilizer on Bavarian arable land. d) The number of registered cars and trucks in Bavaria since 1950.

Between 1950 and 2020, 7.26 million tonnes of sewage sludge and 11.7 million tonnes of compost were added as organic fertilizer on agricultural fields in Bavaria. Hence it can be estimated that 4090 t (min.: 1510 t, max.: 14 500 t) and 1110 t (min.: 358 t, max.: 10 100 t) of MP from sewage sludge and compost, respectively, were dumped on arable land in Bavaria. From that, an average input on the arable land in the Glonn River catchment of 42 100 kg MP from sewage sludge (min.: 15 500 kg, max.: 149 000 kg) and 11 500 kg MP from compost (min.: 3660 kg, max.: 104 000 kg) was calculated. For the arable land in the Glonn River catchment, this means an average annual MP application of 240 kg MP from sewage sludge (min.: 90 kg, max.: 860 kg) and 370 kg from compost (min.: 120 kg, max.: 3390 kg) in 2020 (Table 5). This results in a current entry rate of 1.14 mg MP m^{-2} a^{-1} (min.: 0.42 mg, 4.04 mg) from sewage sludge and 1.75 mg MP m^{-2} a^{-1} (min.: 0.56 mg, max.: 15.8 mg) from compost.

Table 5: MP inputs into arable soils within the test catchment, separated by different sources. All values are listed for the modelled time span 1950–2020 and separately for the year 2020.

	Tire wear	Sewage sludge	Compost	Atmospheric deposition	Unit
		1950–2020			
MP application to arable land	**120 256**	**42 100**	**11 500**	**186**	**kg**
min	43 969	15 500	3660	4.30	
max	288 614	14 9000	104 000	4200	
		2020			
MP application to arable land	**3109**	**240**	**370**	**4.76**	**kg**
min	1137	90	120	0.11	
max	7462	860	3390	107	
MP application rate	**19.67**	**1.14**	**1.75**	**0.02**	**mg MP m^{-2} a^{-1}**
min	7.19	0.43	0.56	0.0005	
max	47.2	4.08	16.03	0.45	

3.2.3.2.2 Atmospheric deposition

For the atmospheric deposition of MP, the data from four bulk deposition measurements (precipitation and dust deposition) in Bavaria (Witzig et al., 2021) were combined with the development of plastics production in Germany since the 1950s. As no better data were available it was assumed that the measured atmospheric deposition of MP in 2020 is proportional to German plastics production in general (Figure 10 a). This results in a mean cumulative atmospheric MP input on arable land in Bavaria of 18 tons of MP (min.: 0.41 t, max.: 407 t). Between

1950 and 2020, the arable land in the Glonn River catchment was loaded with a total of 186 kg of MP (min.: 4.20 kg, max.: 4200 kg). For 2020 an average annual MP immission of 4.76 kg (min.: 0.11 kg, max.: 107 kg) or 0.02 mg MP m^{-2} a^{-1} (min.: 0.0005 mg, max.: 0.5 mg) via atmospheric deposition was calculated (Table 5).

3.2.3.2.3 Tire wear

To determine the tire wear particle input in the Glonn catchment, existing traffic counting data from 2005, 2010, and 2015 were used for the main roads (motorways, federal roads, state roads, and district roads) available from the Bavarian Road Information System (BAYSIS, 2015). Traffic volume for more minor roads (except farm roads) in rural areas was derived from a 1 km x 1 km population density grid following Gehrke et al. (2021). Based on these data, the traffic volume (number of vehicles per km) for each paved road in the Glonn catchment could be estimated for 2005, 2010, and 2015. This was done separately for passenger cars (cars), heavy-duty vehicles (trucks), and motorcycles. For all other years, the traffic volume (number of vehicles per km) per road was linearly extrapolated based on the traffic volume and the number of registered cars and trucks in Bavaria (LfStaD, 2022) (Figure 10 d). No emissions from unpaved roads and agricultural machinery were considered.

Minimum, medium, and maximum scenario were considered based on the quantity of released tire particles specified in the literature. A mean tire wear emission factor of 90 mg TW km-1 (min.: 53 mg, max.: 200 mg) was assumed for cars (a motorcycle represents half a car) and 700 mg TW km-1 (min.: 105 mg, max.: $1{,}7 \cdot 10^3$ mg) for trucks, based on the reviews of Hillenbrand et al. (2005) and Wagner et al. (2018). Based on the length (km) and traffic volume (number of cars, motorbikes, and trucks), the released TW was calculated for each section of the road.

The transport of TW from roads into the surrounding soil systems was estimated based on literature information, assuming that the TW concentration exponentially declines with increasing distance from the road (Figure 12). However, only identify one study could be identified (Müller et al., 2022) that directly measured TW contamination of soils with distance from the road, while most other studies (Motto et al., 1970; Werkenthin et al., 2014; Wheeler and Rolfe, 1979; Wik and Dave, 2009) used chemical markers and the distance from the road to estimate TW distribution. Median behavior was calculated from all these different approaches (Figure 12). As the modeling is performed in a 5 m x 5 m grid, the land-use map may not show all grass or vegetation strips often found along roads, which might lead to overestimating TW input to arable land. Hence, a conservative estimate was used, assuming that at least a 3 m wide grass strip can be found on both sides of any road. Consequently, about 85% of the TW produced on any route (Fig. 12) cannot reach arable fields. The remaining 15% of TW that could potentially get arable land mostly settles within a 50 m distance from the road, whereas background MP concentrations are reached in about 130 m distance (Figure 12).

Compared to the other MP sources considered (sewage sludge, compost, and atmospheric deposition), the estimate for TW was calculated on a field-by-field basis. A land-use map was overlaid on the road network to identify all agricultural fields affected by road-borne TW deposits within a distance of 130 m. For each lot, the area share of the associated road section and the distance to the road were considered when calculating the TW load. The only limitation is that on fields affected by TW, in the model, the amount of TW was distributed evenly over the entire area and not just on the concerned field section near the road (within 130 m).

Between 1950 and 2020, $120*10^3$ kg of tire wear (min.: $44*10^3$ kg, max.: $289*10^3$ kg) ended up on arable land in the Glonn catchment (Table 5). In 2020 the average annual MP application amounted to $3.1*10^3$ kg of tire wear (min.: $1.1*10^3$ kg, max.: $7.5*10^3$ kg) (Table 5). The load from TW in 2020 can reach maximum concentrations of $2.5*10^3$ mg TW m^{-2} a^{-1} on roads with

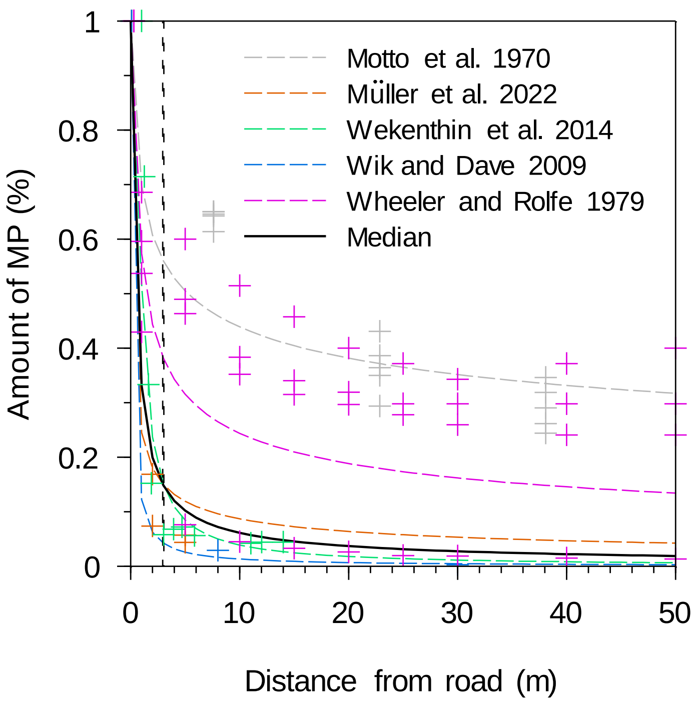

Figure 12: The distribution of tire wear in the soil relative to the distance from the road. Literature values are based on direct detection of tire wear (Müller et al. 2022) or on the estimated concentrations of tire wear particles based on chemical markers (Motto et al. 1970, Wheeler and Dave 2009; Wik and Dave 2009; Wekenthin et al. 2014). The markers show the individual values, the dashed lines show the mean of the respective reference. The black line represents the median of all literature values used for modelling in this study.

heavy traffic use; the average over all affected fields in the Glonn catchment area is 19.7 mg TW m^{-2} a^{-1} (Table 5).

3.2.4 Model testing

It is impossible to validate the modeled MP delivery to the stream network against measured MP loads, as this would call for continuous monitoring of MP delivery for several years at least. However, the modeled sediment delivery can be tested against measured data from the Bavarian State Office for Environment (Bayerisches Landesamt für Umwelt, LfU), which operated a discharge and sediment monitoring gauge in Hohenkammer (Figure 10) between 1968 and 2020. The daily shot was derived from continuous runoff depth measurements in combination with a stage-discharge rating curve at this gauge with a defined river cross-section. In contrast, the stationarity of this rating curve at the measuring cross-section was randomly checked once or twice every year. At the gauging station, a weekly water sample was collected (1968–2020), and its sediment concentration was determined in the laboratory. From 2011 onwards, a turbidity probe (Solitax ts-line; Hach Lange GmbH; Germany) was installed and regularly calibrated against the samples taken by hand. Based on the continuous discharge and the weekly to continuous sediment concentration measurements, the LfU provided daily sediment load data from 1968 to 2020, aggregating to yearly values for this study.

3.2.5 Modelled scenarios

Apart from modelling and analyzing the MP delivery to the stream network via the erosion pathway from 1950 to 2020, three scenarios (S1 to S3) were modeled to discuss potential future paths up to 2100.

Scenario S1 – business-as-usual scenario: In this scenario, it is assumed that the MP input to arable land continues until 2100 with the same input rates estimated for 2020. Given the ongoing increase in plastics production (Chia et al., 2021; Lwanga et al., 2022), this may even be a conservative estimate of a business-as-usual scenario pathway.

Scenario S2 – spatially targeted application of soil amendments: This scenario addresses two aspects. (i) A potential reduction of MP delivery to the stream network due to a targeted application of soil amendments, keeping a distance of at least 100 m from the stream network in the case of compost and sewage sludge application. (ii) More generally illustrating the sensitivity of MP delivery to the stream network in the case of non-homogenous MP inputs in the catchment. For the latter, soil amendments were solely applied near the stream network (max distance 100 m).

Scenario S3 – stop MP input: This scenario is set up to determine how soils function as a long-term source of MP about soil erosion, assuming the MP applied before 2020 remains stable in the soil until 2100. Therefore, a potential decline in MP concentration in the plough layer either results from a lateral loss to neighboring land uses (grassland or forest) or the stream network or is buried below the plough layer due to deposition processes (here, deposition due to water and tillage erosion).

3.3 Results

3.3.1 Sediment delivery

Without any calibration, the model satisfactorily reproduced the measured long-term mean sediment delivery of the Glonn outlet (Figure 13). The modeled sediment deliveries resulted in a mean of 145±18 kg ha^{-1}; the measured mean contained 149±63 kg ha^{-1} kg ha^{-1} (Figure 13). The model could not capture the total variability in the measured yearly sediment delivery (R^2 = 0.51; Figure 13). It underestimates years with high erosion rates while overestimating years with low erosion rates. However, the model performance (especially in reproducing the long-

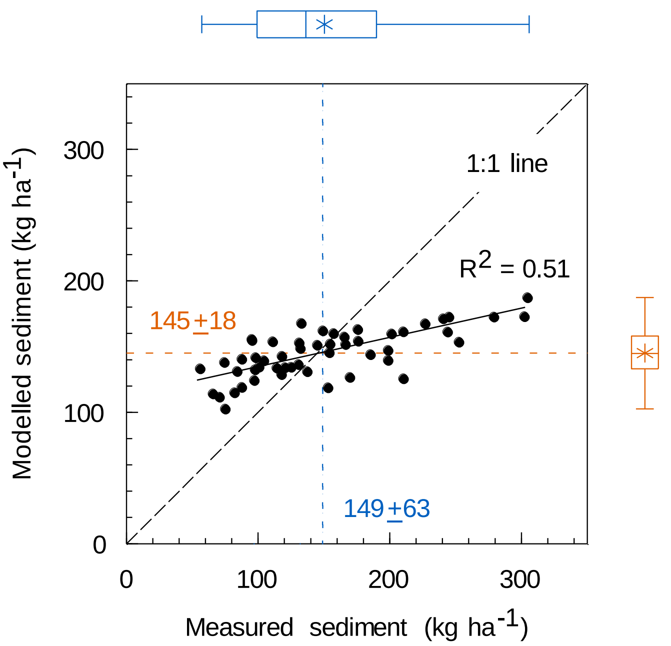

Figure 13: Measured and modelled sediment delivery (1968 to 2020) at the outlet of the Glonn catchment. The blue and orange lines represent the measured and modelled means, respectively. The boxplots show the variability of the data. They show the median (line) and mean (star) and the 1st and 3rd quartile, whiskers give the minimum and maximum.

term mean) gives a solid basis for modeling lateral MP fluxes due to erosion processes. Here it is important to note that the modeling approach aims to estimate the magnitude of the MP erosion transport pathway, which was not analyzed in earlier studies, and that the estimated MP inputs contribute significantly to model uncertainty.

3.3.2 MP erosion and delivery to stream network

The constantly rising MP input to arable soils from different sources (Figure 10) since 1950 is reflected in the steadily increasing, erosion-induced MP delivery into the stream network (Figure 14 a). Due to the long-term fertilization of arable land with sewage sludge, on average, 0.51 kg of MP a^{-1} entered the Glonn stream network in 2020 (Table 6). For compost, it is 0.77 kg of MP a^{-1}, with 0.01 kg of MP a^{-1} from atmospheric deposition (Table 6, Figure 14 a). With compost, sewage sludge, and atmospheric deposition as potential MP inputs to arable land, SPEROS-MP generated a total MP input into the stream network of 1.29 kg MP via the soil erosion pathway in 2020. Deliveries to the stream network have also steadily increased in TW (Figure 14 a), with an average of 5.04 kg of MP a^{-1} delivered to the stream network in 2020 (Table 6).

Between 1950 and 2020, 208.3 kg of MP (134 kg TW, 57 kg sewage sludge, 17 kg compost, and 0.32 kg atmospheric deposition) entered the Glonn stream network (Table 6), while overall, a sediment load of 3.0×10^8 kg was delivered to the catchment outlet. TW was the primary MP source, accounting for 64.3%, followed by sewage sludge with 27.4%, compost with 8.2%, and atmospheric deposition with 0.1%. Taking into account the MP delivery relative to the MP input (i.e., the total amount of MP input into the soil in 1950–2020 vs. complete MP delivery into the stream network from 1950–2020), only 0.14% of the MP released to arable land was transported into the Glonn stream network. This differs slightly for the different MP sources, ranging from 0.17% for atmospheric deposition to 0.11% for tire wear (Table 6).

The spatially distributed model also allowed us to quantify the relocation of MP between different land uses (an example is shown in Figure 15 f). The amount of MP delivered between 1950 and 2020 from arable land to grassland and forest is 1.1×10^3 and 0.2×10^3 kg, respectively (Table 6). The more extensive delivery to grasslands is exciting, as these are mainly located along the stream network (see discussion).

Table 6: Soil erosion-induced MP delivery to the Glonn stream network, as well as redistribution to grassland and forest. The MP vertical loss below the plough layer is also given. All values are listed for the modelled time span 1950–2020 and separately for the year 2020.

	Tire wear	Sewage sludge	Compost	Atmospheric deposition	Unit
		1950–2020			
MP delivery into stream network	134	57	17	0.32	kg
min	49.0	21	5	0.01	
max	322	200	155	9	
Percentage of MP application	*0.11*	*0.14*	*0.15*	*0.17*	*%*
MP delivery into grassland	604	442	82	1.5	kg
min	221	163	24	0	
max	1450	1551	748	42	
Percentage of MP application	*0.50*	*1.05*	*0.71*	*0.81*	*%*
MP delivery into forest	108	97	18	0.34	kg
min	39.5	36	5	0	
max	259	340	164	10	
Percentage of MP application	*0.09*	*0.23*	*0.16*	*0.18*	*%*
MP loss below plough layer	4703	2605	489	14.8	kg
min	1720	961	144	6	
max	11 287	9414	4458	386	
Percentage of MP application	*3.91*	*6.19*	*4.25*	*8*	*%*
		2020			
MP delivery into stream network	5.04	0.51	0.77	0.01	kg MP a^{-1}
min	1.84	0.2	0.2	0.0003	
max	12.1	1.8	7	0.3	

SPEROS-MP not only gives information about the MP relocation between arable land and other land uses. The model also determines the amount of MP allocated below the plough layer (and thus out of reach of water erosion) at depositional sites (an example is shown in Figure 15 e). Between 1950 and 2020, 3.9% of the TW supplied to arable land was moved below the plough layer (Table 6). This corresponds to 4.7 $*10^3$ kg MP or 35 times the amount reaching the stream network via water erosion. For sewage sludge, it is 6.19% (2.6$*10^3$ kg); for compost, 4.25% (489 kg) and for atmospheric deposition, 8% (14.8 kg). Consequently, much more MP was translocated into the subsoil than was transported into the Glonn. This transport into the subsoil was caused by water erosion (48.5%) and tillage erosion (51.5%). Conversely, up to 95% of the MP applied to arable soil over the past 70 years remains in the plough layer (infiltration and bioturbation excluded). Considering the time, the MP concentrations in the plough layer are not substantially changing due to lateral and vertical MP loss. Nevertheless, these

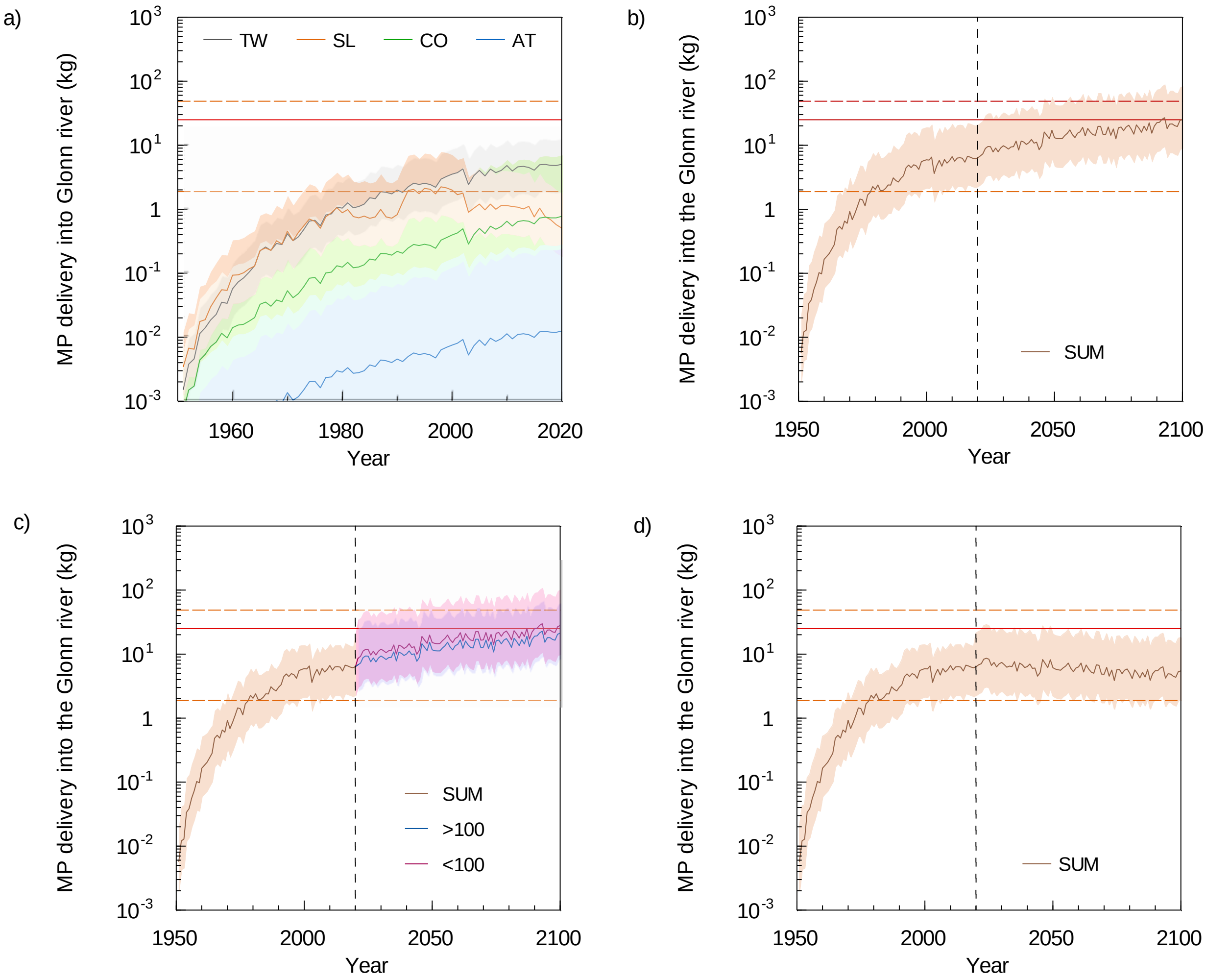

Figure 14: MP delivery into the Glonn shown individually for tire wear (TW), sewage sludge (SL), compost (CO) and atmospheric deposition (AT) or the sum of TW, SL, CO and AT (SUM). The dashed line gives the year 2020 as the starting point for different scenarios. For comparison, the amount of MP delivery through wastewater treatment plants (WWTPs) in 2020 is shown as a red line (min. and max. as dashed lines). a) MP delivery into the Glonn river between 1950 and 2020. b) Result of scenario S1 with the assumption that the MP input will continue as in 2020. c) Result of scenario S2. Compost and sewage sludge are applied to arable land at a distance of > 100 m and < 100 m from water streams. d) Result of scenario S3 with no MP input at all from 2020 onwards.

buried amounts of MP present a huge mass, indicating that tillage erosion is considered a specific process of MP erosion and transport.

3.3.3 Scenario S1 – business-as-usual

If arable soils continue to be loaded with MP the same as in 2020, the annual MP delivery rate into the Glonn stream network will increase by a factor of 4 by 2100. In 2100, 25.2 kg MP

a^{-1} (min.: 9.03 kg; max.: 84.1 kg) through TW, compost, sewage sludge and atmospheric deposition would end up in the stream network (Figure 14 b). Between 1950 and 2100, this would make a total MP input of 1.32 $*10^3$ kg MP (min.: 511 kg; max.: 4.7 $*10^3$ kg) into the stream network.

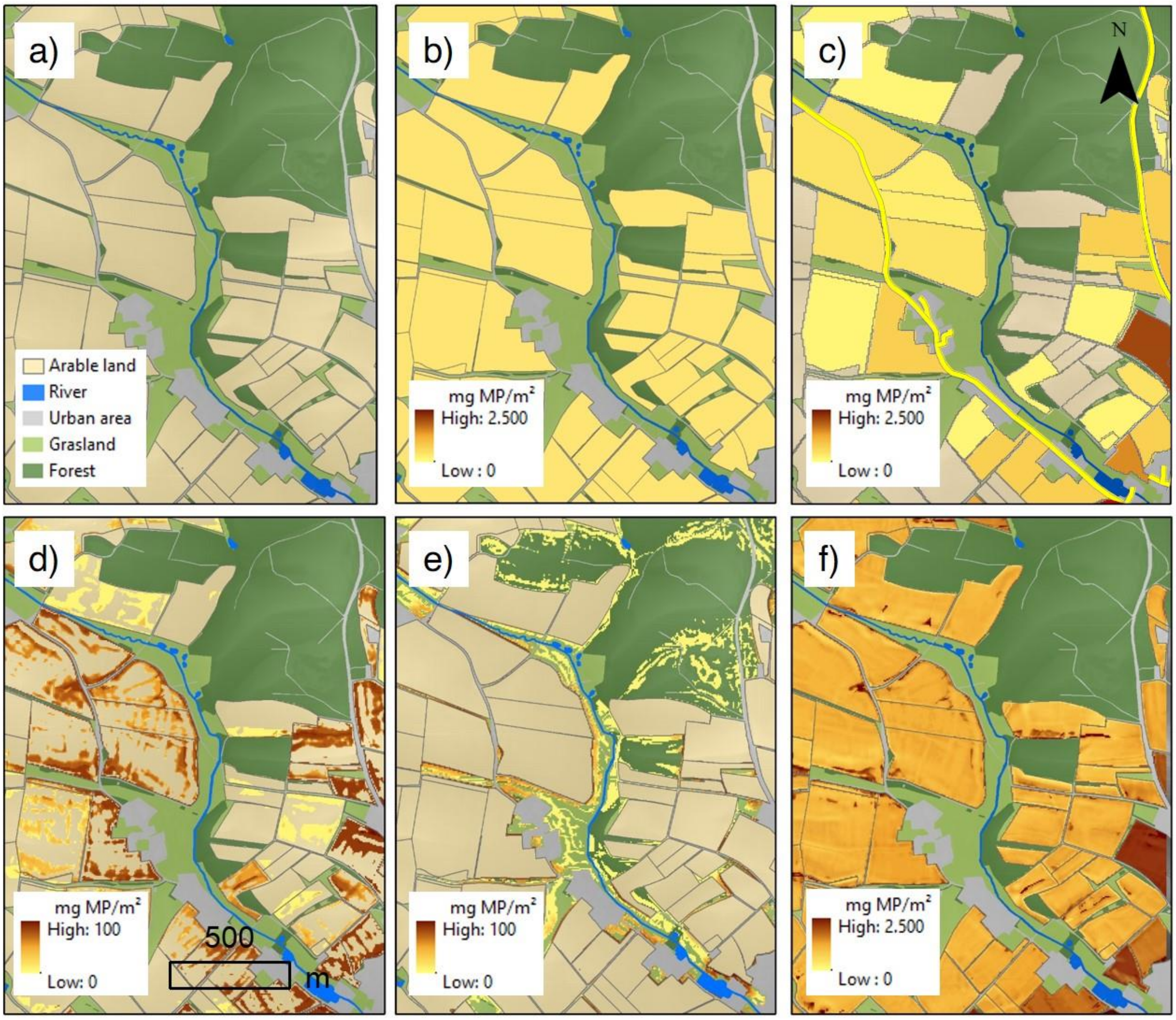

Figure 15: Example of catchment segment (for location, see Figure 10) illustrating microplastic (MP) input on arable land and results of erosion modeling between 1950 and 2020. The maps show the situation in 2020. a) Field-based land use. b) Total MP input from sewage sludge, compost, and atmospheric input (without TW) as a mean value over all arable land. c) MP input from TW, spatially distributed to individual arable fields along the roads. d) MP concentration below the plough layer. e) MP transported to other land uses via soil erosion. f) MP distribution after water and tillage erosion on arable land.

3.3.4 Scenario S2 – spatially targeted application of soil amendments

In S2, MP inputs from atmospheric deposition and TW accumulation continued like in S1. However, the location where the organic fertilizer (sewage sludge and compost) was applied in the catchment was changed. All organic fertilizers were applied at least 100 m from the stream network or within a distance smaller than 100 m along the stream network.

With an application at a distance of < 100 m, on the other hand, it would be 27.9 kg (min.: 10 kg; max.: 102 kg) in 2100 and thus an increase of 10.7% compared to S1 (Figure 14 c). In the case of the application at a distance of > 100 m, the MP delivery in the stream network would be reduced to a total of 21.2 kg (min.: 7.72 kg; max.: 55.9 kg) in 2100 (Figure 14 c). That would correspond to a reduction of 16% compared to S1. Targeted application of MP contaminating organic fertilizer only slightly affected the MP delivery to the stream network as tire wear fluxes dominate this process.

The result becomes clearer considering TW and the organic fertilizers separately. If the distance is > 100 m, the annual MP delivery rate from organic fertilizer (sewage sludge and compost) without TW is 1.1 kg MP a^{-1} (min.: 0.4 kg, max.: 7.8 kg) in 2100 (Figure 16). For 2100, this would result in a 78% reduction of the annual MP delivery rate from organic fertilizer into water bodies compared to S1. From 1950 to 2100, 173 kg MP (min.: 60 kg; max.: $1.0*10^3$ kg), or 46% less MP, from organic fertilizer would end up in the stream network until 2100 (the effect of atmospheric input is negligible).

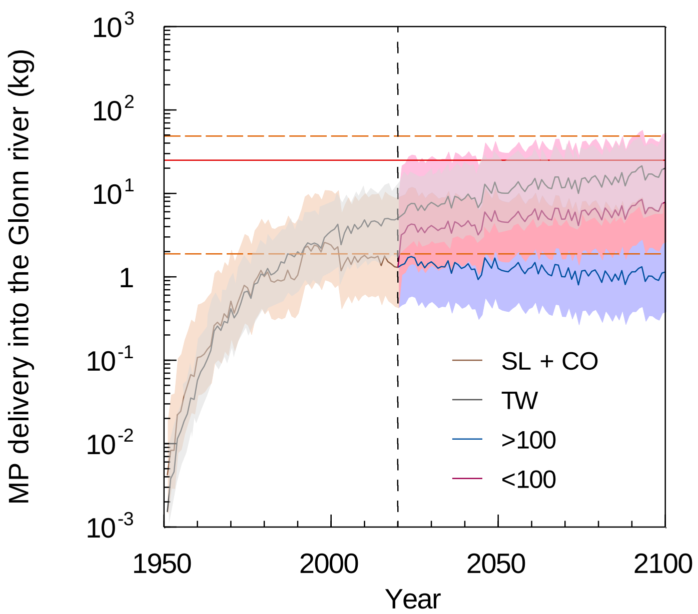

Figure 16: Result of scenario S2 individually shown for tire wear (TW) and sewage sludge (SL) and compost (CO) as organic fertilizer applied to arable land at a distance of > 100 m and < 100 m from water streams. For comparison, the amount of MP delivery through wastewater treatment plants (WWTP) in 2020 as red lines (min and max as dashed lines).

If organic fertilizer is applied along the stream network (max. distance < 100 m), an MP delivery of 7.8 kg a^{-1} (min.: 2.6 kg, max.: 54 kg) is modeled in 2100 (Figure 16). Between 1950 and 2100, a total of 493 kg MP (min.: 168 kg; max.: $3.25*10^3$ kg) would be delivered to the river system by organic fertilizer (without TW).

3.3.5 Scenario S3 – stop MP input:

In scenario S3, MP input stops from 2020 onwards. This abrupt stop in plastic immission is not reflected in the MP delivery rates after 2020 (Figure 14 d). However, in 2100, 5.43 kg of MP a^{-1} (min.: 1.98 kg, max.: 18.2 kg) would still end up in the stream network from arable land due to soil erosion (Figure 14 d). This corresponds to a decrease in the annual MP delivery rate of 14% between 2020 and 2100, with 80 MP-free years (since 2020). Since 1950, 684 kg MP (min.: 246 kg; max.: $2*10^3$ kg) would have ended up in the Glonn stream network.

3.4 Discussion

3.4.1 Modelled erosion rates & sediment delivery

The modeling approach used, with a yearly time step and the missing temporal and spatial variability of most model input data (especially the constant crop cover factor), while only varying yearly rainfall erosivity, leads to model outputs that do not capture the full temporal dynamics of the measured yearly sediment delivery (Figure 13). It is well documented that averaging model input variables over space and time generally leads to overestimating years with low sediment delivery and underestimating years with high sediment delivery (Keller et al., 2021; Meinen and Robinson, 2021). The reduced temporal variability in modeled sediment delivery is expected for two main reasons: (1) the annual model time step averages out years where individual extreme events dominate the yearly sediment delivery, and (2) varying only the annual rainfall erosivity, while all other input parameters (especially cropping dynamics) are kept constant, cannot capture the temporal dynamics. However, without any model calibration, the model reflects the long-term mean sediment delivery between 1968 and 2020 (Figure 13), explaining 51% of the variability in the measured data. Hence, it can be concluded that SPEROS-MP is robust enough for this modeling study which focuses on MP delivery to the stream network in the Glonn catchment, especially as uncertainties associated with the erosion modeling are in any case more minor than the uncertainties associated with estimates of MP immissions to the arable soils in the catchment.

3.4.2 Plausibility of MP soil input estimates

Estimating the cumulative MP-soil immissions from different sources starting from 1950 is, of course, associated with large uncertainties. To account for these uncertainties, we used large ranges of possible inputs in the semi-virtual catchment approach, which in the following discussion are compared with literature values for Germany or Bavaria.

3.4.2.1 MP from sewage sludge, compost and atmospheric deposition

Brandes et al. (2021) calculated mean MP inputs into agricultural soils in Germany for compost (1990–2016) and for sewage sludge (1983–2016). Bavaria's calculation results in compost-MP input rates of 15 and 80 mg MP m^{-2} a^{-1} and sewage sludge-MP input rates between 0 and 190 mg MP m^{-2} a^{-1}. Bertling et al. (2021) also determined MP immissions (TW excluded) to agricultural soils in Germany, resulting in much higher input rates for 2021 for compost and sewage sludge, with up to 702 mg MP m^{-2} a^{-1} and $2.1*10^3$ mg MP m^{-2} a^{-1}, respectively. In contrast to the first authors, Braun et al. (2021) calculate the possible MP load for the legally permissible amount of compost applied to fields in Germany. This maximum permitted amount of compost application results in maximum possible entry rates ranging from 34 to $4.7*10^3$ mg MP m^{-2} a^{-1} into agricultural soils via compost.

For this study, an MP emission to arable soils of between 0.42 and 4 mg MP m^{-2} a^{-1} for sewage sludge and between 0.56 and 15.8 mg MP m^{-2} a^{-1} for compost were calculated for Bavaria. The values are not based on the maximum possible limits but on the most realistic estimates. Therefore, the MP loads remain well below the literature values. Nevertheless, the MP input from the compost will likely be underestimated based on the optical detection of MP > 1 mm (Bläsing and Amelung, 2018; Braun *et al.*, 2021; Weithmann *et al.*, 2018). Currently, much more compost (21*107 t in 2020) is spread on fields in Bavaria than sewage sludge (24*104 t in 2020), causing higher MP emissions from compost (Figure 10 a). This results from reduced sewage sludge application, which has been banned mainly in Bavaria since 2017

(Schleypen, 2017) (Figure 10 c). However, regional policy strategies regarding the use of sewage sludge differ substantially within Germany, making comparisons within the country somewhat difficult (Brandes et al., 2021).

For atmospheric deposition, an average of 771 and 395 MP particles m^{-2} d^{-1} were measured at rural locations in London and Hamburg (Klein and Fischer, 2019; Wright et al., 2019). Brahney et al. (2020) show that airborne microplastic particles accumulate at minimum concentrations of 48±7 MP particles m^{-2} d^{-1} even in the most isolated areas of the United States (national parks and national wilderness areas). Even in Antarctic snow, up to 29 MP particles per melted liter were found (Aves et al., 2022). In this study, the values of Witzig et al. (2021) were used to estimate the MP contribution via atmospheric deposition. They made MP measurements at different locations in Bavaria, ranging from 74±19 to 109±16 MP particles m^{-2} d^{-1}. Even if transferring such particle numbers to mass inputs is associated with additional uncertainties, these amounts are orders of magnitude smaller than the inputs from sewage sludge and compost and hence less critical.

3.4.2.2 MP from tire wear

The large MP mass resulting from tire wear is noticeable in the TW input data and the TW delivery rates into the stream network. With modeled mean TW delivery of 5 kg MP a^{-1} in 2020 into the river system, the equivalent of half a car tire ends up as MP in the Glonn (flow length of 50 km) each year. However, the calculated mean TW input to the Glonn catchment of 200 mg MP m^{-2} in 2020 is in the same range as the estimates in other studies. For example, annual values of between 180 and 370 mg TW m^{-2} were reported for Germany (Baensch-Baltruschat et al., 2020; Kocher et al., 2010; Wagner et al., 2018). The modeled MP input (Figure 12) to arable land in the Glonn catchment was substantially smaller, with a mean of 19.7 mg TW m^{-2}.

Most of the TW remains on the roads or in the immediate vicinity. Some of the TW is expected to be transported directly into surface waters via runoff from the road. Baensch-Baltruschat et al. (2020) estimated that 12–20% of the tire wear released on German roads ends up in surface water via road runoff. The hydrological model estimates of Unice et al. (2019) indicated that 18% of cast tire wear was transported to freshwater in the Seine River catchment. In comparison, focusing on the erosion of MP, which was mixed into the plough layer, only 0.11% of the applied TW to arable soils from 1950 to 2020 reached the river system. Although TW is the largest source of entry in this study, the MP flow to the stream network is a conservative estimate. This mainly results from the assumption that all roads are surrounded by a 3 m grass buffer strip (even if this was not shown in the 5 m x 5 m land-use raster map used), permanently trapping at least 85% of the TW emissions (Figure 12). Yet even this conservative assumption is associated with high uncertainties. The width of the grass strip between the road and the field enormously impacts the MP emission. A 2 m wide buffer strip would retain approximately 80%, and a 1 m wide buffer strip about 65% of the TW emission (Figure 12). Without any assumed grass buffer strips, the MP emission from TW would be eight times higher. Ultimately, spatially distributed tire wear is still associated with uncertainties. The level of TW emissions into the environment (not just arable land) makes other MP sources almost negligible, especially regarding MP saving strategies.

Overall, it can be concluded that the estimates of MP input to the Glonn catchment are in the same order of magnitude, or somewhat smaller, compared to most other studies and hence should be more or less reasonable, even if any estimates are associated with large uncertainties (e.g., extrapolating back to 1950; the small number of studies available for estimating MP concentrations in sewage sludge and compost; errors when transferring particle numbers in particle mass, etc.). However, an error in modeling the MP delivery into the stream network of the test catchment most likely results from the fact that mean application rates (sewage sludge, compost) for the whole of Bavaria were used (Figure 15 b). At the same time, only TW input was calculated on a catchment-specific basis (Figure 15 c). Again, it is essential to note that the Glonn catchment was used as an exemplar to address and discuss the potential magnitude of the MP/soil erosion pathway in mesoscale catchments determined by arable land use.

3.4.3 The modelled fate of MP

As a mass-balanced model, SPEROS-MP calculates the MP input in mass (kg m^2), not particle numbers. Hence, the model does not consider the MP particles' type, shape, density, size, or chemical properties from different MP sources. It thus treats the erodibility of MP from all input pathways equally. However, it can be assumed that particle properties play a decisive role in erosion-induced lateral transport and potential vertical transport. Small MP particles should be translocated faster below the plough layer due to bioturbation and maybe infiltration (Li *et al.*, 2021a; Rehm *et al.*, 2021; Waldschläger and Schüttrumpf, 2020). A subsequent reduction in MP concentration in the plough layer will also reduce MP erosion. On the other hand, smaller MP particles might interact more strongly with soil organic or mineral particles or might even be included in soil aggregates; hence are more likely transported as bulk soil. The long-term plot experiment (chapter 2) demonstrated that smaller PE particles (53–100 µm) are less strongly enriched in delivered sediments compared to larger PE particles (250–300 µm). Such behavior might change again with increasing particle size because if particles transported with sheet flow are larger than the flow depths (mostly < 1 mm), transport in suspension is no longer possible.

In general, the potential decrease in topsoil MP concentration due to infiltration and bioturbation is not accounted for in SPEROS-MP. Vertical MP transport via infiltration and bioturbation has been widely discussed and partially observed in earlier studies, e.g. (Rillig et al., 2017b), while earthworms play an especially important role in directly transporting MP via digestion and excretion (Huerta Lwanga et al., 2017) or in preparing preferential flow pathways for MP leaching (Yu et al., 2019). Ignoring these processes of vertical movement below the plough layer may lead to a slight overestimation of the topsoil MP concentration in the modeling approach presented here.

SPEROS-MP delivers MP into the stream network and redistributes MP within the catchment and the soil profile. As arable land in the catchment is mainly found on the upper slopes and grassland in the flood plains, large amounts of MP are transported from arable land to grassland (Table 6). No-tillage takes place in grassland, leading to high MP concentration in the topsoil. Along the main river, in particular, grassland contaminated with MP (example shown in Figure 15 f) offers a high potential for MP loss during flood events. In the flood plains, the groundwater level is regularly close to the surface; hence the chance of MP leaching into the groundwater increases (Chia et al., 2021; Singh and Bhagwat, 2022; Viaroli et al., 2022).

3.4.4 Soil erosion as a potential MP source for inland waters

Comparing the annual MP input to arable land and the yearly MP loss through soil erosion indicates that only a small proportion (≤ 0.17% since 1950) is delivered to the stream network. The loss rate of TW (0.11%) was the smallest compared to sewage sludge, compost, and atmospheric deposition (Table 6). This is because the TW was not applied to all fields but only to the fields next to a road. The low percentage of input lost to the streams should not lead to the fallacy that MP transport via soil erosion is negligibly small (Schell et al., 2022; Weber et al., 2022). This becomes clearer when comparing the MP input from soil erosion with the MP input from wastewater treatment plants (WWTP) in the study area (Figure 14). Based on the known number and size of the WWTPs in the study area and MP loads in German WWTPs as in the literature (Mintenig et al., 2014), the MP delivery into the Glonn through WWTP outlets can be estimated at an average of 25 kg MP a^{-1} (min.: 1.9 kg, max.: 49 kg) in 2020 (Figure 14). These values represent a maximum scenario since the calculations were based on the possible full capacities of the WWTPs. Within the test catchment, the MP delivery into the stream network was 6.3 kg MP a^{-1} (min.: 2.2 kg, max.: 21 kg) in 2020, but (S1, Figure 14 b) could reach 25.2 kg MP a^{-1} (min.: 9 kg, max.: 84.3 kg) by the end of the century (Figure 14 b).

The field experiment (chapter 2) has shown that due to its low density, MP is preferentially eroded and is enriched by up to a factor of four in delivered sediments. These potential enrichment effects were not included in SPEROS-MP. In addition, this study did not consider other MP input sources, such as plastic used in agriculture (e.g., mulch films) and littering. Therefore, the modeled MP delivery is a conservative estimate in this respect. Overall, our results are in line with other, larger-scale model estimates for the Bavarian section of the Danube catchment, showing that the MP input via soil erosion into water bodies in rural areas outweighs the MP input of WWTP outlets (Witzig et al., 2021). It should, therefore, not be claimed that soil erosion for MP transport is negligible (Schell et al., 2022) while wastewater treatment plants are treated as a significant MP source for inland waters (Cai et al., 2022; Eibes and Gabel, 2022; Murphy et al., 2016).

3.4.5 The MP sink function of soil results in a long-term MP source

Today's MP pollution of arable land represents a long-term MP source for inland waters. With the model scenarios S1 and S3, this study showed that the MP discharge from arable soils into inland waters via soil erosion will still affect many generations, even if MP entry into the terrestrial environment could be avoided. Because of low MP loss rates (≤ 0.17%) via soil erosion and the stability of conventional plastic materials over centuries (Ng et al., 2018), the MP particles accumulate in the soil over the years. As most of the MP stays in the plough layer (Table 6), it is regularly made available to surface runoff and erosion processes. After 80 years without MP input in S3, MP delivery from the soil decreased only by 14%. The MP concentration in the topsoil of arable land decreases over time due to lateral MP loss into the stream network or neighboring grassland and forest areas (example shown in Figure 15 b). The MP concentration in the topsoil also decreases since erosion incorporates MP-free subsoil. Conversely, MP gets below the plough layer at depositional sites (outside the range of water erosion). It is important to note that tillage erosion plays an important role, as it supports the spatial distribution within agricultural fields and the burial of MP below the plough layer (Figure 15 e, Table 6).

S3 is reminiscent of other well-known environmental problems of long-term diffuse pollution, e.g., with phosphorus (Daneshgar et al., 2018; Vaccari, 2009), where a pollutant accumulates in soils but slowly finds its way into inland waters through soil erosion. In this respect, it is essential to note that reducing MP inputs to stream networks coming from point sources, e.g., WWTP, will be easier, whereas the diffuse input will continue for centuries.

3.4.6 Targeted application of MP-loaded organic fertilizer

The predicted increase in plastics production means that more MP inputs into the environment can be expected (Borrelle et al., 2020; Horton, 2022). Because of this, it is necessary to consider measures to reduce or avoid the entry of MP into the various environmental compartments. The results of S2 have shown that applying organic fertilizer (without TW) containing MP at a distance of more than 100 m from the stream network can reduce MP entry into surface waters via soil erosion by up to 46% compared to S1 (Figure 16). By contrast, application of MP-contaminated soil amendments in the proximity of the stream network increases MP supply (by 53% in this scenario).

This highlights the potential impact of optimized landscape management, considering the location of any agricultural management activity. It also shows that, in addition to soil conservation in the field to prevent soil erosion, general changes in catchment management affecting hydrological and sedimentological connectivity have essential implications for transporting sediments and pollutants. Therefore, the location of soil additives, usually used to close production cycles, should be considered for future use. This consideration can significantly influence the subsequent erosion transport and redistribution of, for example, MP within a whole river catchment.

In contrast, tire wear remains the most important source of MP and also contributes most of the MP pollution to water bodies through soil erosion. However, due to its uncontrolled distribution across the landscape, targeted management of tire abrasion is unfeasible. Consequently, the targeted fertilizer application approach ultimately leads to a more modest real reduction of only 16% in MP contamination within the water body until 2100. The decrease via MP-contaminated organic fertilizer has a limited impact on MP delivery into the stream network, given that tire wear remains the dominant contributor to this phenomenon.

3.5 Conclusion

In Chapter 3, the transport of MP eroded from arable land was modeled across a mesoscale landscape. Sewage sludge, compost, atmospheric deposition, and tire wear were considered MP sources. Tire wear not only represented the most considerable MP input to arable land. It also generated the most considerable MP delivery rates to the stream network — although tire wear is not widespread on arable land, only occurring on fields near the roads. In percentage terms, only a tiny fraction (< 0.2%) of all MP applied to arable land ended up directly in the stream network via soil erosion. However, the MP mass delivered into the stream network represented much MP input. The modeled MP delivery into the stream network was in the same range of potential MP inputs from wastewater treatment plants in this rural area.

In addition, it was shown that most of the MP applied to arable soils remains in the topsoil (0–20 cm) for decades. Tillage produces a regular homogenization, and the MP stays available for surface runoff and water erosion in the long term. Based on a series of scenarios modeled up to 2100 with no more MP input from 2020 onwards, similar MP delivery rates (compared to 2020) could still be identified. This implies that arable land represents an MP sink on the one hand and a long-term MP source for inland waters on the other.

Using the soil profile update component in the SPEROS-MP model, the MP concentrations along the soil profile could be determined to a depth of 1 m. It was modeled that 5% of the MP applied to arable land is translocated into the subsoil (> 20 cm) by tillage and water erosion between 1950-2020. Located below the plough horizon, the MP is out of reach for future lateral surface runoff erosion processes. Based on the spatially distributed erosion model, it was also demonstrated that most of the eroded MP leaving arable land is deposited in grassland (1% of applied MP). Especially in areas of the river valleys, these accumulations could represent a concentrated MP entry into the stream network in the event of a flood.

Targeted application of MP contaminated organic fertilizer only slightly affects MP delivery to the stream network as tire wear fluxes dominate this process. In this context, tire abrasion must be considered as a dominant and uncontrollable MP source that remains unaffected by changing application rates of sewage sludge or organic compost as MP contaminated fertilizers. All calculated and modeled cases were dominated by tire wear, which is challenging to manage, especially in regions with a high population and dense road network. Therefore, the most effective protection for arable land would not be to limit or ban the application of MP-contaminated organic fertilizers, but to reduce tire wear emissions. The deliberate creation of grass strips to protect the landscape against erosion would also be an option to reduce MP delivery into the stream network. To preserve soil as a valuable resource and protect the terrestrial and aquatic ecosystem from MP pollution and its effects, we should focus on limiting MP emissions to the environment in general as much as possible.

4 General discussion

The fact that MP is transported through the terrestrial landscape via surface runoff and soil erosion is often mentioned (Windsor *et al.*, 2019; Owens, 2020; Horton *et al.*, 2017) and indirectly indicated by MP measurements in sediment, as well as lake shores and beach sediments (Rodrigues *et al.*, 2018; Fan *et al.*, 2019; Horton *et al.*, 2017). Empirical evidence for this phenomenon is still lacking (Surendran *et al.*, 2023; Bläsing and Amelung, 2018). Specifically, site-specific work is needed to quantify the extent and timing of the redistribution of plastics on soil (Lebreton and Andrady, 2019). The processes, i.e., redistribution in the soil profile and transport by water erosion and runoff, and their influencing factors such as topography, land use, climate, vegetation, particle shape, and size are poorly understood (Nizzetto *et al.*, 2016a; Sa'adu and Farsang, 2023; Saling *et al.*, 2020). This doctoral thesis addresses this knowledge gap. This thesis investigated the erosion, transport, and deposition of MP by water and tillage erosion, while focusing on arable land most prone to erosion. Investigating the link between MP and soil erosion can help to improve our understanding and the identification of potential impacts on ecosystems.

4.1 Specific erosion and transport behavior of MP

The field experiment (chapter 2) shed light on the transport of MP on arable fields during water erosion. Compared to the mineral soil, it was found that the studied microplastic particles (53-300 µm) were preferentially eroded and transported. This was detectable by an apparent accumulation and enrichment of MP particles in the eroded sediment (Figure 7). This verifies the hypothesis that less dense MP particles are preferentially eroded compared to MP contamination of the topsoil. The results are consistent with plot-based studies on MP and soil erosion, where MP was also more easily transported with surface runoff due to its low density (Schell et al., 2022; Han et al., 2022). Other studies focusing on the erosion of particulate organic matter, which is also preferentially eroded due to its low density (Müller-Nedebock and Chaplot, 2015; Wang et al., 2013a; Martínez-Mena et al., 2012) show some analogies to the rare MP-erosion studies. Here it is important to recognize the enrichment of the light-weight POC was not only found in plot (Martínez-Mena *et al.*, 2012; Wang *et al.*, 2013a) but also in watershed studies (Cerro *et al.*, 2014; Bertol *et al.*, 2007).

The hypothesis that MP enrichment increases with decreasing MP size, while overall MP enrichment is more pronounced when MP is in the same or smaller size range as mineral soil particles, was rejected. Based on the experimental results the course MP_c was more enriched in the delivered sediments compared to the fine MP_f. Even if this difference in mean enrichment was not significant due to the overall variability of the different experimental runs (Figure 7). A higher average ER of MP_c in the delivered sediment can be explained by the less pronounced connection to soil particles. The analysis of MP_{free} and MP_{bound} (Figure 8) shows stronger binding forces between the smaller MP_f compared to the course MP_c and the mineral soil.

There were also noticeable differences between the two soil types, with loamy sand showing a substantially larger mean MP ER compared to silty loam. Nonetheless, these differences were not statistically significant due to the high variability of individual sample values (Figure 7). The combination of lower MP enrichment in the case of silty loam (Figure 7 b, d) and the higher erodibility of silty soils in general (Figure 6 c, d) led to equal MP delivery in the case of both soil types. Sandy soils, although considered less erodible, can also be a significant source of MP in soil erosion.

The interactions between MP and soil, such as binding and aggregation, play a critical role in MP erosion. The field experiment has shown that MP erosion rates decrease over time (Figure 6). It was observed that the binding of MP particles to the soil matrix leads to less enrichment of MP in the sediment (Figure 7), indicating an increase in MP_{bound} over time (Figure 8). The MP concentrations in delivered sediments also declined due to lateral and vertical loss of particles in the topsoil. Topsoil MP concentrations declined from RS1-3 due to lateral loss with surface runoff and erosion. On silty loam, there was an average MP_c and MP_f loss of 4.25% and 0.69% per heavy rain event, respectively. On loamy sand, the average MP_c loss was 3.98%, and the average MP_f loss was 0.73% per heavy rain event.

Vertical movement of MPs was observed in the stainless-steel cylinders (Figure 3). The loss below the MP_c application layer (5 cm) was 1.51% and 2.95% for the silty loam and the loamy sand, respectively. The vertical transfer was more significant for MP_f, with 5.01% lost for silty loam and 5.87% for loamy sand below a soil depth of 5 cm. MP_c was found to be lost mainly by lateral erosion transport, while MP_f was translocated mainly below the topsoil layer and thus protected from further erosion. That means larger MP_c particles were especially lost through soil erosion, while smaller MP_f particles were gradually stored below the plough layer. The field experiment verifies the hypothesis about changing MP delivery rates over time as interactions between MP and soil (aggregation and binding to mineral particles) increase and concentrations of MP in topsoil decrease due to subsequent erosion events and vertical transport below the plow layer. However, it must be mentioned that the lateral loss refers to heavy rain events of 60 mm h^{-1}, and the abrupt loss refers to a depth of 5 cm (Figure 3).

The leaching of MP through the soil matrix is limited and depends on the size and shape of the MP and the pore size distribution of the soil matrix. Wan *et al.* (2019) and O'Connor *et al.* (2019) found that not the water volume flowing through a sandy soil column in the laboratory determines the transport of MP to depth, but the number of drying and wetting cycles. Although sandy soil does not shrink like typical clay soils, the importance of these cycles suggests that the soil matrix, combined with a preferential flux mechanism, may lead to increased transport. Dong *et al.* (2021) examined the effects of various soil solution chemical factors on MP transport, such as electrolytes, pH, and humic acids. The study concluded that transport is determined by the size and shape of the MP rather than by chemical factors. The depth to which the MP particles can then be transported likely depends on the depth distribution and connectivity of the macropore network (Yu *et al.*, 2019; Zubris and Richards, 2005). Where the macropores end, the MP particles are limited in their further downward leaching by the pore size distribution of the matrix (Lwanga *et al.*, 2022). The transport of microplastics by soil organisms depends on factors such as microplastic size and organism size. Smaller microplastics and organisms facilitate easier movement, while electrostatic attraction forces influence microplastic aggregation. Earthworms and springtails mechanically introduce microplastics into the soil. Invertebrates also ingest microplastics, observed in earthworms, snails, larvae, nematodes, and mites. Thus, the pathway of MP to shallow groundwater may occur primarily when the bioturbation and the macropores reach the water table (Panno *et al.*, 2019).

Soil interaction and aggregation play a critical role in the fixation of MP in soil (Klíč et al., 2022). By incorporating MP into soil aggregates, the MP becomes embedded in the soil matrix and is less likely to be mobilized. This means that the likelihood of MP being dislodged from the soil and released into the environment by water erosion, wind, or other transport processes is reduced (Liu et al., 2023; Lehmann et al., 2019; Zhang and Liu, 2018). However, the presence of MP in soil aggregates can have several effects. On the one hand, the inclusion supports the fixation of MP particles. On the other hand, the presence of MP can destabilize soil aggregates, leading to increased soil erosion and reduced water-holding capacity (Wang *et al.*, 2022a; Boots *et al.*, 2019). Studies have shown that microplastic particles can affect aggregate formation and stability by reducing adhesion forces between soil particles. This can cause soil aggregates to break down and soil to compact, leading to soil structure degradation (de Souza Machado et al., 2019; Liang et al., 2021). It has to be mentioned that these studies were performed with non-aged MP. The effect may not be as significant with old (oxidized) MP. Destabilization of soil aggregates by MP could also lead to increased soil erosion. When MP destabilizes soil aggregates, the susceptibility of the soil to erosional processes such as water runoff and wind transport increases (Du et al., 2022; Foster et al., 1985). This could lead to increased soil erosion in MP-polluted soils, where valuable soil layers can be removed and entrained MP can enter water bodies or other ecosystems.

4.2 Importance of soil erosion as input pathway to the stream network

This thesis modelled the potential MP input for an arable land within the semi-virtual Glonn catchment. In 2020, it was estimated that more than 3.7 tons of MP were introduced to arable land by tire abrasion, sewage sludge, compost, and atmospheric deposition (Table 5). Since 1950, more than 170 tons have accumulated. Between 1950 and 2020, a total of 208 kg of this applied MP entered the Glonn stream network, with the majority coming from tire wear (64.3%), followed by sewage sludge (27.4%), compost (8.2%), and atmospheric deposition (0.1%) (Table 6). However, considering the MP delivery relative to the MP input, only 0.14% of the MP released to arable land was transported into the Glonn stream network. The SPEROS-MP model also allowed the assessment of MP relocation between different land uses, with a significant amount delivered from arable land to grassland. In the catchment, where arable land is primarily located on the upper slopes and grassland occupies the floodplains, significant amounts of MP are transported from arable land to grassland (Table 6). Due to the absence of tillage practices in grassland, MP concentrations are high in the topsoil. Particularly along the

Glonn River, grassland contaminated with MP (as depicted in Figure 15f) poses a high risk of MP loss during flood events. Additionally, in floodplains, where the groundwater level is often close to the surface, there is an increased likelihood of MP leaching into the groundwater.

Despite the significant connectivity between terrestrial and aquatic systems through soil erosion, it has been demonstrated through both the field experiment (chapter 2) and modeling approach (chapter 3) that most of the MP applied to arable soil remains in the topsoil (0-20 cm) for a long time. Contaminating MP inputs to soils has accumulated over many decades. In addition, regular tillage brings MP to the surface, making it available for long-term surface runoff and water erosion. Even if no further MP enters the soil from 2020 onwards, the modeled scenario until 2100 (chapter 3.3.5) showed similar rates of MP delivery (compared to 2020). This means that the results of this study confirm soil as a "sink" for MP and verifies the hypothesis that the MP load of arable soils is much higher than the potential MP delivery from the fields into a stream system via the water erosion pathway, indicating an MP sink function of the soils. However, at the same time, it acts as a long-term and diffuse source of MP to inland waters.

Based on the soil profile update component in the SPEROS-MP model, it was also possible to determine MP concentrations along the soil profile to a depth of 1 meter. The modeling showed that about 5% of the MP applied to arable land (regardless of its size) was translocated to the subsoil (> 20 cm) by tillage and water erosion, respectively, by deposition (1950-2020). This corresponds to an annual vertical loss of 0.07%, and this transport into the subsoil was more or less equally resulting from water (48.5%) and tillage erosion (51.5%). This redistribution of MP below the plow layer also indicates that water and tillage erosion load to a decrease in MP concentrations at erosional sites, where tillage incorporates subsoil into the plow layer. Even if this effect and its increase due to tillage erosion is relatively small, we still would agree that tillage erosion needs to be accounted. Nevertheless, it is not possible to clearly verify or falsify hypothesis 4, that tillage erosion substantially affects MP delivery to the stream network via water erosion.

This process of burial loss from the plough layer might be even more pronounced if the bioturbation process could have been considered. In the field experiment, the stainless-steel cylinders in which vertical MP movement was analyzed were not exposed to tillage and only to natural precipitation events and bioturbation. Nevertheless, particles could be detected at depths of up to 42 cm. Thus, the depth shift probably occurred along the pores by bioturbation, swelling, and shrinkage when changing from wet to dry conditions (Heinze *et al.*, 2022; Li *et al.*, 2021a; Zhang *et al.*, 2020a). Considering the lateral loss of MP by erosion and the vertical redistribution of MP below the topsoil layer, it becomes clear that the function of MP sources and sinks strongly depends on the size of MP particles and the soil properties.

In agreement with the results of this study, and according to Bläsing and Amelung (2018), most MP particles are retained in the topsoil and may remain there for decades. Weber et al. (2022) also demonstrated soil as a long-term MP sink. After thirty years following sewage sludge application, they could still detect a high concentration of MP in the topsoil, whereas areas with direct sewage sludge application contained the most plastic. Weber et al. (2022) also confirm that the plastic particles are distributed over the arable land by tillage and erosion over time. In the context of the MP cycle, arable soils might better be called MP reservoirs rather than ultimate sinks. Arable soils form a reservoir for human-made MP pollution. New environmental regulations and policies to prevent plastic pollution could be too late (Weber et al., 2022). All known and unknown consequences of plastic pollution on soils, soil organisms, or plants discovered by science will have an impact over a more extended period. Bertling et al. (2021) even see this as a devaluation of the soil that will take place in less than two decades in the worst case.

On erosion modelling results for the Glonn catchment are more or less in line with calculations of potential erosion (no transport and deposition) available via the Erosion Atlas of Bavaria (LfL, 2023). Also the Glonn is located in the erosion prone area of the so called Tertiary Hills, widly dominated by loess-burden soils. The Erosion Atlas of Bavaria in general indicates that erosion is a substantial soil threat throughout the arable areas of Bavaria. Taking the average erosion on arable land in Bavaria or even entire Germany (5.7 t ha^{-1} a^{-1}) into account, clearly indicates the large potential of water erosion as long-term MP source for inland waters.

4.3 Challenges and uncertainties related to erosion-induced MP delivery to the stream network

The largest uncertainty in MP erosion research is in weak knowledge regarding microplastic pollution of the soils. Since no sufficiently measurements of microplastic concentrations in Bavarian arable soils are available up to date, these values used in our modelling study were estimated from a variety of state wide (governmental district) mean data (chapter 3.2.3). For sewage sludge, compost and atmospheric deposition, an average value was assumed for all fields (Figure 15). The application data are not available with parcel accuracy. TW was distributed along the road network (chapter 3.2.3). However, estimates were used here as well, such as the decrease in TW concentration with distance from the road. If it were possible to simply measure MP in the soil, this would mean a great leap in quality for the model results. In addition, statements would be possible specifically for the Glonn River catchment. Currently, the model is to be seen as an analysis tool to present current estimates. The Glonn catchment area in this study is therefore to be seen as a semi-virtual example.

A general estimate of MP transport and deposition in soil is difficult for several reasons. MP enter the soil from a variety of sources, including plastic waste, plasticulture, wastewater, abrasion from tires, etc. (Campanale *et al.*, 2022; Huang *et al.*, 2023a). These different sources have different properties and compositions of MP particles. Therefore, characterizing and tracking these non-uniform particles in soil is challenging. In addition, MP can be transported in soil in several ways. Laterally, it can be moved by wind, water or tillage erosion (Bullard *et al.*, 2021; Han *et al.*, 2022). Vertically, it can move to deeper soil layers through deposition or through transport with water percolation (Klein and Fischer, 2019; Li *et al.*, 2021a) and bioturbation (Heinze *et al.*, 2022; Li *et al.*, 2021a). Considering all of these transport mechanisms and their interactions makes estimating soil translocation difficult. MP can interact with the soil matrix, which can affect their movement and distribution in the soil (Klíč *et al.*, 2022; Liu *et al.*, 2023). Factors such as soil type, moisture, pH, and organic matter can affect the interactions between MP and soil (Zhao *et al.*, 2021). These interactions can affect both the movement of MP in soil and their availability to soil-dwelling organisms (Browne *et al.*, 2013; Waldschläger and Schüttrumpf, 2020). Accurate detection of these interactions requires complex experiments and extensive data on microplastic-soil interactions under real conditions. Moreover, it could be shown that the movement and distribution of MP in soil can change over time. Therefore, to obtain an accurate estimate of microplastic displacement in soil, long-term studies and repeated measurements are needed to capture the temporal dynamics. However, this crucial data basis is still missing in this research field in order to be able to make well-founded statements (He *et al.*, 2023; Hachem *et al.*, 2023; Zhang *et al.*, 2022c).

Interpretation of results on MP in soil requires careful consideration of current scientific knowledge as well as existing uncertainties (Tunali *et al.*, 2023; Rodríguez-Seijo and Pereira, 2019). The results of the field experiment are based on HDPE particles in two size fractions (53-100 µm and 250-300 µm). Other plastics of different size, shape, and density could exhibit different behavior (Kim *et al.*, 2021; Rillig *et al.*, 2021). However, differences in behavior could occur depending on the chemical properties of the polymers, e.g., sorption behavior depending on pH-value. The shape of the MP, especially for fibers (Weber and Opp, 2020), could also affect erosion and transport behavior. Given these uncertainties, it is important to interpret soil microplastic results cautiously and continue to conduct sound scientific research. Long-term studies, standardized analytical methods, and a comprehensive consideration of soil properties and environmental conditions are needed to draw reliable and site-specific conclusions. Considering that topsoil is a long-term source, this fact is of concern, and therefore the urgent appeal remains to conduct specific experiments in the field to estimate the rate of movement of MP particles and to assume the relative role of the various factors that may influence this movement.

The modeling approach used in this study (**chapter 3**) has obvious limitations in terms of temporal dynamics and spatial variability of MP input data. Hence, model results do not capture the full temporal variation in measured annual sediment delivery as well as other erosion input data. Precipitation is incorporated as an average value per year. The averaging model input variables over space and time often leads to overestimation of years with low sediment delivery and underestimation of years with high sediment delivery (Figure 13). However, although the model was not calibrated, it shows the long-term mean sediment input well and explains a significant portion of the variability in the measured data. Considering the uncertainties associated with erosion modeling, the SPEROS-MP model is working robust enough, as shown in several studies (Van Oost *et al.*, 2000; Van Oost *et al.*, 2005a; Fiener *et al.*, 2020).

The SPEROS-MP model calculates the input of MP in terms of mass (kg m^{-2}) and does not consider the specific properties of MP particles, such as type, shape, density, size, or chemical properties. It treats the erodibility of MP from all sources equally. However, these particle properties seem play a role in erosion and potential transport (Zhang *et al.*, 2021; Weber *et al.*, 2022). We are at the beginning of understanding MP-soil interactions which would be essential to address the specific MP erosion, transport, and deposition behavior. Therefore, the only robust pathway of MP erosion modelling for this thesis was to ignore MP properties and enrichment processes in the modelling, even if this potentially led to an underestimation of MP delivery to the stream network. The model recognizes the importance of erosion-induced lateral transport and potential vertical transport of MP (deposition), but it does not account for vertical transport of MP by infiltration and biological activities below the plow layer, which may lead to a potential overestimation of MP concentration in the topsoil. At the same time, the field experiment confirmed that more than 95% of the applied MP did not move below 5 cm within 1.5 years through natural vertical transport. Therefore, this uncertainty is considered small in the model. Nevertheless, such uncertainties should always be taken into account when considering results. Although it is obvious that our modelling results are associated with large uncertainties (as given e.g., in Figure 13), we still conclude that this first attempt to estimate the importance of the MP pathway to aquatic systems helps to understand and recognize this important, long-term diffuse MP input to our aquatic systems.

4.4 Soil erosion a specific MP stressor of inland waters

The results of modeled scenario S2 (chapter 3.5.4) show that applying MP-containing organic fertilizer at a distance of more than 100 m from water bodies can reduce MP inputs via soil erosion by up to 46% of this MP source (1950-2100). Total MP input could be reduced by 16% in 2100, since tire wear cannot be targeted applied. Anyway, this scenario demonstrated the possibility of optimized landscape management and siting of agricultural practices to reduce MP inputs. At the same time, it verifies the hypothesis of spatially targeted MP application and changing MP loads affecting the diffuse MP delivery to the stream network.

The modeling results show that of all MP applied to arable land (1950-2020), only a small fraction (in the case of the modeled catchment less than 0.2%) entered the stream network directly via soil erosion. However, it is emphasized that MP transport via soil erosion is not negligible despite the small percentage. Although the percentage is small, the mass input of MP into the stream network is huge. The calculated MP input to the stream network was similar to the potential MP input from wastewater treatment plants in this modeled rural region. The results are consistent with other model estimates within the Bavarian Danube catchment (Witzig et al., 2021). MP inputs via soil erosion in rural areas may exceed inputs from WWTPs. Therefore, it is emphasized that soil erosion is not negligible, while WWTPs are considered an essential source of MP in inland waters (Liu et al., 2022b; Habib et al., 2020; Edo et al., 2020)

As this work demonstrates, soil erosion creates a link between agricultural land and water bodies, and thus also for the transfer of MP from the terrestrial to the aquatic environment. Thus, transport via soil erosion promotes MP pollution of water bodies with all its consequences. The projected increase in plastic production is expected to lead to an increased release of MP into the environment (Mai et al., 2020; An et al., 2020). To reduce MP input, erosion control measures like mulch seeding, intercropping, and maintaining watercourse edges can be employed. Buffer strips are well known for erosion control, and maintaining a distance from water bodies would also be helpful. However, accumulation of MP in erosion control grassed areas surrounding streams may concentrate MP inputs to the streams during floods.

Regarding distribution in the catchment, TW plays an important role. Chapter 3 considered the different MP sources, sewage sludge, compost, atmospheric deposition, and tire wear. Interestingly, it was found that TW not only caused the most significant input of MP to arable land but also resulted in the highest amounts of MP entering the stream network (5 kg in 2020) (Table 6). This is surprising since TW was calculated with a spatial distribution only on fields near roads compared to the other sources distributed evenly across all agricultural fields within the catchment (chapter 3.2.3.3). The model estimates in this study indicate that only a small fraction of TW that lands on arable fields enters the stream network (0.11%). Nevertheless, the amount of TW reaching the stream system from soil erosion of arable soils alone is many times greater (5 kg MP a^{-1}) than that from MP sources such as sewage sludge (0.51 kg MP a^{-1}) or compost (0.77 kg MP a^{-1}) considered to be distributed over all fields (Table 6). Several scientific studies have underlined the importance of tire abrasion as a high soil-input source of MP (Kole et al., 2017; Andersson-Sköld et al., 2020; Knight et al., 2020a). A study by Kole et al. (2017) found that an estimated 550,000 tons of MP are released annually from TW worldwide. In Germany, a heavily motorized country, the environmental impact of TW is also significant. A study by Baensch-Baltruschat et al. (2021) examined the pollution of TW particles on German roads. It stated it as one of the primary emissions of particular MP in the environment. Goßmann et al. (2021) verified that TW particle concentrations in road dust significantly exceeded those of "conventional" MP (Ø 5 g TW versus 0.3 g MP per kg road dust). Their study shows that abrasion particles from car tires and truck tires were detected in various environmental samples, including air, water, and sediments. A significant portion of TW is deposited on roads and their immediate surroundings. This fraction and the direct input of TW to inland waters from surface runoff or road runoff were neglected in the model. However, other studies indicate that a significant portion of tire abrasion enters surface waters directly via road runoff (Goehler et al., 2022; Arias et al., 2022).

With this work's new insight into the extent to which TW can be distributed, including through the pathway of soil erosion into the aquatic environment, it can be noted that the prevalence and potential consequences of TW particle pollution on the environment still need to be addressed. It should be noted that TW is of paramount importance compared to other MP sources, especially concerning MP reduction measures, not only for soil but also for water bodies and probably all different environmental compartments. Preventing MP in the soil will have little noticeable effect if TW remains unchanged. With this insight, this work puts the issue of TW in the environment in a new light. This is because TW is consequently the biggest problem in terms of impacting soils and, through soil erosion, neighboring systems as well. This problem should be considered more in future studies and interpretation of results (Knight et al., 2020a; Mennekes and Nowack, 2022; Knight et al., 2020b).

Studies on MP mass exposure often do not consider these types of elastomers. There is a lack of data on the composition and concentrations of TW compared to known "traditional" MP polymers such as polyethylene, polypropylene, and polystyrene (Mennekes and Nowack, 2022). Part of the difficulty in detecting tire wear in soils is a complex mixture of materials such as rubber, plastics, metals, and other additives. As a rubber, it also behaves differently than the classic plastic types (e.g., high density). This mixture can disperse in the soil and be mixed with other soil constituents, making accurate identification and quantification difficult. Analyzing tire wear in soil samples is technically challenging (Ding et al., 2023; Mennekes and Nowack, 2022).

Hence, more research is needed to understand the environmental impact of tire wear (TW) particles entering water bodies through soil erosion. TW contains rubber components and up to 60% additives, posing a significant threat as particles are released during daily traffic (Goßmann et al., 2021; Goehler et al., 2022; Yang et al., 2019). Unlike stationary soil particles, dissolved chemicals in water can disperse widely, an aspect underrepresented in microplastics (MP) research. Similar concerns were recognized for heavy metals and chemical leachates in the 1990s (Horner, 1996; Day et al., 1993; Stigliani et al., 1993), warranting attention in MP research (Ding et al., 2023; Sheng et al., 2021; Halle et al., 2021). TW and MP are known to bind pollutants and pathogens (Naqash et al., 2020; Bakir et al., 2012; Ma et al., 2019), including heavy metals, pesticides, and persistent organic pollutants (McCormick et al., 2014; De Tender et al., 2017). While soil studies on MP-related contaminant transport exist, field investigations are limited (Hüffer et al., 2019). The interplay between pollutants and MP mechanisms remains poorly understood (Li et al., 2020), but the risk of pollutants entering water bodies through soil-eroded plastic particles is significant.

Nevertheless, the results of this study confirm that current MP loading to arable soils is a long-term source of inland waters. Even if the input of MP to the environment is prevented, the MP delivery from soils via soil erosion will continue for many generations. Because of the low rates of MP loss through soil erosion and the long life of conventional plastics, MP particles accumulate in the soil over time (Huang et al., 2023a; Williams and Rangel-Buitrago, 2022). This phenomenon is similar to other environmental problems where pollutants accumulate in soils (e.g., phosphorus) and slowly enter inland waters via soil erosion (Daneshgar *et al.*, 2018).

Due to its diffuse nature, soil erosion is a challenging source of microplastic (MP) pollution in stream networks. Wastewater treatment plants, for example, can remove a significant amount of MP (up to 95%) from wastewater (Edo et al., 2020), but some particles still enter water streams as point sources. To reduce MP pollution, improved treatment plant technology, for example, can help with point source inputs, but diffuse inputs, on the other hand, can hardly be entirely controlled or stopped.

5 General conclusion

This comprehensive study has significantly contributed to understanding the transport of MP via soil erosion and the therefore linked the terrestrial MP sinks with the inland water system. Through field studies with plot-based rainfall simulations, it was able to investigate in detail the erosion potential of MP in arable soils and gain valuable insights. The results are based on long-term studies. A field trial was conducted over 1.5 years under actual arable field conditions. The field study allows for an accurate assessment of impacts over an extended period. This makes the results of the study significant and relevant for practice.

The field experiment revealed that MP particles with lower density, ranging from 53-300 µm, were preferentially eroded and transported compared to mineral soil. No significant correlation could be demonstrated concerning MP enrichment and particle size. Nevertheless, the function of MP sources and sinks in the soil is strongly influenced by the size of MP particles. MP_c (250-300 µm) is primarily lost through lateral erosion transport, while MP_f (53-100 µm) is mainly redistributed below the topsoil layer and protected from further erosion. The interaction of MP with soil changed over time, and thus the erosion rates of MP in the field experiment decreased. It was observed that the binding of MP particles to the soil matrix resulted in less accumulation of MP in sediment over time. The smaller MP_f particles were more strongly bound to soil particles than the larger MP_c particles. Aggregate formation plays a critical role in stabilizing MP in soil, reducing its mobility and potential for delivery into the stream network.

These findings show the complexity of the interactions between MP and soil. MP particles of different sizes exhibit different behaviors. This suggests that the size of MP particles is essential in their dispersion and fate in soil. The results also show that the binding of MP to the soil matrix plays an important role in reducing the mobility and potential release of MP to water bodies. The formation of aggregates between MP and soil particles positively affects the stabilization of MP in soil. This reduces the mobility of MP and minimizes the potential for their input into the aquatic network. Aggregate formation thus plays a crucial role in the removal potential of MP. In summary, particle properties and the interaction with soil could be identified as the specific processes of MP erosion and transport during heavy erosion events.

The field experiment is based on plot experiments. Therefore, the interpretation of the results is limited to this scale and may not apply to entire landscapes. Erosion processes such as rill or gully erosion were not considered. The study focuses mainly on the size of HDPE particles and their binding to soil particles. However, it does not view information on other potential influencing factors such as polymer type, agricultural practices, or environmental factors that could affect MP particle erosion and transport. More process-based studies are needed to understand the interaction between MP and soil.

A significant highlight of this work was using the SPEROS-MP model to model the spatially distributed transport of MP in a mesoscale landscape (400 km²). Integrating various data sources and parameters could simulate the behavior and distribution of MP particles in different scenarios and time frames. The estimation of MP sources to arable soils allowed the identification of potential input pathways and the analysis of the relationships between environmental factors and MP contamination in soil. The modeling considered data since 1950 and, in some cases, modeled up to 100 years into the future. This approach gives the work a unique quality, as it is based on comprehensive and long-term research. It opens new perspectives and helps to understand long-term trends and possible scenarios.

The MP transport within an exemplary (semi-virtual) mesoscale landscape via the soil erosion pathway was modeled. Various sources of MP, including sewage sludge, compost, atmospheric deposition, and tire wear TW, were considered. TW caused the most significant input of MP to arable land and was the most critical MP source leading to erosion-induced MP fluxes into a water stream network. Hence, the study highlights the significance of TW as a significant source of MP in the environment. Modeling results showed that only a small fraction (less than 0.2%) of all MP applied to arable land entered the stream network via soil erosion. However, the mass of MP entering the streams was still significant. The input of MP from soil erosion was comparable to the potential influx from wastewater treatment plants in the modeled rural region. This highlights the importance of considering soil erosion as a significant source of MP pollution in inland waters. Soil erosion links agricultural land and water bodies, facilitating the transfer of MP from terrestrial to aquatic environments. Moreover, considering soil redistribution is essential to understand the redistribution of MP within catchments. Consequently, soil erosion plays a significant role in the overall cycle of MP, impacting aquatic life and the environment.

The findings of this thesis reveal that despite the connectivity between terrestrial and aquatic systems through soil erosion, most MP applied to arable soil remains in the topsoil (0-20 cm). Regular tillage practices do change the MP concentration in the plough layer by burying MP below the plough layer. As in the stream network, the buried MP masses below the plough layer should not be ignored. Tillage can contribute to the translocation of MP to the soil surface, making it susceptible to surface runoff and water erosion over the long term. Even if no additional MP enters the soil, modeling scenarios indicate that similar rates of MP delivery can be expected until 2100. This confirms that soil acts as a long-term sink for MP while also serving as a continuous source of MP to inland waters. In conclusion, soils act as long-term reservoirs for MP and continuously release MP to water bodies.

Spatially targeted MP applications and changing MP only slightly affect the diffuse MP delivery to the stream network as tire wear fluxes are dominating this process. As soil erosion is critical in the overall MP cycle and impacts aquatic life and the environment, the study highlights the need for measures to reduce MP inputs, particularly tire abrasion, and to control soil erosion to reduce MP pollution in water bodies.

Overall, this thesis contributes to scientific knowledge and practical relevance of erosion-induced MP redistribution in and MP delivery from arable landscapes, based on long-term studies, field experiments under natural conditions, and model-based analysis of mesoscale catchments. It provides first valuable insights that are important for future research. However, there are still areas for improvement in MP-erosion research, especially in standardized detection methods, quantification of MP pollution in the terrestrial environment, as well as process understanding and adapted model parametrization.

List of figures

Figure 1: Schematic representation of emission and immission processes of microplastics in the soil system, including potential sources, input pathways, and ecological effects (adopted from Rehm and Fiener 2020).. 7

Figure 2: Graphical overview about field experiment and laboratory analysis. In the field experiment, considered and investigated factors related to MP transport behavior and MP topsoil concentration and thus determining effects on the potential transport of HDPE MP particles... 21

Figure 3: Top and side view of the set up in the field for a 1.5 years experiment for lateral (left side) and vertical (right side) high density polyethylene (HDPE) microplastic (MP) movement observation. For lateral movement, MP (MPf is fine MP, 53-100 µm; MPc is coarse MP, 250-300 µm) was added to the topsoil of paired plots (A and B) and treated with a series of rainfall simulations. For vertical movement, stainless-steel cylinders were inserted into the soil to study the vertical movement of MP. 24

Figure 4: Scheme of the laboratory extraction of high density polyethylene (HDPE) microplastic (MP) from the soil samples, considering the micro- and macro-aggregates (MP_{free} is MP not bound to soil particles and aggregates; MP_{bound} is MP bound to soil particles or aggregates). MP_f is fine MP, 53-100 µm; MP_c is coarse MP, 250-300 µm. Grey boxes represent filters that have been analysed with the digital microscope. 29

Figure 5: After density separation, high density polyethylene (HDPE) microplastic (MP) and organic matter particles from the sediment samples were filtered out on black filters (a, c). For the detection of the white MP reference particles a digital microscope was used based on color. The white MP particles were captured (green = detected particles), while the brown colored organic material remained undetected (b, d). 31

Figure 6: Surface run off (a, b), sediment delivery (c, d), coarse microplastic (MP_c, 250-300 µm) delivery (e, f) and fine microplastic (MP_f, 53-100 µm) delivery (g, h) of the rainfall simulations 1, 2 and 3 (RS1, RS2 and RS3) in both soil types (silty loam and loamy sand). Each simulation is shown with two lines, which represent the two installed plots A and B on each soil type. The X-axis shows the time of a rainfall simulation run (0-30 min dry run, 30-60 min wet run).. 35

Figure 8: Microplastic (MP) enrichment ratios of coarse MP (MPc, 250-300 µm) particles (a, b) and fine MP (MPf, 53-100 µm) particles (c, d) in the delivered sediment of two soil types (loamy sand and silty loam) during the rainfall simulations 1, 2 and 3 (RS1, RS2 and RS3). A preferential erosion of MP is shown by a mean enrichment factor >1 in all simulations. Boxes present all single sample values during the runs and show the median and the 1st and

3rd quartile, whiskers give the minimum and maximum; the stars present mean values per run; the dashed line indicates the relative initial concentration in topsoil < 1 cm (factor 1). 37

Figure 9: The increasing amount of coarse microplastic ($MP_{c\ bound}$, 250-300 µm) particles (a, b) and fine microplastic ($MP_{f\ bound}$, 53-100 µm) particles (c, d) in the delivered sediment which was bound to soil particles or aggregates during the rainfall simulations 1, 2 and 3 (RS1, RS2 and RS3) on two soil types (loamy sand and silty loam). Boxplots present all single sample values during the rainfall simulation runs and show the median and the 1st and 3rd quartile, whiskers give the minimum and maximum; the stars present mean values per run. 38

Figure 10: Graphical overview about the model based analysis. The model-based approach considered and investigated factors related to MP transport through the landscape of a mesoscale river basin. 47

Figure 11: The Glonn catchment (400 km²) representing a typical intensively used arable landscape in Southern Germany with highly erosion rates. The left and right illustration shows the land use and the soil erosion in t ha^{-1} a^{-1} within in the catchment, respectively. The black rectangle in the catchment marks the section of the detailed maps in Fig. 13. 48

Figure 12: a) The MP emissions for arable land in Bavaria from the different sources, tire wear (TW), sewage sludge (SL), compost (CO) and atmospheric deposition (AT), from 1950 to 2020. b) The development of plastics production in Germany and the population of Bavaria since 1950. c) Amount of application of sewage sludge and compost as fertilizer on Bavarian arable land. d) The number of registered cars and trucks in Bavaria since 1950. 55

Figure 13: The distribution of tire wear in the soil relative to the distance from the road. Literature values are based on direct detection of tire wear (Müller et al. 2022) or on the estimated concentrations of tire wear particles based on chemical markers (Motto et al. 1970, Wheeler and Dave 2009; Wik and Dave 2009; Wekenthin et al. 2014). The markers show the individual values, the dashed lines show the mean of the respective reference. The black line represents the median of all literature values used for modelling in this study........... 58

Figure 14: Measured and modelled sediment delivery (1968 to 2020) at the outlet of the Glonn catchment. The blue and orange lines represent the measured and modelled means, respectively. The boxplots show the variability of the data. They show the median (line) and mean (star) and the 1st and 3rd quartile, whiskers give the minimum and maximum. 60

Figure 15: MP delivery into the Glonn shown individually for tire wear (TW), sewage sludge (SL), compost (CO) and atmospheric deposition (AT) or the sum of TW, SL, CO and AT (SUM). The dashed line gives the year 2020 as the starting point for different scenarios. For comparison, the amount of MP delivery through wastewater treatment plants (WWTPs) in 2020 is shown as a red line (min. and max. as dashed lines). a) MP delivery into the Glonn river between 1950 and 2020. b) Result of scenario S1 with the assumption that the MP input will continue as in 2020. c) Result of scenario S2. Compost and sewage sludge are applied to arable land at a distance of > 100 m and < 100 m from water streams. d) Result of scenario S3 with no MP input at all from 2020 onwards. 63

Figure 16: Example of catchment segment (for location, see Figure 10) illustrating microplastic (MP) input on arable land and results of erosion modeling between 1950 and 2020. The maps show the situation in 2020. a) Field-based land use. b) Total MP input from sewage sludge, compost, and atmospheric input (without TW) as a mean value over all arable land. c) MP input from TW, spatially distributed to individual arable fields along the roads. d) MP concentration below the plough layer. e) MP transported to other land uses via soil erosion. f) MP distribution after water and tillage erosion on arable land. 64

Figure 17: Result of scenario S2 individually shown for tire wear (TW) and sewage sludge (SL) and compost (CO) as organic fertilizer applied to arable land at a distance of > 100 m and < 100 m from water streams. For comparison, the amount of MP delivery through wastewater treatment plants (WWTP) in 2020 as red lines (min and max as dashed lines). 65

List of tables

Table 1: Used microplastic (MP) concentrations (I-IV) (mg g^{-1} soil) for quality controlof the microplastic extraction method. Each concentration was mixed with 20 g soil and presents 3 replicates in two soil types (total n = 48). MP_f = fine MP, 53-100 µm; MP_c = coarse MP, 250-300 µm.. 32

Table 2: Mean soil moisture conditions measured at ten plot locations before starting the rainfall simulations (RS), 15 min after the dry runs and 15 min after the wet run; within plot moisture, variability is indicated as ± standard deviation. 33

Table 3: Mean lateral microplastic (MP_f = fine MP, 53-100 µm; MP_c = coarse MP, 250-300 µm) loss after rainfall simulation 1, 2 and 3 (RS1, RS2 and RS3) and mean vertical MP_c and MP_f loss (steel cylinders) relative to MP_c and MP_f amounts added to topsoil at the beginning of the experiment in percent. The lateral loss presents the mean of two plots per soil type (n = 2), vertical loss presents mean ± standard deviation of three pipes per soil type (n = 3)......... 34

Table 4: USLE factors used in SPEROS-MP.. 51

Table 5: MP inputs into arable soils within the test catchment, separated by different sources. All values are listed for the modelled time span 1950–2020 and separately for the year 2020. 56

Table 6: Soil erosion-induced MP delivery to the Glonn stream network, as well as redistribution to grassland and forest. The MP vertical loss below the plough layer is also given. All values are listed for the modelled time span 1950–2020 and separately for the year 2020. 62

References

Accinelli, C., Abbas, H. K., Bruno, V., Vicari, A., Little, N. S., Ebelhar, M. W. & Shier, W. T. (2021). Minimizing abrasion losses from film-coated corn seeds. *Journal of Crop Improvement* 35(5): 666-678.

Adhikari, S., Kelkar, V., Kumar, R. & Halden, R. U. (2022). Methods and challenges in the detection of microplastics and nanoplastics: a mini-review. *Polymer International* 71(5): 543-551.

Ajith, N., Arumugam, S., Parthasarathy, S., Manupoori, S. & Janakiraman, S. (2020). Global distribution of microplastics and its impact on marine environment-a review. *Environmental Science and Pollution Research*. (27): 25970-25986.

Amadei, A. M., Sanyé-Mengual, E. & Sala, S. (2022). Modeling the EU plastic footprint: Exploring data sources and littering potential. *Resources, Conservation and Recycling* (178): 106086.

Angers, D. A., Bullock, M. & Mehuys, G. (2008). Aggregate stability to water. *Soil Sampling and Methods of Analysis* 2: 811-819.

Auerswald, K., Kainz, M., Schröder, D. & Martin, W. (1992). Comparison of German and Swiss rainfall simulators-experimental setup. *Zeitschrift für Pflanzenernährung und Bodenkunde* 155(1): 1-5.

Aves, A. R., Revell, L. E., Gaw, S., Ruffell, H., Schuddeboom, A., Wotherspoon, N. E., LaRue, M. & McDonald, A. J. (2022). First evidence of microplastics in Antarctic snow. *The Cryosphere* 16(6): 2127-2145.

Baensch-Baltruschat, B., Kocher, B., Kochleus, C., Stock, F. & Reifferscheid, G. (2021). Tyre and road wear particles-A calculation of generation, transport and release to water and soil with special regard to German roads. *Science of the Total Environment* (752): 141939.

Barnes, D. K. A., Galgani, F., Thompson, R. C. & Barlaz, M. (2009). Accumulation and fragmentation of plastic debris in global environments. *Philosophical Transactions of the Royal Society B-Biological Sciences* 364(1526): 1985-1998.

Baruah, A., Sharma, A., Sharma, S. & Nagraik, R. (2022). An insight into different microplastic detection methods. *International Journal of Environmental Science and Technology* 19(6): 5721-5730.

Bastos, D. & De las Nieves, F. (1994). Colloidal stability of sulfonated polystyrene model colloids. Correlation with electrokinetic data. *Colloid and Polymer Science* 272(5): 592-597.

BAYSIS, B. S. (2015). Straßenverkehrszählungen (SVZ). Zählerstellenauswahl. https://www.baysis.bayern.de/internet/verdat/svz/zaehlstelle/index.html (06.07.2023)

Bergmann, M., Almroth, B. C., Brander, S. M., Dey, T., Green, D. S., Gundogdu, S., Krieger, A., Wagner, M. & Walker, T. R. (2022). A global plastic treaty must cap production. *Science* 376(6592): 469-470.

Bertling, J., Zimmermann, T. & Rödig, L. (2021). Kunststoffe in der Umwelt: Emissionen in landwirtschaftlich genutzte Böden. Fraunhofer UMSICHT. Oberhausen.

Bertol, I., Engel, F., Mafra, A., Bertol, O. & Ritter, S. (2007). Phosphorus, potassium and organic carbon concentrations in runoff water and sediments under different soil tillage systems during soybean growth. *Soil and Tillage Research* 94(1): 142-150.

Bhattacharyya, S., Gorain, S., Patra, M., Rajwar, A. K., Gope, D., Giri, S. K., Pal, J., Mahato, M., Barik, S. & Biswas, S. J. (2022). Microplastics, Their toxic effects on living Organisms in soil biota and their fate: an appraisal. *In: Shit, P.K., Adhikary, P.P., Bhunia, G.S., Sengupta, D. (eds) Soil Health and Environmental Sustainability. Environmental Science and Engineering. Springer, Cham.*

Bläsing, M. & Amelung, W. (2018). Plastics in soil: Analytical methods and possible sources. *Science of the Total Environment* 612: 422-435.

Boardman, J., Vandaele, K., Evans, R. & Foster, I. D. (2019). Off-site impacts of soil erosion and runoff: Why connectivity is more important than erosion rates. *Soil Use and Management* 35(2): 245-256.

Boots, B., Russell, C. W. & Green, D. S. (2019). Effects of microplastics in soil ecosystems: Above and below Ground. *Environmental Science & Technology*. 53,19.

Borrelle, S. B., Ringma, J., Law, K. L., Monnahan, C. C., Lebreton, L., McGivern, A., Murphy, E., Jambeck, J., Leonard, G. H. & Hilleary, M. A. (2020). Predicted growth in plastic waste exceeds efforts to mitigate plastic pollution. *Science* 369(6510): 1515-1518.

Bouchard, D., Zhang, W. & Chang, X. (2013). A rapid screening technique for estimating nanoparticle transport in porous media. *Water Research* 47(12): 4086-4094.

Brahney, J., Hallerud, M., Heim, E., Hahnenberger, M. & Sukumaran, S. (2020). Plastic rain in protected areas of the United States. *Science* 368(6496): 1257-1260.

Brandes, E. (2020). Die Rolle der Landwirtschaft bei der (Mikro-) Plastik-Belastung in Böden und Oberflächengewässern.*Mitt Umweltchen Ökotox* (4): 111-114.

Brandes, E., Henseler, M. & Kreins, P. (2021). Identifying hot-spots for microplastic contamination in agricultural soils - a spatial modelling approach for Germany. *Environmental Research Letters* 16(10): 104041.

Brandhuber, R., Auerswald, K., Lang, R., Müller, A. & Treisch, M. (2018). ABAG interaktiv, Version 2.0. Bayerische Landesanstalt für Landwirtschaft, Freising. https://www.lfl.bayern.de/mam/cms07/publikationen/daten/informationen/bodenerosion-lfl-information.pdf (06.07.2023)

Braun, M., Mail, M., Heyse, R. & Amelung, W. (2021). Plastic in compost: Prevalence and potential input into agricultural and horticultural soils. *Science of the Total Environment* (760): 143335.

Braun, U., Altmann, K., Bannick, C. G., Becker, R., Ritter, H., Bochow, M., Dierkes, G., Enders, K., Eslahian, K. & Fischer, D. (2020). Mikroplastik-Analytik: Probenahme, Probenaufbereitung und Detektionsverfahren. Statuspapier im Rahmen des Forschungsschwerpunktes" Plastik in der Umwelt-Quellen, Senken, Lösungsansätze". https://bmbf-plastik.de/sites/default/files/2020-11/Statuspapier_Mikroplastik%20Analytik_Plastik%20in%20der%20Umwelt_2020.pdf (06.08.2023)

Brown, R. W., Chadwick, D. R., Thornton, H., Marshall, M. R., Bei, S., Distaso, M. A., Bargiela, R., Marsden, K. A., Clode, P. L. & Murphy, D. V. (2022). Field application of pure polyethylene microplastic has no significant short-term effect on soil biological quality and function. *Soil Biology and Biochemistry* (165): 108496.

Browne, M. A., Niven, S. J., Galloway, T. S., Rowland, S. J. & Thompson, R. C. (2013). Microplastic moves pollutants and additives to worms, reducing functions linked to health and biodiversity. *Curr Biol* 23(23): 2388-2392.

Bullard, J. E., Ockelford, A., O'Brien, P. & Neuman, C. M. (2021). Preferential transport of microplastics by wind. *Atmospheric Environment* (245): 118038.

Cai, Y., Wu, J., Lu, J., Wang, J. & Zhang, C. (2022). Fate of microplastics in a coastal wastewater treatment plant: Microfibers could partially break through the integrated membrane system. *Frontiers of Environmental Science & Engineering* 16(7): 1-10.

Campanale, C., Galafassi, S., Savino, I., Massarelli, C., Ancona, V., Volta, P. & Uricchio, V. F. (2022). Microplastics pollution in the terrestrial environments: Poorly known diffuse sources and implications for plants. *Science of The Total Environment* (805): 150431.

Cerro, I., Sanchez-Perez, J. M., Ruiz-Romera, E. & Antigüedad, I. (2014). Variability of particulate (SS, POC) and dissolved (DOC, NO3) matter during storm events in the Alegria agricultural watershed. Hydrological Processes 28(5): 2855-2867.

Chauhan, S. & Basri, S. (2022). Microplastics in terrestrial soils: Occurrence, analysis, and remediation. In: *New Trends in Emerging Environmental Contaminants. Energy, Environment, and Sustainability*. Springer, Singapore.

Chen, H., Zou, X., Ding, Y., Wang, Y., Fu, G. & Yuan, F. (2022). Are microplastics the 'technofossils' of the Anthropocene? *Anthropocene Coasts* 5(1): 8.

Chia, R. W., Lee, J.-Y., Jang, J., Kim, H. & Kwon, K. D. (2022). Soil health and microplastics: a review of the impacts of microplastic contamination on soil properties. *Journal of Soils and Sediments* 22(10): 2690-2705.

Chia, R. W., Lee, J.-Y., Kim, H. & Jang, J. (2021). Microplastic pollution in soil and groundwater: A review. *Environmental Chemistry Letters* 19(6): 4211-4224.

Colin, G., Cooney, J., Carlsson, D. & Wiles, D. (1981). Deterioration of plastic films under soil burial conditions. *Journal of Applied Polymer Science* 26(2): 509-519.

Coppock, R. L., Cole, M., Lindeque, P. K., Queirós, A. M. & Galloway, T. S. (2017). A small-scale, portable method for extracting microplastics from marine sediments. *Environmental pollution* (230): 829-837.

Corcoran, P. L. (2022). Degradation of microplastics in the environment. In *Handbook of Microplastics in the Environment*, 531-542: Springer. Cham.

Crossman, J., Hurley, R. R., Futter, M. & Nizzetto, L. (2020). Transfer and transport of microplastics from biosolids to agricultural soils and the wider environment. *Science of the Total Environment* (724): 138334.

Da Luz, J. M., Paes, S. A., Bazzolli, D. M., Totola, M. R., Demuner, A. J. & Kasuya, M. C. (2014). Abiotic and biotic degradation of oxo-biodegradable plastic bags by Pleurotus ostreatus. *PLoS One* 9(11): e107438.

Daneshgar, S., Callegari, A., Capodaglio, A. G. & Vaccari, D. (2018). The potential phosphorus crisis: resource conservation and possible escape technologies: a review. *Resources* 7(2): 37.

De Silva, Y., Rajagopalan, U. & Kadono, H. (2021). Microplastics on the growth of plants and seed germination in aquatic and terrestrial ecosystems. *Global Journal of Environmental Science and Management* 7(3): 347-368.

De Souza Machado, A. A., Kloas, W., Zarfl, C., Hempel, S. & Rillig, M. C. (2017). Microplastics as an emerging threat to terrestrial ecosystems. *Global Change Biology*. 24(4), 1405-1416.

De Souza Machado, A. A., Lau, C. W., Kloas, W., Bergmann, J., Bachelier, J. B., Faltin, E., Becker, R., Görlich, A. S. & Rillig, M. C. (2019). Microplastics can change soil properties and affect plant performance. *Environmental Science & Technology* 53(10): 6044-6052.

De Souza Machado, A. A., Lau, C. W., Till, J., Kloas, W., Lehmann, A., Becker, R. & Rillig, M. C. (2018). Impacts of microplastics on the soil biophysical environment. *Environmental Science & Technology* 52(17): 9656-9665.

Desmet, P. & Govers, G. (1996). A GIS procedure for automatically calculating the USLE LS factor on topographically complex landscape units. *Journal of Soil and Water Conservation* 51(5): 427-433.

Dierkes, G., Lauschke, T., Becher, S., Schumacher, H., Földi, C. & Ternes, T. (2019). Quantification of microplastics in environmental samples via pressurized liquid extraction and pyrolysis-gas chromatography. *Analytical and Bioanalytical Chemistry* 411(26): 6959-6968.

Ding, J., Liu, C., Chen, Q., Zhang, Z., Han, J., Liang, A., Zhu, D., Wang, H., Lv, M. & Chen, L. (2022). Extractable additives in microplastics: A hidden threat to soil fauna. *Environmental Pollution* (294): 118647.

Dlugoß, V., Fiener, P., Van Oost, K. & Schneider, K. (2012). Model based analysis of lateral and vertical soil carbon fluxes induced by soil redistribution processes in a small agricultural catchment. *Earth Surface Processes and Landforms* 37(2): 193-208.

Dong, S., Xia, J., Sheng, L., Wang, W., Liu, H. & Gao, B. (2021). Transport characteristics of fragmental polyethylene glycol terephthalate (PET) microplastics in porous media under various chemical conditions. *Chemosphere* (276): 130214.

Dris, R., Imhof, H., Sanchez, W., Gasperi, J., Galgani, F., Tassin, B. & Laforsch, C. (2015). Beyond the ocean: contamination of freshwater ecosystems with (micro-)plastic particles. *Environmental Chemistry* 12(5): 539-550.

Du, X., Jian, J., Du, C. & Stewart, R. D. (2022). Conservation management decreases surface runoff and soil erosion. *International Soil and Water Conservation Research* 10(2): 188-196.

Dümichen, E., Barthel, A.-K., Braun, U., Bannick, C. G., Brand, K., Jekel, M. & Senz, R. (2015). Analysis of polyethylene microplastics in environmental samples, using a thermal decomposition method. *Water Research* (85): 451-457.

Deutscher Wetterdienst DWD (2020). Klimadaten direkt zum Download. 3. Rasterfelder für Deutschland. https://www.dwd.de/DE/leistungen/cdc/cdc_ueberblick-klimadaten.html (06.07.2023)

Edo, C., González-Pleiter, M., Leganés, F., Fernández-Piñas, F. & Rosal, R. (2020). Fate of microplastics in wastewater treatment plants and their environmental dispersion with effluent and sludge. *Environmental Pollution* (259): 113837.

Ehlers, S. M., Manz, W. & Koop, J. H. (2019). Microplastics of different characteristics are incorporated into the larval cases of the freshwater caddisfly Lepidostoma basale. *Aquatic Biology* (28): 67-77.

Eibes, P. M. & Gabel, F. (2022). Floating microplastic debris in a rural river in Germany: Distribution, types and potential sources and sinks. *Science of the Total Environment* (816): 151641.

Elert, A. M., Becker, R., Duemichen, E., Eisentraut, P., Falkenhagen, J., Sturm, H. & Braun, U. (2017). Comparison of different methods for MP detection: What can we learn from them, and why asking the right question before measurements matters? *Environmental Pollution.* 231(Pt 2): 1256-1264.

Van Emmerik, T., Mellink, Y., Hauk, R., Waldschläger, K. & Schreyers, L. (2022). Rivers as plastic reservoirs. *Frontiers in Water* (3): 212.

Espí, E., Salmerón, A., Fontecha, A., García, Y. & Real, A. I. (2016). PLastic Films for Agricultural Applications. *Journal of Plastic Film & Sheeting* 22(2): 85-102.

Fan, Y., Zheng, K., Zhu, Z., Chen, G. & Peng, X. (2019). Distribution, sedimentary record, and persistence of microplastics in the Pearl River catchment, China. *Environmental Pollution* (251): 862-870.

Feuilloley, P., César, G., Benguigui, L., Grohens, Y., Pillin, I., Bewa, H., Lefaux, S. & Jamal, M. (2005). Degradation of polyethylene designed for agricultural purposes. *Journal of Polymers and the Environment* 13(4): 349-355.

Fiener, P., Dlugoß, V. & Van Oost, K. (2015). Erosion-induced carbon redistribution, burial and mineralisation - Is the episodic nature of erosion processes important? *Catena* (133): 282-292.

Fiener, P., Dostál, T., Krása, J., Schmaltz, E., Strauss, P. & Wilken, F. (2020). Operational USLE-based modelling of soil erosion in Czech Republic, Austria, and Bavaria - Differences in model adaptation, parametrization, and data availability. *Applied Sciences* 10(10): 3647.

Fiener, P., Govers, G. & Van Oost, K. (2008). Evaluation of a dynamic multi-class sediment transport model in a catchment under soil-conservation agriculture. *Earth Surface Processes and Landforms* (33): 1639-1660.

Fiener, P., Wilken, F., Aldana-Jague, E., Deumlich, D., Gómez, J., Guzmán, G., Hardy, R., Quinton, J., Sommer, M. & Van Oost, K. (2018). Uncertainties in assessing tillage erosion–how appropriate are our measuring techniques? *Geomorphology* (304): 214-225.

Foster, G., Young, R., Römkens, M. & Onstad, C. (1985). Processes of soil erosion by water. *Soil erosion and crop productivity*: 137-162. American Society of Agronomy. Madison.

Franzluebbers, A. & Stuedemann, J. (2002). Particulate and non-particulate fractions of soil organic carbon under pastures in the Southern Piedmont USA. *Environmental Pollution* (116): S53-S62.

Frias, J. P. & Nash, R. (2019). Microplastics: Finding a consensus on the definition. *Marine Pollution Bulletin* (138): 145-147.

Fries, E., Dekiff, J. H., Willmeyer, J., Nuelle, M.-T., Ebert, M. & Remy, D. (2013). Identification of polymer types and additives in marine microplastic particles using pyrolysis-GC/MS and scanning electron microscopy. *Environmental Science: Processes & Impacts* 15(10): 1949-1956.

Gasperi, J., Wright, S. L., Dris, R., Collard, F., Mandin, C., Guerrouache, M., Langlois, V., Kelly, F. J. & Tassin, B. (2018). Microplastics in air: Are we breathing it in? *Current Opinion in Environmental Science & Health* (1): 1-5.

Gehrke, I., Dresen, B., Blömer, J., Sommer, H., Lindow, F. & Röckle, R. (2021). Tyre Wear Mapping. Digitales Planungs- und Entscheidungsinstrument zur Verteilung, Ausbreitung und Quantifizierung von Reifenabrieb in Deutschland. Schlussbericht. Fraunhofer UMSICHT. Oberhausen.

Geyer, R., Jambeck, J. R. & Law, K. L. (2017). Production, use, and fate of all plastics ever made. *Science Advances* 3(7): e1700782.

Gong, J. & Xie, P. (2020). Research progress in sources, analytical methods, eco-environmental effects, and control measures of microplastics. *Chemosphere* (254): 126790.

Govers, G., Vandaele, K., Desmet, P., Poesen, J. & Bunte, K. (1994). The role of tillage in soil redistribution on hillslopes. *European Journal of Soil Science* (45): 469-478.

Guo, J.-J., Huang, X.-P., Xiang, L., Wang, Y.-Z., Li, Y.-W., Li, H., Cai, Q.-Y., Mo, C.-H. & Wong, M.-H. (2020). Source, migration and toxicology of microplastics in soil. *Environment International* (137): 105263.

Guo, Z., Boeing, W. J., Xu, Y., Borgomeo, E., Mason, S. A. & Zhu, Y.-G. (2021). Global meta-analysis of microplastic contamination in reservoirs with a novel framework. *Water Research* (207): 117828.

Habib, R. Z., Thiemann, T. & Al Kendi, R. (2020). Microplastics and wastewater treatment plants—a review. *Journal of Water Resource and Protection* 12(01): 1.

Hachem, A., Vox, G. & Convertino, F. (2023). Prospective scenarios for addressing the agricultural plastic waste issue: Results of a territorial analysis. *Applied Sciences* 13(1): 612.

Hale, R. C., Seeley, M. E., La Guardia, M. J., Mai, L. & Zeng, E. Y. (2020). A global perspective on microplastics. *Journal of Geophysical Research-Oceans* 125(1), e2018JC014719.

Han, N., Zhao, Q., Ao, H., Hu, H. & Wu, C. (2022). Horizontal transport of macro-and microplastics on soil surface by rainfall induced surface runoff as affected by vegetations. *Science of the Total Environment* (831): 154989.

Haregeweyn, N., Poesen, J., Verstraeten, G., Govers, G., de Vente, J., Nyssen, J., Deckers, J. & Moeyersons, J. (2013). Assessing the performance of a spatially distributed soil erosion and sediment delivery model (WATEM/SEDEM) in Northern Ethiopia. *Land Degradation & Development* 24(2): 188-204.

He, L., Li, Z., Jia, Q. & Xu, Z. (2023). Soil microplastics pollution in agriculture. *Science* 379(6632): 547-547.

He, Y. T., Wan, J. & Tokunaga, T. (2008). Kinetic stability of hematite nanoparticles: the effect of particle sizes. *Journal of Nanoparticle Research* 10(2): 321-332.

Heinze, W. M., Mitrano, D. M. & Cornelis, G. (2022). Bioturbation-driven transport of microplastic fibres in soil. EGU General Assembly 2022, Vienna, Austria, 23–27 May 2022, EGU22-7987, https://doi.org/10.5194/egusphere-egu22-7987, 2022.

Hillenbrand, T., Toussaint, D., Boehm, E., Fuchs, S., Scherer, U., Rudolphi, A. & Hoffmann, M. (2005). Discharges of copper, zinc and lead to water and soil. Analysis of the emission pathways and possible emission reduction measures; (Eintraege von Kuper, Zink und Blei in Gewaesser und Boeden. Analyse der Emissionspfade und moeglicher Emissionsminderungsmassnahmen.). https://www.osti.gov/etdeweb/biblio/21097529 (06.07.2023)

Hodkovicova, N., Hollerova, A., Svobodova, Z., Faldyna, M. & Faggio, C. (2022). Effects of plastic particles on aquatic invertebrates and fish – A review. *Environmental Toxicology and Pharmacology* (96): 104013.

Horton, A. A. (2022). Plastic pollution: when do we know enough? *Journal of Hazardous Materials* (422): 126885.

Horton, A. A., Walton, A., Spurgeon, D. J., Lahive, E. & Svendsen, C. (2017). Microplastics in freshwater and terrestrial environments: Evaluating the current understanding to identify the knowledge gaps and future research priorities. *Science of the Total Environment* (586): 127-141.

Hu, F., Xu, C., Li, H., Li, S., Yu, Z., Li, Y. & He, X. (2015). Particles interaction forces and their effects on soil aggregates breakdown. *Soil and Tillage Research* (147): 1-9.

Huang, H., Mohamed, B. A. & Li, L. Y. (2023). Accumulation and fate of microplastics in soils after application of biosolids on land: A review. *Environmental Chemistry Letters* (21): 1745-1759.

Huang, Z., Hu, B. & Wang, H. (2023b). Analytical methods for microplastics in the environment: a review. *Environmental Chemistry Letters* 21(1): 383-401.

Huerta Lwanga, E., Gertsen, H., Gooren, H., Peters, P., Salanki, T., van der Ploeg, M., Besseling, E., Koelmans, A. A. & Geissen, V. (2016). Microplastics in the terrestrial ecosystem: Implications for Lumbricus terrestris (Oligochaeta, Lumbricidae). *Environmental Science Technology* 50(5): 2685-2691.

Huerta Lwanga, E., Thapa, B., Yang, X., Gertsen, H., Salanki, T., Geissen, V. & Garbeva, P. (2017). Decay of low-density polyethylene by bacteria extracted from earthworm's guts: A potential for soil restoration. *Science of the Total Environment* (624): 753-757.

Hurley, R. R. & Nizzetto, L. (2018). Fate and occurrence of micro(nano)plastics in soils: Knowledge gaps and possible risks. *Current Opinion in Environmental Science & Health* (1): 6-11.

Jahn, A. (2020).Microplastic in our environment: A review of the biggest perpetrators and possible solutions. Wien.

Ju, H., Zhu, D. & Qiao, M. (2019). Effects of polyethylene microplastics on the gut microbial community, reproduction and avoidance behaviors of the soil springtail, Folsomia candida. *Environmental Pollution* (247): 890-897.

Junghänel, T., Ertel, H., Deutschländer, T. & Wetterdienst, D. (2010). KOSTRA-DWD-2010R. *Bericht zur Revision der koordinierten Starkregenregionalisierung und-auswertung des Deutschen Wetterdienstes in der Version*. https://www.dwd.de/DE/leistungen/kostra_dwd_rasterwerte/download/bericht_revision_kostra_dwd_2010.pdf?__blob=publicationFile&v=6 (06.07.2023)

Kainz, M., Auerswald, K. & Vöhringer, R. (1992). Comparison of German and Swiss rainfall Simulators-utility, labour demands and costs. *Zeitschrift fuer Pflanzenernaehrung und Bodenkunde (Germany, FR)*, 155.7-11 (1997).

Kappler, A., Windrich, F., Loder, M. G., Malanin, M., Fischer, D., Labrenz, M., Eichhorn, K. J. & Voit, B. (2015). Identification of microplastics by FTIR and Raman microscopy: a novel silicon filter substrate opens the important spectral range below 1300 cm(-1) for FTIR transmission measurements. *Anal Bioanal Chem* 407(22): 6791-6801.

Keller, B., Centeri, C., Szabó, J. A., Szalai, Z. & Jakab, G. (2021). Comparison of the applicability of different soil erosion models to predict soil erodibility factor and event soil losses on loess slopes in Hungary. *Water* 13(24): 3517.

Khan, M. A., Huang, Q., Khan, S., Wang, Q., Huang, J., Fahad, S., Sajjad, M., Liu, Y., Mašek, O. & Li, X. (2023). Abundance, spatial distribution, and characteristics of microplastics in agricultural soils and their relationship with contributing factors. *Journal of Environmental Management* (328): 117006.

Kim, Y.-N., Yoon, J.-H. & Kim, K.-H. J. (2021). Microplastic contamination in soil environment–a review. *Soil Science Annual* 71(4): 300-308.

Klein, M. & Fischer, E. K. (2019). Microplastic abundance in atmospheric deposition within the metropolitan area of Hamburg, Germany. *Science of the Total Environment* (685): 96-103.

Klíč, R., Kravka, M., Wimmerová, L., Viruez, J. L. G., Válová, M. & Miháliková, M. (2022). Microplastics locked in water-stable aggregates of the haplic luvisol and role of land use on their potential mobility. *Water, Air & Soil Pollution* 233(2): 1-13.

Klingelhöfer, D., Braun, M., Quarcoo, D., Brüggmann, D. & Groneberg, D. A. (2020). Research landscape of a global environmental challenge: Microplastics. *Water Research* (170): 115358.

Knight, L. J., Parker-Jurd, F. N., Al-Sid-Cheikh, M. & Thompson, R. C. (2020). Tyre wear particles: an abundant yet widely unreported microplastic? *Environmental Science and Pollution Research* (27): 18345-18354.

Kocher, B., Brose, S., Feix, J., Görg, C., Peters, A. & Schenker, K. (2010). Stoffeinträge in den Straßenseitenraum-Reifenabrieb. Berichte der Bundesanstalt fuer Strassenwesen. Unterreihe Verkehrstechnik (188). https://bast.opus.hbz-nrw.de/opus45-bast/frontdoor/deliver/index/docId/60/file/V188.pdf (06.07.2023)

Koelmans, A. A., Redondo-Hasselerharm, P. E., Nor, N. H. M., de Ruijter, V. N., Mintenig, S. M. & Kooi, M. (2022). Risk assessment of microplastic particles. *Nature Reviews Materials* 7(2): 138-152.

Koutnik, V. S., Leonard, J., Alkidim, S., DePrima, F., Ravi, S., Hoek, E. & Mohanty, S. K. (2021). Distribution of microplastics in soil and freshwater environments: Global analysis and framework for transport modeling. *Environmental Pollution* (274): 116552.

Krasa, J., Dostal, T., Van Rompaey, A., Vaska, J. & Vrana, K. (2005). Reservoirs' siltation measurments and sediment transport assessment in the Czech Republic, the Vrchlice catchment study. *Catena* 64(2-3): 348-362.

Krekelbergh, N., Li, J., Hu, J., Sleutel, S., Parakhonskiy, B., Skirtach, A. & De Neve, S. (2022). Fluorescence microscopy versus Raman spectroscopy for direct identification of small (< 2 µm) microplastics in soils. https://eartharxiv.org/repository/view/3287/

Kumar, A., Mishra, S., Pandey, R., Yu, Z. G., Kumar, M., Khoo, K. S., Thakur, T. K. & Show, P. L. (2022). Microplastics in terrestrial ecosystems: Un-ignorable impacts on soil characterises, nutrient storage and its cycling. *TrAC Trends in Analytical Chemistry* (158), 116869.

Lal, R. (2015). Restoring soil quality to mitigate soil degradation. *Sustainability* 7(5): 5875-5895.

Lambert, S. & Wagner, M. (2018). Microplastics are contaminants of emerging concern in freshwater environments: an overview. In *Freshwater Microplastics*, 1-23: Springer. Frankfurt.

Lamichhane, G., Acharya, A., Marahatha, R., Modi, B., Paudel, R., Adhikari, A., Raut, B., Aryal, S. & Parajuli, N. (2022). Microplastics in environment: global concern, challenges, and controlling measures. *International Journal of Environmental Science and Technology* (20): 4673–4694.

Lebreton, L. & Andrady, A. (2019). Future scenarios of global plastic waste generation and disposal. *Palgrave Communications* 5(1): 1-11.

Lechthaler, S. (2020). Makroplastik in der Umwelt. Betrachtung terrestrischer und aquatischer Bereiche. Springer. Vieweg. XIV, 77.

Van Leeuwen, J., Walker, T. R. & Vince, J. (2022). Plastic pollution: The challenges of uncertainty and multiplicity in global marine governance. In *Routledge Handbook of Marine Governance and Global Environmental Change*, 253-262: Routledge. London.

Lehmann, A., Fitschen, K. & Rillig, M. C. (2019). Abiotic and Biotic Factors Influencing the Effect of Microplastic on Soil Aggregation. *Soil Systems* 3(1): 21.

Lehmann, A., Leifheit, E. F., Gerdawischke, M. & Rillig, M. C. (2021). Microplastics have shape-and polymer-dependent effects on soil aggregation and organic matter loss–an experimental and meta-analytical approach. *Microplastics and Nanoplastics* 1(1): 1-14.

Lehrsch, G. A. & Jolley, P. M. (1992). Temporal changes in wet aggregate stability. *Transactions of the American Society of Agricultural Engineers* (35): 493-498.

LfL (2023). Erosionsatlas Bayern. https://www.lfl.bayern.de/iab/boden/029288/ (06.07.2023).

LfStaD (2022). Statistisches Jahrbuch für Bayern. https://www.statistik.bayern.de/produkte/jahrbuch/ (06.07.2023).

LfU (1990-2020). Abfallwirtschaft–Hausmüll in Bayern – Bilanzen. *Joh.Walch GmbH & Co. KG,* Augsburg. https://www.lfu.bayern.de/abfall/index.htm (06.08.2023)

Li, H., Liu, L., Xu, Y. & Zhang, J. (2022a). Microplastic effects on soil system parameters: a meta-analysis study. *Environmental Science and Pollution Research* (29): 11027-11038.

Li, H., Lu, X., Wang, S., Zheng, B. & Xu, Y. (2021a). Vertical migration of microplastics along soil profile under different crop root systems. *Environmental Pollution* (278): 116833.

Li, J., Yu, S., Yu, Y. & Xu, M. (2022b). Effects of microplastics on higher plants: a review. *Bulletin of Environmental Contamination and Toxicology* 109(2): 241-265.

Li, S., Ding, F., Flury, M., Wang, Z., Xu, L., Li, S., Jones, D. L. & Wang, J. (2022c). Macro- and microplastic accumulation in soil after 32 years of plastic film mulching. *Environmental Pollution* (300): 118945.

Li, Z., Nie, X., Chang, X., Liu, L. & Sun, L. (2016). Characteristics of soil and organic carbon loss induced by water erosion on the loess plateau in China. *PLOS ONE* 11(4): e0154591

Li, Z., Wang, X., Liang, S., Li, H. & Sun, L. (2021b). Pyr-GC-MS analysis of microplastics extracted from farmland soils. *International Journal of Environmental Analytical Chemistry*, 1-18.

Lian, J., Liu, W., Meng, L., Wu, J., Zeb, A., Cheng, L., Lian, Y. & Sun, H. (2021). Effects of microplastics derived from polymer-coated fertilizer on maize growth, rhizosphere, and soil properties. *Journal of Cleaner Production* (318): 128571.

Liang, Y., Lehmann, A., Yang, G., Leifheit, E. F. & Rillig, M. C. (2021). Effects of microplastic fibers on soil aggregation and enzyme activities are organic matter dependent. *Frontiers in Environmental Science* (9): 650155.

Liu, E. K., He, W. Q. & Yan, C. R. (2014). 'White revolution' to 'white pollution'—agricultural plastic film mulch in China. *Environmental Research Letters* 9(9).

Liu, F., Olesen, K. B., Borregaard, A. R. & Vollertsen, J. (2019). Microplastics in urban and highway stormwater retention ponds. *Science of The Total Environment* (671): 992-1000.

Liu, H., Yang, X., Liu, G., Liang, C., Xue, S., Chen, H., Ritsema, C. J. & Geissen, V. (2017). Response of soil dissolved organic matter to microplastic addition in Chinese loess soil. *Chemosphere* (185): 907-917.

Liu, S., Niu, S.-H., Xiang, L., Liao, X.-D. & Xing, S.-C. (2023). Effects of the oversized microplastic pollution layer on soil aggregates and organic carbon at different soil depths. *Journal of Hazardous Materials* (450): 131014.

Liu, S., Shang, E., Liu, J., Wang, Y., Bolan, N., Kirkham, M. & Li, Y. (2022a). What have we known so far for fluorescence staining and quantification of microplastics: a tutorial review. *Frontiers of Environmental Science & Engineering* (16): 1-14.

Liu, Y., Shao, H., Liu, J., Cao, R., Shang, E., Liu, S. & Li, Y. (2021). Transport and transformation of microplastics and nanoplastics in the soil environment: A critical review. *Soil Use and Management*. 37(2). 224-242.

Liu, Y., Wang, B., Pileggi, V. & Chang, S. (2022b). Methods to recover and characterize microplastics in wastewater treatment plants. *Case Studies in Chemical and Environmental Engineering* (5): 100183.

Löder, M. G. J., Kuczera, M., Mintenig, S., Lorenz, C. & Gerdts, G. (2015). Focal plane array detector-based micro-Fourier-transform infrared imaging for the analysis of microplastics in environmental samples. *Environmental Chemistry* 12(5): 563-581.

Lozano, Y. M., Lehnert, T., Linck, L. T., Lehmann, A. & Rillig, M. C. (2021). Microplastic Shape, Polymer Type, and Concentration Affect Soil Properties and Plant Biomass. *Frontiers in Plant Science* (12): 169.

Luan, X., Kou, X., Zhang, L., Chen, L., Liu, W. & Cui, Z. (2022). Estimation and prediction of plastic losses to the environment in China from 1950 to 2050. *Resources, Conservation and Recycling* (184): 106386.

Luk, S. H. (1983). Effect of aggregate size and microtopography on rainwash and rainsplash erosion. Z*eitschrift für Geomorphologie.* (27): 283-295.

Lutz, N., Fogarty, J., Rate, A. & Hackett, M. J. (2022). Accumulation and potential for transport of microplastics in stormwater drains into marine environments, Perth region, Western Australia. *Marine Pollution Bulletin* (168): 112362.

Lwanga, E. H., Beriot, N., Corradini, F., Silva, V., Yang, X., Baartman, J., Rezaei, M., van Schaik, L., Riksen, M. & Geissen, V. (2022). Review of microplastic sources, transport pathways and correlations with other soil stressors: a journey from agricultural sites into the environment. *Chemical and Biological Technologies in Agriculture* 9(1): 1-20.

Lwanga, E. H., Thapa, B., Yang, X. M., Gertsen, H., Salanki, T., Geissen, V. & Garbeva, P. (2018). Decay of low-density polyethylene by bacteria extracted from earthworm's guts: A potential for soil restoration. *Science of the Total Environment* (624): 753-757.

Maass, S., Daphi, D., Lehmann, A. & Rillig, M. C. (2017). Transport of microplastics by two collembolan species. *Environmental Pollution* (225): 456-459.

Machado, A. A. D., Kloas, W., Zarfl, C., Hempel, S. & Rillig, M. C. (2018). Microplastics as an emerging threat to terrestrial ecosystems. *Global Change Biology* 24(4): 1405-1416.

MacLeod, M., Arp, H. P. H., Tekman, M. B. & Jahnke, A. (2021). The global threat from plastic pollution. *Science* 373(6550): 61-65.

Mai, L., Bao, L.-J., Wong, C. S. & Zeng, E. Y. (2018).Microplastics in the terrestrial environment. In *Microplastic Contamination in Aquatic Environments*, 365-378. https://www.sciencedirect.com/science/article/abs/pii/B9780128137475000126 (06.07.2023).

Mansa, R. & Zou, S. (2021). Thermogravimetric analysis of microplastics: A mini review. *Environmental Advances* (5): 100117.

Martínez-Mena, M., López, J., Almagro, M., Albaladejo, J., Castillo, V., Ortiz, R. & Boix-Fayos, C. (2012). Organic carbon enrichment in sediments: Effects of rainfall characteristics under different land uses in a Mediterranean area. *Catena* (94): 36-42.

Meinen, B. U. & Robinson, D. T. (2021). Agricultural erosion modelling: Evaluating USLE and WEPP field-scale erosion estimates using UAV time-series data. *Environmental Modelling & Software* (137): 104962.

Miklos, D., Obermaier, N. & Jekel, M. (2016). Mikroplastik: Entwicklung eines Umweltbewertungskonzepts. *Erste Überlegungen zur Relevanz von synthetischen Polymeren in der Umwelt. Umweltbundesamt, Dessau-Roßlau*. https://www.researchgate.net/profile/David_Miklos/publication/296676671_Mikroplastik_Entwicklung_eines_Umweltbewertungskonzeptes/links/56d7f0de08aebabdb4030ee2.pdf (06.08.2023).

Mintenig, S., Int-Veen, I., Löder, M. & Gerdts, G. (2014). Mikroplastik in ausgewählten Kläranlagen des Oldenburgisch-Ostfriesischen Wasserverbandes (OOWV) in Niedersachsen. https://www.gruene-bad-oldesloe.de/userspace/SH/ov_bad-oldesloe/Dateien/Abschlussbericht_Mikroplastik_in_Klaeranlagen-3.pdf (06.07.2023).

Mitrano, D. M. & Wohlleben, W. (2020). Microplastic regulation should be more precise to incentivize both innovation and environmental safety. *Nature Communications* 11(1): 5324.

Moritz, J. & Echterhoff, J. (2016). Growing threat in a throwaway society. In *European Conference on Plastics in Freshwater Environments 21–22 June 2016 in Berlin*, 93. https://www.researchgate.net/profile/Stefanie-Felsing/publication/316284914_European_Conference_on_Plastics_in_Freshwater_Environments_21_-_22_June_2016_in_Berlin/links/58f9c0cbaca2723d79d5c476/European-Conference-on-Plastics-in-Freshwater-Environments-21-22-June-2016-in-Berlin.pdf#page=95 (06.07.2023).

Moshood, T. D., Nawanir, G., Mahmud, F., Mohamad, F., Ahmad, M. H. & Abdul Ghani, A. (2022a). Biodegradable plastic applications towards sustainability: A recent innovations in the green product. *Cleaner Engineering and Technology* (6):100404.

Moshood, T. D., Nawanir, G., Mahmud, F., Mohamad, F., Ahmad, M. H. & AbdulGhani, A. (2022b). Sustainability of biodegradable plastics: New problem or solution to solve the global plastic pollution? *Current Research in Green and Sustainable Chemistry* (5): 100273.

Motto, H. L., Daines, R. H., Chilko, D. M. & Motto, C. K. (1970). Lead in soils and plants: its relation to traffic volume and proximity to highways. *Environmental Science & Technology* 4(3): 231-237.

Moulé, A. J. (2010). Power from plastic. *Current Opinion in Solid State and Materials Science* 14(6): 123-130.

Müller-Nedebock, D. & Chaplot, V. (2015). Soil carbon losses by sheet erosion: a potentially critical contribution to the global carbon cycle. *Earth Surface Processes and Landforms* 40(13): 1803-1813.

Müller, A., Kocher, B., Altmann, K. & Braun, U. (2022). Determination of tire wear markers in soil samples and their distribution in a roadside soil. *Chemosphere* (294): 133653.

Murphy, F., Ewins, C., Carbonnier, F. & Quinn, B. (2016). Wastewater Treatment Works (WwTW) as a source of microplastics in the aquatic environment. *Environmental Science Technology.* 50(11): 5800-5808.

Nadeu, E., Gobin, A., Fiener, P., Van Wesemael, B. & Van Oost, K. (2015). Modelling the impact of agricultural management on soil carbon stocks at the regional scale: the role of lateral fluxes. *Global Change Biology* (21): 3181-3192.

Nasseri, S. & Azizi, N. (2022).Occurrence and fate of microplastics in freshwater resources. In *Microplastic Pollution*, 187-200: Springer. Cham.

Ng, E. L., Lwanga, E. H., Eldridge, S. M., Johnston, P., Hu, H.-W., Geissen, V. & Chen, D. (2018). An overview of microplastic and nanoplastic pollution in agroecosystems. *Science of the Total Environment* (627): 1377-1388.

Nizzetto, L., Bussi, G., Futter, M. N., Butterfield, D. & Whitehead, P. G. (2016a). A theoretical assessment of microplastic transport in river catchments and their retention by soils and river sediments. *Environmental Science-Processes & Impacts* 18(8): 1050-1059.

Nizzetto, L., Futter, M. & Langaas, S. (2016b). Are Agricultural Soils Dumps for Microplastics of Urban Origin? *Environmental Science & Technology* 50(20): 10777-10779.

Nizzetto, L., Langaas, S. & Futter, M. (2016c). Do microplastics spill on to farm soils? *Nature* 537(7621): 488-488.

Nunes, J. P., Wainwright, J., Bielders, C. L., Darboux, F., Fiener, P., Finger, D. & Turnbull, L. (2018). Better models are more effectively connected models. *Earth Surface Processes and Landforms* 43(6), 1355-1360.

O'Connor, D., Pan, S., Shen, Z., Song, Y., Jin, Y., Wu, W.-M. & Hou, D. (2019). Microplastics undergo accelerated vertical migration in sand soil due to small size and wet-dry cycles. *Environmental Pollution* (249): 527-534.

Okoye, C. O., Addey, C. I., Oderinde, O., Okoro, J. O., Uwamungu, J. Y., Ikechukwu, C. K., Okeke, E. S., Ejeromedoghene, O. & Odii, E. C. (2022). Toxic chemicals and persistent organic pollutants associated with micro-and nanoplastics pollution. *Chemical Engineering Journal Advances* (11):100310.

Owens, P. N. (2020). Soil erosion and sediment dynamics in the Anthropocene: a review of human impacts during a period of rapid global environmental change. *Journal of Soils and Sediments* (20): 4115-4143.

Panno, S. V., Kelly, W. R., Scott, J., Zheng, W., McNeish, R. E., Holm, N., Hoellein, T. J. & Baranski, E. L. (2019). Microplastic contamination in karst groundwater systems. *Groundwater*. 57(2), 189-196.

Pérez-Reverón, R., González-Sálamo, J., Hernández-Sánchez, C., González-Pleiter, M., Hernández-Borges, J. & Díaz-Peña, F. J. (2022). Recycled wastewater as a potential source of microplastics in irrigated soils from an arid-insular territory (Fuerteventura, Spain). *Science of the Total Environment* (817): 152830.

Pervez, R., Wang, Y., Mahmood, Q. & Jattak, Z. (2020). Stereomicroscopic and Fourier transform infrared (FTIR) spectroscopic characterization of the abundance, distribution and composition of microplastics in the beaches of Qingdao, China. *Analytical Letters* 53(18): 2960-2977.

Praveena, S. M., Aris, A. Z. & Singh, V. (2022). Quality assessment for methodological aspects of microplastics analysis in soil. *Trends in Environmental Analytical Chemistry*. 34 (2022): e00159.

Primpke, S., Fischer, M., Lorenz, C., Gerdts, G. & Scholz-Böttcher, B. M. (2020). Comparison of pyrolysis gas chromatography/mass spectrometry and hyperspectral FTIR imaging spectroscopy for the analysis of microplastics. *Analytical and Bioanalytical Chemistry* (412): 8283-8298

Qiao, R., Mortimer, M., Richter, J., Rani-Borges, B., Yu, Z., Heinlaan, M., Lin, S. & Ivask, A. (2022). Hazard of polystyrene micro-and nanospheres to selected aquatic and terrestrial organisms. *Science of the Total Environment* (853): 158560.

R: Development Core Team (2021). R: a language and environment interaction for statistical computing. *R Foundation for Statistical Computing, Vienna, Austria*.

Raclot, D. & Albergel, J. (2006). Runoff and water erosion modelling using WEPP on a Mediterranean cultivated catchment. *Physics and Chemistry of the Earth* 31(17): 1038-1047.

Radford, F. (2023). Microplastics in agricultural soils: Methods, sources and fate. University of Southampton. https://eprints.soton.ac.uk/473412/1/FreyaRadford_thesis_final_copy.pdf (06.07.2023).

Rafique, A., Irfan, M., Mumtaz, M. & Qadir, A. (2020). Spatial distribution of microplastics in soil with context to human activities: a case study from the urban center. *Environmental Monitoring and Assessment* (192): 1-13.

Raj, D. & Maiti, S. K. (2023). Critical assessment of approach towards estimation of microplastics in environmental matrices. *Land Degradation & Development*. 34(10). 2735-2749.

Ramkumar, M., Balasubramani, K., Santosh, M. & Nagarajan, R. (2022). The plastisphere: A morphometric genetic classification of plastic pollutants in the natural environment. *Gondwana Research* (108): 4-12.

Rehm, R., Grashey-Jansen, S. & Thalheimer, M. (2018). Plastik im Boden. Ein noch unbekanntes Problem im Obst- und Weinbau? *obstbau weinbau* (11): 13-16.

Rehm, R., & Fiener, P. (2020). Der unsichtbare Plastikmüll: wie viel Mikroplastik steckt in unseren Böden? https://opus.bibliothek.uni-augsburg.de/opus4/frontdoor/deliver/index/docId/81051/file/Rehm_R_Fiener_P_2020.pdf (06.07.2023)

Rehm, R., & Fiener, P. (2023). Model-based analysis of erosion-induced microplastic delivery from arable land to the stream network of a mesoscale catchment. EGUsphere, 2023, 1-43.

Rehm, R., Zeyer, T., Schmidt, A. & Fiener, P. (2021). Soil erosion as transport pathway of microplastic from agriculture soils to aquatic ecosystems. *Science of the Total Environment* (795): 148774.

Rezaei, M., Riksen, M. J., Sirjani, E., Sameni, A. & Geissen, V. (2019). Wind erosion as a driver for transport of light density microplastics. *Science of The Total Environment* (669): 273-281.

Rhoton, F., Emmerich, W., Goodrich, D., Miller, S. & McChesney, D. (2006). Soil geomorphological characteristics of a semiarid watershed: influence on carbon distribution and transport. *Soil Science Society of America Journal* 70(5): 1532-1540.

Rillig, M. C. (2012). Microplastic in terrestrial ecosystems and the soil? *Environmental Science & Technology* 46(12): 6453-6454.

Rillig, M. C., Ingraffia, R. & Machado, A. A. D. (2017a). Microplastic incorporation into soil in agroecosystems. *Frontiers in Plant Science* 8. 8(2017):1805.

Rillig, M. C., Lehmann, A., de Souza Machado, A. A. & Yang, G. (2019). Microplastic effects on plants. *New Phytologist*. 223(3), 1066-1070.

Rillig, M. C., Leifheit, E. & Lehmann, J. (2021). Microplastic effects on carbon cycling processes in soils. *PLoS Biology* 19(3): e3001130.

Rillig, M. C., Ziersch, L. & Hempel, S. (2017b). Microplastic transport in soil by earthworms. *Scientific Reports* 7(1): 1362.
Rochman, C. M. (2018). Microplastics research - from sink to source. *Science* 360(6384): 28-29.
Rodrigues, M., Abrantes, N., Gonçalves, F., Nogueira, H., Marques, J. & Gonçalves, A. (2018). Spatial and temporal distribution of microplastics in water and sediments of a freshwater system (Antuã River, Portugal). *Science of the Total Environment* (633): 1549-1559.
Rodríguez-Seijo, A. & Pereira, R. (2019). Microplastics in agricultural soils: are they a real environmental hazard? In *Bioremediation of agricultural soils*, 45-60. Tylor & Francis Group, LCC. Boca Raton.
Ryan, P. G. (2015). A brief history of marine litter research. In: *Marine anthropogenic litter*. 1-25. Springer. Cham.
Sa'adu, I. & Farsang, A. (2023). Plastic contamination in agricultural soils: a review. *Environmental Sciences Europe* 35(1): 1-11.
Saggau, P., Kuhwald, M., Hamer, W. B. & Duttmann, R. (2022). Are compacted tramlines underestimated features in soil erosion modeling? A catchment-scale analysis using a process-based soil erosion model. *Land Degradation & Development* 33(3): 452-469.
Sajjad, M., Huang, Q., Khan, S., Khan, M. A., Yin, L., Wang, J., Lian, F., Wang, Q. & Guo, G. (2022). Microplastics in the soil environment: A critical review. *Environmental Technology & Innovation* (27): 102408.
Saling, P., Gyuzeleva, L., Wittstock, K., Wessolowski, V. & Griesshammer, R. (2020). Life cycle impact assessment of microplastics as one component of marine plastic debris. *The International Journal of Life Cycle Assessment* (25): 2008-2026.
Samuel, I. D. (2004). Fantastic plastic. *Nature* 429(6993): 709-710.
Santander, F. A. C. (2021).Development and application of tests for microplastic detection in soil. Wageningen University and Research. Wageningen.
Sarker, A., Deepo, D. M., Nandi, R., Rana, J., Islam, S., Rahman, S., Hossain, M. N., Islam, M. S., Baroi, A. & Kim, J.-E. (2020). A review of microplastics pollution in the soil and terrestrial ecosystems: A global and Bangladesh perspective. *Science of the Total Environment* (733): 139296.
Schell, T., Hurley, R., Buenaventura, N. T., Mauri, P. V., Nizzetto, L., Rico, A. & Vighi, M. (2022). Fate of microplastics in agricultural soils amended with sewage sludge: Is surface water runoff a relevant environmental pathway? *Environmental Pollution* (293): 118520.
Schell, T., Rico, A. & Vighi, M. (2020). Occurrence, fate and fluxes of plastics and microplastics in terrestrial and freshwater ecosystems. *Reviews of Environmental Contamination and Toxicology* (250): 1-43.
Scheurer, M. & Bigalke, M. (2018). Microplastics in Swiss floodplain soils. *Environmental Science & Technology*. 52(6), 3591-3598.
Schleypen, P. (2017). Abwasserbehandlung (nach 1945). *Historisches Lexikon Bayerns*. https://www.historisches-lexikon-bayerns.de/Lexikon/Abwasserbehandlung_(nach_1945) (06.07.2023).
Schmidt, J., v. Werner, M. & Michael, A. (1999). Application of the EROSION 3D model to the CATSOP watershed, The Nederlands. *Catena*. 37(3-4), 449-456.
Schwertmann, U., Vogl, W. & Kainz, M. (1987). Bodenerosion durch Wasser. Ulmer Verlag, Stuttgart.

Sharma, S., Sharma, B. & Sadhu, S. D. (2022). Microplastic profusion in food and drinking water: are microplastics becoming a macroproblem? *Environmental Science: Processes & Impacts* 24(7): 992-1009.

Shekhar, A. R., Kumar, A., Syamsai, R., Cai, X. & Pol, V. G. (2022). Is the Plastic Pandemic a Greater Threat to Humankind than COVID-19? *ACS Sustainable chemistry & Engineering* 10(10): 3150-3154.

Shim, W. J., Hong, S. H. & Eo, S. E. (2017). Identification methods in microplastic analysis: a review. *Analytical Methods* 9(9): 1384-1391.

Sierra, I., Chialanza, M. R., Faccio, R., Carrizo, D., Fornaro, L. & Pérez-Parada, A. (2020). Identification of microplastics in wastewater samples by means of polarized light optical microscopy. *Environmental Science and Pollution Research* (27): 7409-7419.

Singh, S. & Bhagwat, A. (2022). Microplastics: A potential threat to groundwater resources. *Groundwater for Sustainable Development* (19): 100852.

Sintim, H. Y. & Flury, M. (2017). Is biodegradable plastic mulch the solution to agriculture's plastic problem? *Environmental Science Technology*. 51(3):1068-1069.

Six, J., Elliott, E. & Paustian, K. (1999). Aggregate and soil organic matter dynamics under conventional and no-tillage systems. *Soil Science Society of America Journal* 63(5): 1350-1358.

Six, J., Paustian, K., Elliott, E. T. & Combrink, C. (2000). Soil structure and organic matter I. Distribution of aggregate-size classes and aggregate-associated carbon. *Soil Science Society of America Journal* 64(2): 681-689.

Sommer, F., Dietze, V., Baum, A., Sauer, J., Gilge, S., Maschowski, C. & Gieré, R. (2018). Tire abrasion as a major source of microplastics in the environment. *Aerosol and Air Quality Research* 18(8): 2014-2028.

Su, L., Xiong, X., Zhang, Y., Wu, C., Xu, X., Sun, C. & Shi, H. (2022). Global transportation of plastics and microplastics: a critical review of pathways and influences. *Science of the Total Environment* (831): 154884.

Surendran, U., Jayakumar, M., Raja, P., Gopinath, G. & Chellam, P. V. (2023). Microplastics in terrestrial ecosystem: Sources and migration in soil environment. *Chemosphere* (318): 137946.

Swanson, N. P. & Dedrick, A. R. (1967). Soil particles and aggregates transported in water runoff under various slope conditions using simulated rainfall. *Transactions of the American Society of Agricultural Engineers* (10): 246-247.

Tábi, T. (2022). Biodegradable bio-based plastics: Compostable or recyclable? *Express Polymer Letters* 16(2): 115-115.

Tagg, A. S. & do Sul, J. A. I. (2019). Is this your glitter? An overlooked but potentially environmentally-valuable microplastic. *Marine Pollution Bulletin* (146): 50-53.

Tang, K. H. D. & Hadibarata, T. (2021). Microplastics removal through water treatment plants: Its feasibility, efficiency, future prospects and enhancement by proper waste management. *Environmental Challenges* (5): 100264.

Tekman, M. B., Walther, B., Peter, C., Gutow, L. & Bergmann, M. (2022). *Impacts of plastic pollution in the oceans on marine species, biodiversity and ecosystems.* WWW Germany. Berlin.

Tian, L., Jinjin, C., Ji, R., Ma, Y. & Yu, X. (2022). Microplastics in agricultural soils: sources, effects, and their fate. *Current Opinion in Environmental Science & Health* (25): 100311.

Tunali, M., Adam, V. & Nowack, B. (2023). Probabilistic environmental risk assessment of microplastics in soils. *Geoderma* (430): 116315.

Unice, K. M., Weeber, M. P., Abramson, M. M., Reid, R. C. D., van Gils, J. A. G., Markus, A. A., Vethaak, A. D. & Panko, J. M. (2019). Characterizing export of land-based microplastics to the estuary - Part I: Application of integrated geospatial microplastic transport models to assess tire and road wear particles in the Seine watershed. *Science of the Total Environment* (646): 1639-1649.

Vaccari, D. A. (2009). Phosphorus: a looming crisis. *Scientific American* 300(6): 54-59.

Van Oost, K., Govers, G., De Alba, S. & Quine, T. (2006). Tillage erosion: a review of controlling factors and implications for soil quality. *Progress in Physical Geography* 30(4): 443-466.

Van Oost, K., Govers, G. & Desmet, P. (2000). Evaluating the effects of changes in landscape structure on soil erosion by water and tillage. *Landscape Ecology* 15(6): 577-589.

Van Oost, K., Govers, G., Quine, T. A., Heckrath, G., Olesen, J. E., De Gryze, S. & Merckx, R. (2005a). Landscape-scale modeling of carbon cycling under the impact of soil redistribution: The role of tillage erosion. *Global Biogeochemical Cycles* 19(4).

Van Oost, K., Quine, T., Govers, G. & Heckrath, G. (2005b).Modeling soil erosion induced carbon fluxes between soil and atmosphere on agricultural land using SPEROS-C. In *Advances in soil science. Soil erosion and carbon dynamics*, 37-51 (Eds E. J. Roose, R. Lal, C. Feller, B. Barthes and B. A. Stewart). CRC Press,.Boca Raton,

Van Rompaey, A. J., Verstraeten, G., Van Oost, K., Govers, G. & Poesen, J. (2001). Modelling mean annual sediment yield using a distributed approach. *Earth Surface Processes and Landforms* 26(11): 1221-1236.

Verla, A. W., Enyoh, C. E., Verla, E. N. & Nwarnorh, K. O. (2019). Microplastic–toxic chemical interaction: a review study on quantified levels, mechanism and implication. *SN Applied Sciences* 1(11): 1-30.

Verstraeten, G. & Prosser, I. P. (2008). Modelling the impact of land-use change and farm dam construction on hillslope sediment delivery to rivers at the regional scale. *Geomorphology* 98(3-4): 199-212.

Viaroli, S., Lancia, M. & Re, V. (2022). Microplastics contamination of groundwater: Current evidence and future perspectives. A review. *Science of the Total Environment* (24): 153851.

Vollertsen, J., & Hansen, A. A. (Eds.) (2017). Microplastic in Danish wastewater: Sources, occurrences and fate. The Danish Environmental Protection Agency. Environmental Project Vol. 1906 http://mst.dk/service/publikationer/publikationsarkiv/2017/mar/mikroplast-i-renseanlaeg/ (06.07.2023)

Wagner, S., Cattle, S. R. & Scholten, T. (2007). Soil-aggregate formation as influenced by clay content and organic-matter amendment. *Journal of Plant Nutrition and Soil Science* 170(1): 173-180.

Wagner, S., Hüffer, T., Klöckner, P., Wehrhahn, M., Hofmann, T. & Reemtsma, T. (2018). Tire wear particles in the aquatic environment-a review on generation, analysis, occurrence, fate and effects. *Water Research* (139): 83-100.

Waldschläger, K., Lechthaler, S., Stauch, G. & Schüttrumpf, H. (2020). The way of microplastic through the environment–Application of the source-pathway-receptor model. *Science of the Total Environment* (713): 136584.

Waldschläger, K. & Schüttrumpf, H. (2020). Infiltration behavior of microplastic particles with different densities, sizes, and shapes - From glass spheres to natural sediments. *Environmental Science & Technology* 54(15): 9366-9373.

Walker, H. W. & Bob, M. M. (2001). Stability of particle flocs upon addition of natural organic matter under quiescent conditions. *Water Research* 35(4): 875-882.

Wan, Y., Wu, C., Xue, Q. & Hui, X. (2019). Effects of plastic contamination on water evaporation and desiccation cracking in soil. *Science of the Total Environment* (654): 576-582.

Wang, F., Wang, Q., Adams, C. A., Sun, Y. & Zhang, S. (2022). Effects of microplastics on soil properties: current knowledge and future perspectives. *Journal of Hazardous Materials* (424): 127531.

Wang, Q., Feng, X., Liu, Y., Cui, W., Sun, Y., Zhang, S. & Wang, F. (2022b). Effects of microplastics and carbon nanotubes on soil geochemical properties and bacterial communities. *Journal of Hazardous Materials* (433): 128826.

Wang, Z., Govers, G., Oost, K. V., Clymans, W., den Putte, A. V. & Merckx, R. (2013a). Soil organic carbon mobilization by interrill erosion: Insights from size fractions. *Journal of Geophysical Research: Earth Surface* 118(2): 348-360.

Wang, Z., Govers, G., Van Oost, K., Clymans, W., Van den Putte, A. & Merckx, R. (2013b). Soil organic carbon mobilization by interrill erosion: Insights from size fractions. *Journal of Geophysical Research* 118(2): 348-360.

Weber, C. J. & Opp, C. (2020). Spatial patterns of mesoplastics and coarse microplastics in floodplain soils as resulting from land use and fluvial processes. *Environmental Pollution* (267): 115390.

Weber, C. J., Santowski, A. & Chifflard, P. (2022). Investigating the dispersal of macro-and microplastics on agricultural fields 30 years after sewage sludge application. *Scientific Reports* 12(1): 1-13.

Weithmann, N., Möller, J. N., Löder, M. G., Piehl, S., Laforsch, C. & Freitag, R. (2018). Organic fertilizer as a vehicle for the entry of microplastic into the environment. *Science Advances* 4(4): eaap8060.

Werkenthin, M., Kluge, B. & Wessolek, G. (2014). Metals in European roadside soils and soil solution–A review. *Environmental Pollution* (189): 98-110.

Wheeler, G. & Rolfe, G. (1979). The relationship between daily traffic volume and the distribution of lead in roadside soil and vegetation. *Environmental Pollution.* 18(4): 265-274.

Wik, A. & Dave, G. (2009). Occurrence and effects of tire wear particles in the environment–A critical review and an initial risk assessment. *Environmental Pollution* 157(1): 1-11.

Wilken, F., Sommer, M., Van Oost, K., Bens, O. & Fiener, P. (2017). Process-oriented modelling to identify main drivers of erosion-induced carbon fluxes. *SOIL* 3(2): 83-94.

Williams, A. T. & Rangel-Buitrago, N. (2022). The past, present, and future of plastic pollution. *Marine Pollution Bulletin* (176): 113429.

Windsor, F. M., Durance, I., Horton, A. A., Thompson, R. C., Tyler, C. R. & Ormerod, S. J. (2019). A catchment-scale perspective of plastic pollution. *Global Change Biology* 25(4): 1207-1221.

Witzig, C., Wörle, K., Földi, C., Rehm, R., Reuwer, A.-K., Ellerbrake, K., Cieplik, S., Rehorek, A., Freier, K., Dierkes, G., Wick, A., Ternes, T., Fiener, P., Klasmeier, J. & Zumbülte, N. (2021). Mikroplastik in Binnengewässern. Untersuchung und Modellierung des Eintrags und Verbleibs im Donaugebiet als Grundlage für Maßnahmenplanung. *MICBIN Abschlussbericht.* *https://www.micbin.de/download/Abschluss_MicBin_02-11-2021-Final.pdf (06.07.2023)*

WRB (2015). World reference base for soil resources 2014, update 2015. Internation soil classification sstem for naming soils and creating legends for soil maps. *World Soil Resources Reports No. 106. FAO*. Rome.

Wright, S., Ulke, J., Font, A., Chan, K. & Kelly, F. (2019). Atmospheric microplastic deposition in an urban environment and an evaluation of transport. *Environment International* (136): 105411.

Xu, C. Y., Zhang, B. B., Gu, C. J., Shen, C. S., Yin, S. S., Aamir, M. & Li, F. (2020). Are we underestimating the sources of microplastic pollution in terrestrial environment? *Journal of Hazardous Materials* (400): 123228.

Yu, M., van der Ploeg, M., Lwanga, E. H., Yang, X. M., Zhang, S. L., Ma, X. Y., Ritsema, C. J. & Geissen, V. (2019). Leaching of microplastics by preferential flow in earthworm (Lumbricus terrestris) burrows. *Environmental Chemistry* 16(1): 31-40.

Yurtsever, M., Kaya, A. T. & Bayraktar, S. Ç. (2018). A Research on microplastic presence in outdoor air. In *Proceedings of the International Conference on Microplastic Pollution in the Mediterranean Sea*, 89-97. Springer. Cham.

Zhang, G. & Liu, Y. (2018). The distribution of microplastics in soil aggregate fractions in southwestern China. *Science of the Total Environment* (642): 12-20.

Zhang, H., Huang, Y., An, S. & Zhu, Z. (2022a). A Review of Microplastics in Soil: Distribution Within Pedosphere Compartments, Environmental Fate, and Effects. *Water, Air, & Soil Pollution* 233(9): 380.

Zhang, J., Ren, S., Xu, W., Liang, C., Li, J., Zhang, H., Li, Y., Liu, X., Jones, D. L. & Chadwick, D. R. (2022b). Effects of plastic residues and microplastics on soil ecosystems: A global meta-analysis. *Journal of Hazardous Materials* (435): 129065.

Zhang, K., Hamidian, A. H., Tubić, A., Zhang, Y., Fang, J. K., Wu, C. & Lam, P. K. (2021). Understanding plastic degradation and microplastic formation in the environment: A review. *Environmental Pollution* (274): 116554.

Zhang, L., Xie, Y., Liu, J., Zhong, S., Qian, Y. & Gao, P. (2020). An overlooked entry pathway of microplastics into agricultural soils from application of sludge-based fertilizers. *Environmental Science & Technology* 54(7): 4248-4255.

Zhang, S., Liu, X., Hao, X., Wang, J. & Zhang, Y. (2020b). Distribution of low-density microplastics in the mollisol farmlands of northeast China. *Science of The Total Environment* (708): 135091.

Zhang, Y., Gao, T., Kang, S., Shi, H., Mai, L., Allen, D. & Allen, S. (2022b). Current status and future perspectives of microplastic pollution in typical cryospheric regions. *Earth-Science Reviews* (226): 103924.

Zhao, S., Zhang, Z., Chen, L., Cui, Q., Cui, Y., Song, D. & Fang, L. (2022). Review on migration, transformation and ecological impacts of microplastics in soil. *Applied Soil Ecology* (176): 104486.

Zhao, T., Lozano, Y. M. & Rillig, M. C. (2021). Microplastics increase soil pH and decrease microbial activities as a function of microplastic shape, polymer type, and exposure time. *Frontiers in Environmental Science* (9): 675803.

Zubris, K. A. & Richards, B. K. (2005). Synthetic fibers as an indicator of land application of sludge. *Environmental Pollution* 138(2): 201-211.

Zylstra, E. (2013). Accumulation of wind-dispersed trash in desert environments. *Journal of Arid Environments* (89): 13-15.

During my doctoral period, the following publications were produced:

Rehm, Raphael, Fiener, P. (2024): Model-based analysis of erosion-induced microplastic delivery from arable land to the stream network of a mesoscale catchment. Soil. https://doi.org/10.5194/soil-10-211-2024.

Rehm, R., Zeyer, T., Schmidt, A., Fiener, P. (2021): Soil erosion as transport pathway of microplastic from agriculture soils to aquatic ecosystems. Science of the Total Environment, 795, 148774. https://doi.org/10.1016/j.scitotenv.2021.148774.

Rehm, R., Fiener, P. (2020): Der unsichtbare Plastikmüll: wie viel Mikroplastik steckt in unseren Böden? Geographische Rundschau, 2020(7-8), 32-36.

Pinheiro Machado Rehm, R.; Grashey-Jansen, S.; Thalheimer, M. (2018): Plastik im Boden. Ein noch unbekanntes Problem im Obst-und Weinbau? Obstbau Weinbau-Fachmagazin des Südtiroler Beratungsringes, 2018, 55. Jg., Nr. 11, S. 13-16.

Microplastic (MP) contamination has been detected in all ecosystems and environments worldwide and is currently dominating various research fields. It is now known that MP particles not only pollute marine waters, but also freshwaters and terrestrial ecosystems. Contamination with MP can be detected almost everywhere and across the board. This is partly due to the fact that MP also spreads and is deposited via the atmosphere. It is also suspected that soils contain more MP than the oceans. Arable land in particular represents a large man-made MP sink due to agricultural practice and recycling management such as e.g. fertilization with MP contaminated sewage sludge, where MP is applied concentrated to the fields. Even in compost, the basis for healthy soil, MP concentrations with up to several hundred plastic particles per kilogram were already detected. The fate of the MP particles after deposition on arable land and how they are spatially distributed in the agricultural landscape, e.g. by water erosion, is largely unknown.

Universität Augsburg
Institut für Geographie

WATER ||| SOIL
RESOURCES